AD 663715

ARL 67-0202
OCTOBER 1967

Aerospace Research Laboratories

AN EXPERIMENTAL INVESTIGATION OF SHOCK INITIATED DETONATION WAVES IN A FLOWING COMBUSTIBLE MIXTURE

LEONARD ANTHONY HAMILTON, LT. COL., USAF
AIR FORCE INSTITUTE OF TECHNOLOGY (AU)
WRIGHT-PATTERSON AIR FORCE BASE, OHIO

Project No. 7065

DDC
RECEIVED
JAN 15 1968
C

This document has been approved for public release and sale; its distribution is unlimited.

OFFICE OF AEROSPACE RESEARCH
United States Air Force

197

NOTICES

When Government drawings, specifications, or other data are used for any purpose other than in connection with a definitely related Government procurement operation, the United States Government thereby incurs no responsibility nor any obligation whatsoever, and the fact that the Government may have formulated, furnished, or in any way supplied the said drawings, specifications, or other data, is not to be regarded by implication or otherwise as in any manner licensing the holder or any other person or corporation, or conveying any rights or permission to manufacture, use, or sell any patented invention that may in any way be related thereto.

Agencies of the Department of Defense, qualified contra ..s and other government agencies may obtain copies from the

Defense Documentation Center
Cameron Station
Alexandria, Virginia 22314

This document has been released to the

CLEARINGHOUSE
U.S. Department of Commerce
Springfield, Virginia 22151

for sale to the public.

Copies of ARL Technical Documentary Reports should not be returned to Aerospace Research Laboratories unless return is required by security considerations, contractual obligations or notices on a specified document.

300 - January 1967 - CO455 - 18-367

ARL 67-0202

AN EXPERIMENTAL INVESTIGATION OF SHOCK INITIATED DETONATION WAVES IN A FLOWING COMBUSTIBLE MIXTURE

LEONARD ANTHONY HAMILTON, LT. COL., USAF

AIR FORCE INSTITUTE OF TECHNOLOGY (AU)
WRIGHT-PATTERSON AIR FORCE BASE, OHIO

Submitted to the Faculty of the Graduate School of
The Ohio State University
in partial fulfillment of the requirements
for the degree of
DOCTOR OF PHILOSOPHY

OCTOBER 1967

Project 7065

This document has been approved for public release and sale; its distribution is unlimited.

AEROSPACE RESEARCH LABORATORIES
OFFICE OF AEROSPACE RESEARCH
UNITED STATES AIR FORCE
WRIGHT-PATTERSON AIR FORCE BASE, OHIO

FOREWORD

This technical report was prepared by Lt. Col. Leonard A. Hamilton of the Department of Mechanical Engineering of the Air Force Institute of Technology (AFIT), Wright-Patterson AFB, Ohio, and was presented to the Department of Aeronautical and Astronautical Engineering of the Ohio State University in partial fulfillment of the requirements for the degree of Doctor of Philosophy. This report is based on work accomplished on a cooperative research project, designated AFIT C-66-3, in which the Aerospace Research Laboratories (ARL) provided a portion of the support. Dr. R. G. Dunn of ARL was the Coordinator.

This report also constitutes the final report on AFIT Research Project C-66-3.

ABSTRACT

This investigation was concerned with the initiation of detonation waves in a subsonically flowing mixture of gaseous hydrogen and oxygen by means of shock waves injected opposite to the direction of the flow. Nominally stoichiometric mixtures at near ambient pressure and stagnation temperature were flowed through a constant area tube at Mach Numbers of approximately .2, .5, and .8. The shock waves were produced by a simple shock tube driver employing helium and mylar diaphragms. Piezoelectric pressure transducers, thin film heat transfer gages, and ionization probes were used to measure the various wave velocities. Results showed that detonation waves can easily be produced in such a flowing mixture. The minimum incident shock wave Mach Number above which detonation always occurred was 2.12 for $M_{Exit} = .2$; 1.75 for $M_{Exit} = .5$; and 1.56 for $M_{Exit} = .8$. The temperatures behind these shock waves were far below the ignition temperature predicted by the thermal explosion limit theory. It was suggested that the low temperature ignition phenomena could be accounted for by an increase in the degree of ionization of the flowing mixture with flow velocity, due to frictional effects and possible impurities normally present in the gases. Additional experimental work is required in order to establish conclusively the explanation of the observed phenomena.

ACKNOWLEDGMENTS

I wish to express my thanks to Dr. A. J. Shine, Head of the Department of Mechanical Engineering, AHIT, for his interest in and support of the project, and for making the test facility, technician support, and time available to me to conduct the research. I also thank Dr. R. G. Dunn of ARL for his immediate interest in the project and for his willingness to provide financial support to the project.

I wish to express my gratitude to my advisor, Professor Rudolph Edse, for his interest, advice, and guidance throughout the research program, and for the many hours of stimulating and enlightening discussion which we had throughout my Ph.D. program.

I wish to acknowledge my indebtedness, and offer my thanks to the following people for the assistance they gave me during the program:

Major Ralph Prete, ARL, who designed the circuit and procured the components for the heat transfer gage signal amplifier.

Dr. U. Grimm, ARL, who collaborated in the design of the heat transfer gage holder, and who constructed most of the heat transfer gages used in the program.

Dr. G. Mueller, ARL, who eagerly supplied suggestions, and who loaned several components of the instrumentation system to me.

Dr. W. C. Bahr, AFIT (now deceased), for convincing me of the usefulness of the digital computer in the reduction of the data, and for doing most of the programming involved.

Mr. Howard Toms, ARL, who provided vitally needed solenoid valves and other components required in the gas supply and control system.

Mr. John Parks, AFIT, who was my laboratory technician, for his interest and for all of the fine work which he accomplished.

Mr. Millard Wolfe, supervisor of the AFIT School Shops, for collaborating in the design of many of the modifications to the equipment.

Mrs. Anna Brown, secretary in the Department of Mechanical Engineering, AFIT, who typed the draft.

I would also like to express my appreciation to the many supervisors and workers on the base who were sympathetic to my many requests for "as soon as possible" service. Their friendly cooperation made it possible to complete the project in the time allotted.

Finally, I want to express my thanks to my wife and children for their patience and understanding throughout the years when I was so busy studying or working.

VITA

June 19, 1928	Born -- Lebanon, Kentucky
1949-1967 .	Officer, United States Air Force
1953 . . .	B.S. Equivalent, Air Force Institute of Technology, Wright-Patterson AFB, Ohio (WPAFB, O.)
1953-1957 .	Project Engineer, and Senior Project Engineer, Liquid Propellant Rocket Engine Development Section, Power Plant Laboratory, WPAFB, O.
1958 . . .	M.S.M.E., Purdue University West Lafayette, Indiana
1958-1962 .	Instructor, Assistant Professor, and Associate Professor, Department of Mechanical Engineering, Air Force Institute of Technology, WPAFB, O.
1958-1962 .	Part-Time Graduate Student, Department of Mechanical Engineering, The Ohio State University Graduate Center, WPAFB, O.
1962-1964 .	Graduate Student, Department of Aeronautical and Astronautical Engineering, The Ohio State University, Columbus, Ohio
1964-1965 .	Research Assistant, Department of Mechanical Engineering, Air Force Institute of Technology, WPAFB, O.
1964-1967 .	Part-Time Graduate Student, Department of Aeronautical and Astronautical Engineering, The Ohio State University Graduate Center, WPAFB, O.
1965-1967 .	Associate Professor, Department of Mechanical Engineering, Air Force Institute of Technology, WPAFB, O.

FIELDS OF STUDY

Major Field: Aeronautical and Astronautical Engineering

Studies in Propulsion. Professor Rudolph Edse

Studies in Compressible Aerodynamics and Boundary Layer Theory. Professor John D. Lee

Studies in Mathematics. Professor Albert B. Carson

Studies in Physics. Professor L. C. Brown

TABLE OF CONTENTS

LIST OF TABLES

LIST OF ILLUSTRATIONS

LIST OF SYMBOLS

Symbol	Meaning
A	Cross sectional area available to the flowing gas in square inches
$A(5)$	Speed of sound at the exit of the flowing gas section. (Table 5)
C_d	Discharge coefficient - used in Equation 1
D	Inside diameter of the flowing gas section in inches (in)
L_{Max}	Parameter used in Fanno Line Theory, defined on page 155
M	Mach Number
M_{Exit}	Mach Number of the flowing mixture at the plane of the ionization probe located 3.44 inches from the exit of the flowing gas section - the calculated flow velocity divided by the speed of sound in the flowing mixture at the same location.
M_{SE}	Mach Number of the transmitted shock wave relative to the flowing mixture at a station located 14 1/2 inches from the driver transition section exit diaphragm.
M_{SI}	Mach Number of the incident shock wave relative to the ambient, stationary air in the inert section prior to reaching the driver transition section exit diaphragm.
$\mathfrak{M}$	Average molecular weight of the gas mixture in lb_m/lbmole
P	Static pressure in pounds per square inch absolute (psia)

Symbol	Meaning
P^*	Static pressure at a station in the flowing mixture where the Mach Number is one, psia
ΔP	Difference in static pressures in pounds per square inch (psi)
R_o	Universal gas constant, 1545 $\frac{\text{ft lb}_f}{\text{lbmole R}}$
T	Absolute Temperature in R
T_o	Stagnation or total temperature in R
V	Velocity in feet per second (ft/sec)
V_{C-J}	The theoretical Chapman-Jouget detonation wave velocity, ft/sec
V_{SE}	Velocity of the transmitted shock wave relative to the flowing mixture at a station located 14 1/2 inches from the driver transition section exit diaphragm, in ft/sec.
Y_a	Compressibility correction factor, used in Equation 1
a	Speed of sound in ft/sec
d	Venturi throat diameter, in
f	Friction factor used in the Fanno Line Theory $= \frac{2\tau_w}{\rho V^2}$
g_c	Dimensional conversion factor 32.2 $\frac{\text{lb}_m \text{ ft}}{\text{lb}_f \text{ sec}^2}$
k	Ratio of the specific heat at constant pressure to the specific heat at constant volume
$\dot{m}$	Mass flow rate in pounds mass per second (lb_m/sec)
ρ	Density in lb_m/ft^3
τ_w	Wall shear stress in psi

Subscripts	Meaning
0	Oxygen
H	Hydrogen
(1)	Flow station at the exit of the mixing section - used in Table 5
Exit, or (5)	Flow station at the plane of the ionization probe located 3.44 inches from the exit of the flowing gas section - denoted (5) in Table 5.

I. INTRODUCTION

Background

The occurrence of detonation waves in combustible gases was discovered over eighty years ago, and this phenomenon has been subjected to extensive experimental and theoretical investigation throughout the intervening years up to the present time. Summaries of the results of these investigations, along with extensive lists of references have been presented by Lewis and von Elbe [1]*, Jost [2], Wolfson [3], and Oppenheim, et al. [4], to which the reader is referred for general information. The major portion of these early experiments were conducted in long cylindrical tubes of circular or rectangular cross section in which the gas was initially at rest. Combustion was initiated by one of several methods, such as, electric sparks, hot wires, squibs, blasting caps, or by externally produced detonation or shock waves.

In the past few years attention has been directed to the initiation and propagation of detonation waves in flowing gases. In addition to the fundamental knowledge

---

*Numbers in brackets refer to references at the end.

to be gained from such studies, the results obtained also have potential application in the current and future aircraft and missile propulsion technology. One of the few remaining problems in rocket engine technology is high frequency combustion instability. Many investigators believe that detonative processes in the combustion chamber, along with their associated pressure waves, play an important role in this phenomenon [5]. Furthermore, supersonic combustion ramjets (Scramjets) are under study for application to the propulsion of the hypersonic flight vehicles of the future. At the present time the major efforts in the area of supersonic combustion are being directed at the spontaneous combustion process which results when the fuel is injected into a high temperature supersonic air stream. In this process combustion occurs in a supersonic stream, but the combustion reaction rate is limited by the rate at which the fuel can be mixed with the air by turbulence and diffusion. Thus, the combustion zone does not move supersonically with respect to the air stream, and a relatively long (and heavy) combustion chamber is required for the reaction to reach equilibrium, since the reacting mixture is carried downstream with the supersonic flow. If this combustion process could be replaced with a process which is capable of moving at supersonic speed with respect to the reactants, that is, with a detonation wave moving upstream into the

supersonic gas stream entering the combustor with a velocity equal to the stream velocity, a standing detonation wave would be produced. Since a detonation wave is known to have a very short reaction zone length (of the order of a few millimeters) a drastic reduction in combustion chamber length would be made possible. Therefore, a substantial weight saving would result from the use of such a combustion process. (It should be noted that research has not yet led to the stabilization of a true Chapman-Jouget detonation wave such that it was stationary in laboratory coordinates.) It would seem, therefore, that in addition to the fundamental knowledge to be gained, which is sufficient justification in itself for many researchers, there are also possible technological gains to be realized from continued research into detonative phenomena in flowing gas streams.

Since this dissertation is concerned with shock induced detonation waves in a flowing combustible mixture, a brief review of pertinent literature will now be presented in order to provide a frame of reference for the present work.

Shock induced detonations

Review of the literature did not reveal any instances in which an externally produced shock wave had been used to initiate a detonation wave in a flowing combustible gas. However, there were several references in which

experiments were described in which ignition and detonation were produced in stationary gases by externally produced shock waves. Some of these experiments revealed information which is of value to the present work, and they will now be discussed.

Berets, Greene, and Kistiakowski [6] conducted experiments in which detonation waves were produced by shock waves introduced into static mixtures of hydrogen and oxygen, acetylene and oxygen, methane and oxygen, and benzene and oxygen. The shock waves were produced in a separate initiating tube which was filled with a mixture of acetylene and oxygen. This mixture was isolated from the test mixture by means of two diaphragms which enclosed a 10 centimeter long column of air. In order to produce the shock waves the acetylene-oxygen initiator mixture was ignited by an electric spark, and a detonation wave was quickly formed in the initiator. The detonation wave passed through the first diaphragm and entered the air "buffer" section where the chemical reaction was quenched. The remaining shock wave passed through the second diaphragm and entered the test gas. The shock speed was varied by changing the composition and, in a few cases, the initial pressure of the initiator gas. These investigators found that the weakest shock waves were transmitted by the test gas without chemical reaction and with a slow decay in velocity, as would be the

case if the shock were moving through an inert gas. Shocks whose peak temperature exceeded the ignition temperature of the test gas were propagated with a slowly increasing velocity, and when the initial shocks were more intense, this phase was followed by the development of a full detonation wave. The initial propagation velocity of the detonation waves formed from these shock waves generally exceeded the steady state value, and oscillated as it decayed to the steady value. The strongest initiating shocks produced immediate detonation waves in which the propagation velocity did not overshoot or oscillate. The calculated temperatures behind the shock waves which were strong enough to initiate detonation in various gas mixtures were slightly in excess of the explosion limit temperature values found in the literature for the same mixtures.

Shepherd [7] conducted experiments involving shock induced detonation waves in static mixtures of methane-oxygen and ethylene-oxygen at atmospheric pressure. A simple shock tube was used with air as the driver gas. The shock strength was varied by using different diaphragm materials and thicknesses. The results showed that ignition of the test gas was initiated by shock waves produced by diaphragms which ruptured at surprisingly low pressures --- 64 psig for a 28% methane - 71% oxygen mixture, which corresponds to an ignition

temperature of only 520 K, and less than 50 psig for an ethylene-oxygen mixture. Some experiments were conducted with a 15 centimeter long buffer section containing air inserted between the diaphragm and the test gas. This buffer section was closed at the downstream end by a sliding shutter, which was opened prior to breaking the diaphragm. When using this device higher bursting pressures were required to ignite the test gas; however, it was still possible to ignite a mixture of ethylene and oxygen using a shock wave which produced a calculated temperature of only 390 K and a pressure of 3.5 atmospheres.

In discussing the work reported in [6], Fay [8] expressed the view that results obtained with shock waves which were produced from decaying detonation waves may not compare with results obtained using shock waves produced in the normal manner in a shock tube, since in the former case the shock wave is closely followed by a rarefaction wave. This closely coupled rarefaction wave reduces the time during which the pressure and temperature behind the wave are at high values. Fay conducted experiments similar to those of Shepherd using a stoichiometric mixture of hydrogen and oxygen at one atmosphere initial pressure as the test gas. The strength of the shock waves produced was expressed in terms of the shock Mach Number, which was calculated from the pressure ratio

existing across the diaphragm before its rupture. In experiments using a simple shock tube without a buffer section, ignition of the test gas was effected by a shock wave propagating at a Mach Number of only 1.55, corresponding to an ignition temperature of only 400 K. Experiments were then conducted with a 2 ft long buffer section containing an inert gas installed between the main diaphragm and the test gas. When the buffer gas was separated from the test gas by a thin cellophane diaphragm (having a breaking pressure of 20 inches of mercury) the results were the same as those obtained without the buffer section. When the cellophane diaphragm was physically removed prior to rupturing the main diaphragm, the incident shock Mach Number required to ignite the test gas increased to about 2.6, which corresponds to an ignition temperature of 630 K. These ignition temperatures are considerably less than those obtained in thermal explosion experiments conducted in glass bulbs [1].

Steinberg and Kaskan [9] studied the ignition of stoichiometric hydrogen-oxygen mixtures at initial pressures of 200 and 300 millimeters of mercury (mm Hg) by means of shock waves. The shock tube used in this investigation incorporated a 2 ft long buffer section, and special precautions were taken during the construction of the shock tube to insure that there were no

mismatched surfaces, projections, or cavities which would result in reflected shock waves. The buffer section was filled with an inert gas mixture which was contained by a sliding shutter on the downstream end. During an experiment the shutter was opened, and the final amount of the buffer gas was admitted, prior to rupturing the diaphragm. This procedure moved the interface between the buffer gas and the test gas approximately 12 inches downstream from the shutter station. This procedure was employed in order to insure that the combustible mixture was far removed from the site of possible reflected shock waves generated at the shutter station. Using this apparatus and procedure, it was possible to transmit incident shock waves through the test gas at Mach Numbers up to about 3.1 without causing ignition by the incident shock wave. The lowest temperatures at which ignition occurred behind shock waves reflected from the end of the shock tube were approximately 800 K. For corresponding pressures the thermal explosion limit temperature is 760 K [1].

Belles and Ehlers [10] conducted experiments with stoichiometric and with near limit mixtures of hydrogen and oxygen at initial pressures of 25 and 50 mm Hg. A simple shock tube without a buffer section, and several different diaphragm materials, including mylar, were used. Consistent data was obtained when the initial test gas

pressure was 25 mm Hg, but excessive scatter occurred when experiments were conducted with stoichiometric mixtures at initial pressures of 50 mm Hg. This erratic behavior did not occur when dilute mixtures were tested at the higher pressure. The authors concluded that a buffer section was needed for the stoichiometric mixture when the initial pressure was 50 mm Hg. The experiments with the stoichiometric mixture at an initial pressure of 25 mm Hg showed that the critical incident shock Mach Number was 2.93. That is, ignition did not occur behind the incident shock wave when its Mach Number was less than 2.93; but if the incident shock Mach Number was equal to or greater than 2.93, ignition occurred and, for sufficiently strong shocks, detonation occurred in the shock tube. The post-shock temperature and pressure associated with the critical shock speed were 780 K and 250 mm Hg, respectively. This temperature compares favorably with the calculated explosion limit temperature at this pressure, which is 810 K. Similar experiments were conducted with several near limit mixtures of stoichiometric hydrogen-oxygen and argon, and hydrogen-air. When the results of these experiments were compared with the predictions of the thermal explosion limit theory [1] for the mixtures concerned, the agreement was poor. Ignition of the hydrogen-air mixture was obtained at temperatures as much as 150 K less than the predicted

explosion temperature, and the hydrogen-oxygen-argon mixtures did not ignite until the temperature was approximately 100 K above the predicted value. Based on these results, Belles and Ehlers conclude that the agreement between the experimentally determined shock ignition temperature and the thermal explosion limit temperature for stoichiometric hydrogen-oxygen mixtures is fortuitous. They explain that there is really no reason to expect that the two ignition temperatures should be the same, because of the great difference in experimental conditions. The "ignition temperature" of a particular combustible mixture is not a unique quantity. The value of the temperature at which the ignition of a particular combustible mixture occurs depends on such factors as the size of the container, the nature of the surface of the container and other solid bodies in contact with the mixture, the type of ignition source used, the rate at which energy is supplied to the mixture, the size of the region to which the energy is supplied, and the existence of forced or free convection currents in the mixture. Ignition occurs when the above factors interact to produce a sufficiently high concentration of chemically active species (free radicals and ions) in a sufficiently large region of the gas, regardless of what the bulk temperature of the mixture may be.

In summary, the references just cited reveal the following information pertaining to stationary combustible gas mixtures which are of interest in the present investigation:

1. Detonation waves can be initiated by externally produced shock waves.

2. In order to avoid spuriously low ignition temperatures, a buffer section must be interposed between the diaphragm and the test gas if the test gas pressure is at or above 50 mm Hg.

3. The minimum shock Mach Number required to produce detonation in a stoichiometric mixture of hydrogen and oxygen at standard temperature in a buffered shock tube is approximately 3, and the corresponding ignition temperature is in the neighborhood of 800 K.

Detonation initiation in flowing gases

Search of the literature revealed only a few cases in which attempts had been made to initiate detonation waves in flowing combustible mixtures, and in none of these cases was an externally produced shock wave used to initiate the detonation.

Jost [11], studying the effects of turbulence on detonation induction distance, successfully initiated detonation waves in mixtures of ethylene and oxygen which were flowing in a 1 inch diameter tube at velocities up

to 100 meters per second. The mixture was ignited by a flame which was injected through a small hole in the side of the tube located several meters from the downstream end. Two detonation waves were produced in each experiment -- one progressing upstream, and one progressing downstream. The results showed that the induction distance for the wave moving upstream was always less than the induction distance for the wave moving downstream. In general, the induction distances for both waves decreased as the flow velocity increased.

Bollinger, et al. [12] conducted similar experiments using several different mixtures of hydrogen and oxygen at flow velocities up to 100 meters per second. Some methane-oxygen mixtures were also tested with flow velocities up to 30 meters per second. Ignition of the gases was accomplished by an ignitor made from a length of .005 inch diameter Pyrofuze wire (a palladium-aluminum alloy) which burned upon the application of a small electric current. The results obtained were qualitatively the same as those obtained by Jost, except that the induction distance for the methane-oxygen mixtures did not change appreciably with flow velocity over the velocity range investigated.

McKenna [13] conducted experiments in which a detonation wave was injected head-on into a stoichiometric mixture of hydrogen and oxygen which was flowing in a

constant area tube. The Mach Number of the flowing mixture was varied from .14 to 4.0. The detonation wave was produced in a stationary mixture of hydrogen and oxygen which was ignited with a spark plug. The results of the experiments showed that the propagation velocity of a detonation wave relative to a subsonic flow was independent of the flow speed -- the wave propagated as a Chapman-Jouget detonation. However, when the detonation wave was injected into a supersonic flow, its propagation velocity relative to the flow increased as the flow velocity increased -- the wave propagated as a strong detonation. This behavior was attributed to the axial pressure profile existing in the tube when the flow was supersonic.

It is felt that reference should also be made to the research on "standing detonation waves" which has been conducted at the University of Michigan and at the Fairchild Engine Division for the last several years. Nichols [14, 15] has summarized the results obtained by both organizations. Workers at both facilities have demonstrated that hydrogen will ignite spontaneously downstream of the Mach reflected shock disc produced aerodynamically in preheated supersonic air streams. At Michigan the reflected shock pattern was produced by a highly underexpanded convergent-divergent nozzle which exhausted into the atmosphere. Hydrogen was injected

into the air stream near the throat of the nozzle, and ignition occurred at some distance downstream of the Mach disc which formed in the free jet beyond the nozzle exit. The distance between the shock and the beginning of the combustion zone was related to the ignition time lag, which was evaluated for a wide range of experimental variables. Successful experiments were conducted with air stagnation temperatures ranging from 1950 to 2600 R and with calculated flow Mach Numbers upstream of the normal shock ranging from 3.5 to 6.2.

The investigators at Fairchild obtained a stationary reflected shock pattern in their combustor by placing it in a supersonic wind tunnel. The oblique shock waves attached to the inlet of the combustor intersected downstream, and produced a normal shock wave across its centerline. Hydrogen was injected upstream of the combustor, and ignition occurred behind the normal shock wave. Experiments were conducted with an inlet Mach Number of 3, and with air stagnation temperatures up to 1060 R.

Both groups of researchers referred to the phenomena produced as "standing detonation waves", but it has been suggested that the terminology "shock induced combustion" would be more appropriate. The author of this dissertation prefers the latter terminology. Regardless of which terminology is preferred, it is noted that this phenomenon differs from the classical detonation wave, at least in

the following respect: The shock wave does not depend upon energy derived from the chemical reaction for its sustenance.

In summary, a review of the literature did not disclose any evidence of prior work in which a detonation wave had been produced in a flowing combustible gas by injecting a pure gasdynamic shock wave into the flow. The present study was conducted in order to explore this untouched region in the domain of detonation research.

Scope of the investigation

The general objective of this investigation was to determine the phenomena which result when a shock wave is caused to move upstream into a flowing combustible gas. More specifically, it was desired to determine the minimum incident shock strength required to initiate a detonation wave in a stoichiometric mixture of hydrogen and oxygen which was flowing subsonically in a constant area tube. Flow nominal Mach Numbers of .2, .5, and .8 were chosen in order to determine the influence of the flow velocity on the minimum incident shock strength required to produce detonation. Some tests were also conducted with an exit Mach Number of approximately zero. Data obtained during these experiments also provided information on the induction distance for those shock waves which were of sufficient strength to initiate a detonation wave.

The remainder of this dissertation is devoted to a description of the test apparatus, instrumentation, and test procedures used; the presentation and discussion of the results obtained; and a statement of the conclusions reached.

II. APPARATUS AND INSTRUMENTATION

Apparatus

Design considerations

The design effort required in this investigation was minimized by the availability of the equipment designed and used by McKenna [13] in his research program. It was only necessary to consider what modifications were required to make the equipment suitable for the present investigation. Information revealed as a result of the literature search indicated that it probably would be necessary to produce shock waves having a Mach Number of 3 or higher, and that a buffer section was required between the main diaphragm and the test gas. The major components of the equipment used by McKenna were the flowing gas detonation tube, the initiator detonation tube, the transition section joining them, and the exhaust duct. A schematic diagram of the final configuration of the apparatus as it was used in this investigation is presented in Figure 1. Since it was desired to initiate a detonation wave only in the flowing gas, McKenna's "initiator detonation tube" was re-named "driver" to be consistent with conventional shock tube terminology. A photograph showing the physical arrangement of the

apparatus is contained in Figure 2. Each of the major components of the system will be described in the following paragraphs.

Flowing gas detonation tube

The flowing gas detonation tube (Figure 3) consisted of a 2 foot long mixing section, followed by three instrumented sections having a total length of 7 feet, and a 1 foot long transition section. The tube was constructed from a length of type 304 stainless steel tubing having an inside diameter of 1 1/2 inches and a wall thickness of 1/2 inch. During the construction of the tube special attention was given to providing for precise alignment of the sections at the flange joints in order to prevent flow disturbances at these locations. Each flange joint was provided with an O-ring seal.

Hydrogen and oxygen entered the upstream end of the mixing section through fittings which were placed 180 degrees apart. This configuration was selected in order to provide a maximum of turbulence and mixing action for the two gas streams. The end plate of the mixing section was provided with a fitting through which purge gas was admitted immediately following each experimental run. Other features which were installed on the mixing section were a chromel-alumel thermocuple, which was connected to the automatic shutdown system, and a static pressure tap.

Two of the three flanged sections were 2 feet long and the third was 3 feet long. Bosses for mounting ionization probes were installed on each of these sections. Five probe mounts were installed on each of the 2 foot sections, and eight were installed on the 3 foot section. These mounting stations were approximately 4 inches apart, except when a flange joint intervened. The location of the probe stations on the inside of the tube was determined to an accuracy of ± .001 inch. The only modification to the flowing gas detonation tube required for this study was the addition of mounting provisions for a heat transfer gage in the same axial plane as each of the ionization probe mounts (18 total). This modification was accomplished by milling a 2 1/16 inch long by 3/4 inch wide flat on the side of the tube, drilling and reaming a .281 inch diameter hole through the tube wall, and drilling and tapping two holes for the gage retention screws. After these operations were completed, the tube sections were honed to a mirror finish in order to remove all surface irregularities caused by the drilling operation. The tube inside diameter was then measured in several locations, and was found to be 1.564 ± .001 inches.

The transition section, which was mounted on the downstream end of the flowing gas detonation tube, diverged conically to an exit diameter of 3.46 inches. The purpose of this section was to guide the flow smoothly around the

end of the driver transition section which was inserted into it 3 inches, and also to minimize the losses experienced by the shock wave as it emerged from the end of the driver transition section.

Driver

The driver was constructed from a 7 foot length of the same material used for the flowing gas detonation tube. When this experimental program was conceived it was not known what incident shock Mach Number would be required to initiate a detonation wave in the flowing mixture. It was felt that the required Mach Number would probably lie between the value required for static mixtures (approximately 3) and that at which a Chapman-Jouget detonation wave propagated in this mixture (approximately 5.5). With air in the driver transition section and helium as the driver gas, the driver pressure ratio required in a simple shock tube for this range of shock Mach Numbers ranges from 45 to 1200 [16, Figure 4.1.1]. Since subsonic flow was selected for the test gas, the pressure in the transition section would be approximately atmospheric. Thus, the pressure required in the driver before diaphragm rupture would be 660 to 17,600 psia. In order to avoid the requirement for such unrealistically high pressures, it was decided to convert the simple driver to a combustion driver in which a mixture of hydrogen, oxygen, and helium was burned, essentially at constant

volume. Hall [16, Figure 4.2.18] indicates that such a driver burning a mixture composed of stoichiometric hydrogen and oxygen plus 80% helium would theoretically produce a shock wave Mach Number of 5.5 with a driver pressure ratio after combustion of 100, and with air as the driven gas. Since the final pressure after constant volume combustion of such a mixture is approximately 7 1/2 times the pressure before combustion [16, Figure 4.2.8], it can be seen that the initial pressure requirement of such a device would be quite reasonable. The modifications to the driver were based on information reported by Hall [16, Figure 6.2.5] and by Nagamatsu and Martin [17].

Preliminary tests using the combustion driver to inject shock waves into a flowing mixture of hydrogen and oxygen showed that the original estimates of the difficulty of producing detonation waves in such a mixture were greatly overestimated -- it was not feasible to produce a shock wave with this driver which was weak enough not to cause essentially immediate detonation in the flowing gas. Therefore, the combustion feature of the driver was abandoned, and it was used as a simple driver, pressurized with room temperature helium, and equipped with a mylar diaphragm in all subsequent experiments. A photograph of the driver, installed in the exhaust duct, is presented in Figure 4.

Exhaust duct

The purpose of the exhaust duct was to provide a means of collecting the combustible gas as it flowed out of the transition section, diluting it with air, and conducting the mixture to the exit of the test cell. The exhaust duct was originally a 10 foot long, 12 3/4 inch outside diameter, 3/16 inch wall thickness, stainless steel cylinder, with two access ports cut near one end. For use in this investigation, the duct was modified by cutting it into sections, as shown in Figures 4 and 5. This modification was accomplished in order to make the driver and diaphragm station more accessible. A diametrical cut was made along the axis of the duct for approximately 7 feet, at which point a 180 degree circumferential cut was made. Stainless steel 90 degree angles were welded along the axial edges of both sections. In the run configuration, the angles were clamped together with vise-grip pliers. An effective seal along these surfaces of contact was provided by a strip of rubber, which was cemented to the bottom section. Safety cables, anchored to I-beams in the floor of the test cell, were provided after it was learned that detonations occurring in the system at moderate to high mass flow rates were capable of breaking all of the vise-grip pliers, and lifting the heavy exhaust duct cover into the air.

Dilution of the combustible gases entering the exhaust duct was accomplished by a blower (shown in Figure 2), which delivered 1500 standard cubic feet of air per minute, and a high pressure compressed air trailer, which could deliver up to 4000 standard cubic feet of air per minute.

Inert section

A 2 foot long section, equipped with a diaphragm retention capability at both ends was interposed between the driver and the driver transition section. This section was constructed from the same type of material used in the other tube sections, and its outside and inside diameters, respectively, were made identical to those of the other sections. This section, which was filled with helium during the combustion driver tests, and air for all later tests, was required for several reasons: (1) during the combustion driver tests, it provided an inert medium in which any residual combustion reactions would be quenched before they reached the test gas, (2) for all tests it provided a means of isolating the main diaphragm opening process from the test gas, (3) it provided a sufficient length for the shock wave to become fully formed before it entered the region occupied by the test gas, and (4) it provided space for mounting instrumentation required for the determination of the incident shock wave speed.

Driver transition section
exit diaphragm

Some preliminary cold flow tests were conducted to determine how far hydrogen would penetrate into the open-ended driver-transition section during time intervals comparable to normal run times. The exit diaphragm of the inert section was not installed for these tests. Several gas samples were extracted at different locations while using various hydrogen-oxygen flow rates and sampling times. The samples were qualitatively analyzed with a gas chromatograph. The results showed that an appreciable concentration of hydrogen extended at least as far as 14 7/8 inches beyond the entrance to the driver transition section, even at the lowest contemplated hydrogen-oxygen flow velocity, and only 5 seconds after the flow had been initiated. Consideration of these results led to the decision to install a diaphragm at the exit of the driver transition section. The exit diaphragm retaining mechanism is shown in Figure 6. The requirement imposed on the diaphragm material was that it be the weakest material which could withstand the flow pressures for a 10 second period without breaking. After testing several types of paper and plastic materials, graph paper (tracing paper grade) was found to be suitable for the .2 and .5 Mach Number flows, but the .8 Mach Number flow required the use of .003 inch thick mylar.

Gas supply and control system

The major portion of the gas supply and control system used in this investigation had been in operation for several years. A description of the facility and the operating procedures are contained in [18]. Slight modifications to the system were required for this investigation; for example, the addition of the driver helium supply and control system. A schematic diagram of the complete gas supply, control, and metering system is contained in Figure 7. Both hydrogen and air were supplied from 38 cylinder high pressure gas trailers. The oxygen, nitrogen, and helium were supplied from standard high pressure bottles. The oxygen and nitrogen bottles were connected to manifolds in order to provide the desired mass flow rate capacity for each gas. The helium bottles were connected directly to the driver fill lines. One helium bottle, usually at a low pressure, was used to preload the driver to an intermediate pressure, and two high pressure bottles were used to accomplish the final pressurization and rupture of the diaphragm. The nitrogen was used to purge the hydrogen and oxygen supply lines, and as a pressurizing medium for the dome pressure regulators.

Each of the test gases (hydrogen and oxygen) entered the test cell from its source at high pressure, and passed through a dome pressure regulator, which delivered an output pressure corresponding to the nitrogen pressure

which was preset in the dome by means of a dome loader located in the control room. After leaving the pressure regulators, the gases passed through Herschel venturi flow meters, manually operated isolation valves, solenoid operated shutoff valves, check valves, and then entered the mixing section of the flowing gas detonation tube. The air control system was similar to the other two, except that the dome loader for its pressure regulator was located in the test cell, and two solenoid valves were used. One valve controlled the admission of air into the upstream end of the exhaust duct, and the other admitted air into the upstream end of the mixing section of the flowing gas detonation tube.

The system incorporated an automatic shut-down feature which stopped the flow of hydrogen and oxygen, initiated the nitrogen purge, and admitted air into the mixing section when an electrical signal was received from either of two sources. The primary shut-down signal was delivered by a pressure transducer located in the inert section, which sensed the passage of the incident shock wave. A secondary, or back-up signal was provided by a thermocouple located in the mixing section, which was connected to an adjustable meter relay located in the control room. This secondary system provided an automatic shut-down capability in the event of malfunction of the primary system, or in the event of spontaneous combustion or detonation not

involving the passage of a shock wave over the pressure transducer. The flow could also be stopped by manual operation of the proper electrical switches, if desired.

Except for the manually operated gas cylinder valves and isolation valves, all other components of the combustible gas supply and control system were operated remotely from the safety of the control room. A photograph of the control room, showing the flow control panel and the data recording equipment, which will be discussed in the next section, is presented in Figure 8.

Instrumentation

The instrumentation used in this investigation can be classified into two functional groups: (1) that which was used in determining the mass flow rates and flow conditions in the flowing gas detonation tube; and (2) that which was used for determining wave speeds. Each of these two groups will be discussed in the following sections.

Mass flow rates and flowing gas parameters

Herschel venturi meters were used to provide data required for the calculation of the hydrogen and oxygen mass flow rates. The location of these venturi meters is shown schematically in Figure 7. Strain gage type pressure transducers were used to measure the flowing

gas static pressure upstream of the meters, and the pressure drop across the meters. Iron-constantan thermocouples were used to measure the temperature of the flowing gas upstream of the meters. The output from each of the pressure transducers was fed into a Consolidated Electrodynamics Corporation (CEC) Type 1-113B amplifier. The amplified signals were supplied to an 18 channel CEC oscillograph where they were recorded as a function of time. The output voltages from the thermocouples did not require amplification; therefore, they were directed through the required external damping resistances to the galvanometers in the recorder.

Two additional iron-constantan thermocouples were installed in the system to indicate the temperature of each gas just prior to its entry into the mixing section of the flowing gas detonation tube. Also, a sensitive pressure transducer was used to measure the static pressure of the gas mixture at the exit of the mixing section. This transducer was protected from overpressurization by the high pressures behind the detonation waves by a Statham Model S-214 gage saver, which was installed in the line between the pressure source and the transducer. Signals from these thermocouples, and from the pressure transducer, were also recorded by the oscillograph, making a total of 5 pressures and 4 temperatures which were recorded.

Wave speeds

Instrumentation was selected which provided data from which the speed of the incident shock wave, the transmitted shock wave, and the detonation wave could be determined. A block diagram showing the equipment used to obtain this wave speed data is presented in Figure 9. All components except the oscilloscopes were located in the test cell. The oscilloscopes were located in the control room (Figure 8). Each oscilloscope was equipped with a Tektronix Model C-12 oscilloscope camera with a Polaroid roll film back.

Incident shock wave speed. - The speed of the incident shock wave was determined from the signals produced by two Kistler quartz crystal piezoelectric pressure transducers which were mounted in the inert section. A photograph showing the installation of these transducers is presented in Figure 10. The first transducer was located 13 1/2 tube diameters from the diaphragm, and the distance between the centers of the transducers was 5.012 ± .001 inches. These transducers were used in conjunction with Kistler Model 566 electrostatic charge amplifiers, which accepted the electric charge output from the transducers and converted it into a voltage. This voltage was then amplified and made available at the output of the amplifier. In this installation the

amplified output from the first transducer (the one nearest to the diaphragm of the driver) was applied to the external trigger circuit of a Tektronix Model 551 dual beam oscilloscope, which was adjusted to provide a single horizontal sweep of the electron beams. The amplified output of the second transducer was applied to the vertical deflection input for the upper beam of the oscilloscope. Thus, when the incident shock wave passed the first transducer, a signal was generated which started the horizontal sweep of the oscilloscope's electron beams. When the shock wave passed the second transducer, a signal was generated which caused an almost vertical deflection of the upper beam trace. The oscilloscope camera was adjusted so as to obtain a photograph of the path of the electron beam. The time required for the shock wave to traverse the distance between the two transducers is related to the distance measured on the photograph from the beginning of the upper beam trace to the point of vertical deflection of the beam. (Sample calculations are presented in the Appendix.)

A Fairchild Instruments Corporation, Model 781A, time mark generator provided the time base reference for all three of the oscilloscopes. The accuracy of this time mark generator was checked using a digital counter which could be read to one-tenth of a microsecond. This counter was maintained as a secondary standard by the

Physics Department at AFIT. Based on this comparison, the output of the time mark generator was correct to within ± .1%.

Transmitted shock wave speed. - Two thin film platinum heat transfer gages provided the signals which were used to determine the transmitted shock wave speed. These two gages were installed near the exit of the flowing gas detonation tube, upstream from the transition section. The gages were installed approximately in the same planes as were the first two ionization probes, and the distance between their centers was 4.005 ± .001 inches.

A photograph showing the components of a heat transfer gage is presented in Figure 11. The sensitive element of the heat transfer gage was a thin film of platinum, having a nominal resistance of 50 ohms, which was painted and baked on one edge of a quartz disc. The details of this process have been reported by Frye [19]. The edge of the disc on which the platinum was applied was ground and polished to a radius of .786 inches so that it could be mounted flush with the inside wall of the flowing gas detonation tube. After the platinum film and the electrical leads were attached to the disc, it was cemented into the slot in the brass gage holder with Sauerisen cement. An O-ring seal was provided at the base of the gage holder to prevent the leakage of high temperature gases around the sides of the gage element. A phenolic

insulator was installed between the top of the gage holder and the aluminum "Minibox". The Minibox was used to provide a secure mounting place for the required electrical terminals. A schematic diagram of the gage electrical circuit is presented in Figure 12. A 24-volt wet cell battery was used as the power source for the gages.

The principle of operation of the heat transfer gages, as used in this application, is as follows: A steady state current is established in the circuit composed of the battery, the 1000 ohm resistor, and the gage element. Thus, under ambient conditions there is a certain voltage drop across the thin film element, which depends on its temperature, since its resistance depends on its temperature. When a shock wave passes the gage element, it experiences a step increase in temperature and, therefore, resistance. This step increase in resistance causes a step increase in voltage drop across the thin film. (The response time of the film is of the order of the time it takes the shock wave to pass over the film.) This change in voltage drop across the platinum film is amplified by the heat transfer gage signal amplifier, and then is applied to a pulse forming circuit. The resulting voltage pulse is displayed on an oscilloscope.

A circuit diagram for the heat transfer gage signal amplifier and pulse forming circuit used in this investigation is presented in Figure 13. This circuit has two

features which make it especially desirable when the signals from two or more heat transfer gages are displayed on one oscilloscope. Heat transfer gages are quite sensitive to electromagnetic "noise", and tend to give an output when nearby electrical equipment, such as a solenoid valve, is actuated. This circuit has a sensitivity adjustment, which can be set so that the pulse forming circuitry will not respond to any input signals below a desired value. The second feature of the circuit is that once an output pulse has been generated, the output circuit will not produce another pulse for approximately 1000 microseconds. The duration of this cut-off period depends somewhat on the strength of any subsequent input signals, which may be generated by reflected waves, a combustion zone, or the contact surface. These two features make it possible to obtain noise free traces on the oscilloscope. Of course, the heat transfer gage output signal must be greater than the noise level which is rejected, or no output pulse will be obtained. This situation is possible with weak shock waves, or with heat transfer gages with excessively low resistance.

The oscilloscope used to display the signals from the heat transfer gages was a Tektronix Model 545B which had the Tektronix Raster Modification incorporated at the factory. The raster modification makes it possible

to extend the horizontal sweep time by folding the trace back and forth in a zig-zag fashion from the bottom to the top of the cathode ray tube. This feature permits the use of faster sweep speeds, which make possible more accurate measurements of time intervals from pictures of the oscilloscope trace. Also, the time of triggering of the oscilloscope sweep becomes less critical, since a longer time interval is available for observation of the trace. This oscilloscope was equipped with a vertical amplifier plug-in unit (Tektronix Type D) which accepted two input signals, and the leads could be connected so that a positive input voltage would move the electron beam either up or down. By making use of this feature, the pulse from the first heat transfer gage was pointed down, and the pulse from the second one was pointed up. In this way it could be determined from which gage a pulse originated. In this investigation this oscilloscope was adjusted to provide a single sweep upon the application of an external trigger signal, which was obtained from the oscilloscope used to record the incident shock speed data. The availability of this trigger signal coincided with the beginning of the horizontal sweep of the latter oscilloscope. The oscilloscope camera was used to record the data.

Detonation wave speed. - The speed of the detonation wave was determined from the signals produced by single

electrode ionization probes. Eighteen of these probes were spaced along an 80 inch length of the flowing gas detonation tube so that the speed of the wave could be determined as it progressed along the tube. The spacing between the probes was determined to within ± .001 inch. The probe installation is shown in Figure 3. The configuration of these probes was that developed by McKenna [13]. A photograph showing some details of this probe design is presented in Figure 14. A length of .032 inch diameter stainless steel wire served as the electrode. This wire was inserted into a length of Teflon "spaghetti", which served as an insulator. The wire and insulator were retained in the cylindrical housing by frictional forces caused by tightening the set screw, which compressed the teflon sleeve against the insulator. Internal and external sealing was accomplished by means of rubber O-rings. The length of the probe which projected beyond the bottom of the cylindrical housing was adjusted so that, when installed in the detonation tube, the end of the probe was flush with the inside surface of the tube. The assembly was retained in the boss welded to the detonation tube by the threaded fitting shown on the right. A length of plastic tubing was used to provide rigidity to that portion of the probe wire which extended beyond the fitting. When the probe was installed on the tube,

the gap between the end of the electrode and the tube wall, which served as the second electrode, was approximately .019 inches.

The electrical circuit used with the probes was similar to one recommended by Gaydon and Hurle [20]. A schematic diagram of the circuit used is presented in Figure 15. Power was supplied to this circuit by a Hewlett-Packard Type 712A, 0-500 volt, direct current power supply, shown in Figure 2. The circuit operated as follows: When power was applied to the circuit the gap between the probe and the tube wall was not conductive, so the only action that took place was the charging of the capacitors. When the detonation wave (or any zone of combustion) passed over the end of the probe, the gap was filled with a conductive medium, due to the ions and free electrons present in the reaction zone. When the gap became sufficiently conductive, the capacitor discharged through the series circuit composed of the load resistor, the probe gap, and the diode, producing a voltage pulse across the load resistor. This voltage pulse was the output signal, and it was directed to an oscilloscope, where it caused a vertical deflection of the electron beam. With the probes connected in parallel, as shown, the diode was necessary to prevent the shorting of the output signals from all of the probes except the first one.

The oscilloscope and camera used to record the signals from the ionization probes were identical (except a Tektronix Type G Plug-In Unit was used) to the equipment used for recording the heat transfer gage signals. The oscilloscope was adjusted to provide a single sweep of the electron beam upon receipt of an external trigger signal. The trigger signal was obtained from the front panel of the other Type 545B oscilloscope. The output circuit for three of the probes (numbers 1, 6, and 12) was connected to the oscilloscope so that the pulses they produced caused an upward deflection of the trace. All of the other probes produced a downward deflection of the trace. This arrangement provided a means of determining the direction of travel of the wave, and also made it possible to identify a malfunctioning probe, if necessary.

III. EXPERIMENTAL PROCEDURE

The experimental procedures discussed in this section pertain to the experiments in which the final configuration of the apparatus was used. The procedures used during the development of the apparatus have been omitted.

Calibration

All of the instrumentation used for the determination of the mass flow rates and flow parameters was calibrated before any experiments were conducted with flowing gases. A dead weight tester was used for calibrating the pressure transducers used in the hydrogen system. The dead weight tester was not considered suitable for calibration of the transducers used in the oxygen and mixed gas systems because of possible contamination of the transducers with hydraulic oil, the pressurizing medium used by the tester. Instead, pressure was applied to these transducers with gaseous nitrogen. The magnitude of the applied pressures was read on precision laboratory pressure gages which were accurate to within 1% of full scale. Three gages with pressure ranges of 0-15, 0-100, and 0-1000 psig, respectively, were used, as applicable. A mercury manometer was used as the pressure reference when calibrating

the pressure transducers used for measuring the static pressure drop in the flowing gas detonation tube. The output of each of the transducers was recorded by the oscilloscope recorder. Calibration curves of applied pressure vs recorder trace deflection were prepared from this data for each of the data channels, which consisted of the specific transducer, electrical cables, amplifier, and galvanometer used during the calibration. These components were used as a unit thereafter.

An electrical calibration of the amplifiers used with the pressure transducers was accomplished daily. In this procedure, the gain of each amplifier was adjusted so that the galvanometer deflection caused by an internal calibration resistor was the same as it was at the time of calibration of the system. The validity of the calibration curves was spot-checked frequently, and only one transducer required complete recalibration during the course of the experimental program.

The calibration of the thermocouples was accomplished by recording the galvanometer trace deflections when the thermocouples were immersed in water at various temperatures. The water temperature was determined with a mercury-in-glass thermometer, which was read to the nearest degree Fahrenheit. Calibration curves of temperature vs galvanometer trace deflection were prepared from this data.

The curves were linear, and were extrapolated for use when the measured temperatures were below 32 F.

After the calibration of the instrumentation was completed, a series of experiments was conducted to determine the pressures required in the domes of the hydrogen and oxygen pressure regulators in order to obtain the desired mixture ratio and flow Mach Numbers at the exit of the flowing gas detonation tube. During these experiments, the pressure drop across the instrumented portion of the tube was measured. This measurement was accomplished after temporarily converting the ionization probe mounting station nearest the exit to a static pressure port. A differential pressure transducer was connected between this station and the pressure tap located at the end of the mixing section. Data obtained in this series of experiments was used to prepare curves of mass flow rate vs dome pressure for each of the test gases. This data also made it possible to calculate the friction factor of the flowing gas section under the flow conditions actually existing in the tube at the desired flow Mach Numbers. The friction factors were required in order to calculate the flow velocities at various points in the flowing gas section. The data reduction and other calculations are described in the Appendix.

The time base of each of the oscilloscopes was calibrated by taking a photograph of a single sweep of the

electron beam with the output of the time mark generator applied to the vertical input. A scale factor, expressed in terms of microseconds per inch, was determined from measurements taken from the photograph using a comparator, which could be read to four decimal places. This calibration was accomplished daily, because of the desire to obtain the various wave speeds as accurately as possible.

The input sensitivity of the heat transfer gage amplifiers was also checked daily. A square wave calibrating voltage obtained from the oscilloscope used to record the heat transfer gage signals was applied to the input of the amplifiers, one at a time, and the input sensitivity potentiometer was adjusted until the desired response was obtained. For most of the experimental runs the amplifiers were adjusted so that they produced an output pulse when a 2 millivolt peak-to-peak signal was applied to the input, but produced no output when a 1 millivolt signal was applied. Toward the end of the experimental program when weaker shock waves were used, this setting had to be changed to 1 and .5 millivolt, respectively, in order to obtain signals from the heat transfer gages.

Since the Kistler pressure transducers were not used for quantitative data, but just as event markers, they were not calibrated.

Some non-flow experiments were conducted to determine the effect of the driver transition section exit diaphragm on the strength of the transmitted shock wave. The transmitted shock speed was measured for a range of incident shock speeds, both with and without the exit diaphragm in place. In these experiments air was in both the inert and the flowing section. These experiments showed that the exit diaphragm had a negligible effect on the strength of the transmitted shock wave for the range of incident shock speeds tested. Based on the results, no correction was made to the incident shock wave speed to account for the present of the exit diaphragm.

The test program

It was initially planned to conduct tests at flow nominal Mach Numbers of .2, .5, and .8, but an additional series of tests with no flow velocity in the flowing section was added to the program. The tests were conducted in the following sequence of flow Mach Numbers: .2, .5, 0, and .8. A series of tests, in which the incident shock wave speed was varied, was conducted at each flow Mach Number. The incident shock speed was varied by using diaphragms of different thicknesses in the driver. Mylar was used as the driver diaphragm material for all tests except the preliminary tests using

the combustion driver. The following diaphragm thicknesses were available: .001, .002, a limited number of .0022, and .005 inches, respectively. By combining the available thicknesses in various ways, tests were conducted with diaphragm thicknesses as follows: .002 combination and solid, .003, .004, .005 combination and solid, .0052, .006, .010, and .015 inches, respectively. In the normal operation of the driver it was evacuated to a pressure of approximately .1 inch of mercury before being filled with helium. Additional variation of the incident shock wave speed was effected by not evacuating the driver for a portion of the runs. The higher molecular weight of the resulting mixture of air and helium resulted in the production of a weaker shock wave than that produced with the same diaphragm thickness when the driver was evacuated before filling. In all tests the diaphragms were preloaded to a pressure of approximately one-half of their breaking pressure prior to the initiation of the flow.

The following procedure was used in conducting the experiments with no flow in the flowing gas section: A flow of hydrogen and oxygen was established in the tube under the conditions required to produce a Mach Number of .2 at the exit; the solenoid valves in the feed lines were then closed, which terminated the flow without initiating a purge of the system; the dilution air flowing

into the exhaust duct was cut off at the same time, and approximately five seconds later the diaphragm was broken. This procedure was employed because it was desired to make these tests without changing the configuration of the detonation tube or transition section in any way. This restriction was imposed so that the results obtained could be compared with those obtained when the combustible gas was in motion. It was necessary to establish a flow in the tube in order to effect mixing of the gases.

Operation of the flowing gas detonation system

The gas flow control and instrumentation systems used in this investigation were composed of many components, each of which had to operate in the proper sequence in order to produce a one hundred percent successful run. A detailed operational check list was prepared, and was used during all experimental runs in order to insure that no required step was overlooked. A brief description of the sequence of operations is presented in the following paragraphs.

In preparing the test equipment for an operational run, the first action was to turn on the power to all three oscilloscopes, the time mark generator, all amplifiers, the ionization probe power supply, and the oscillograph recorder. All of this equipment required a minimum

of 30 minutes of warm-up time in order to insure stable operation. During this time the shut-off valves for the proper number and type of gas supply bottles were opened, and the manifold and isolation valves were opened. A resistance check was performed on all ionization probes and heat transfer gages, and the heat transfer gage power was turned on. After the equipment was warmed-up the transducer bridge circuits were balanced, the amplifier gains were checked, and adjusted if necessary, the proper attenuations were set, and the recorder zero signal traces were obtained. The barometric pressure was read and recorded prior to each run. Next, the heat transfer gage amplifier input sensitivities were adjusted. Then the oscilloscopes were checked for the proper sweep and gain settings, a time base calibration photograph was taken for each oscilloscope, and the trigger levels and stability adjustments were set and checked. These operations readied the instrumentation for an experimental run.

The driver was then prepared for the run. The proper exit and main diaphragms were installed, and the exhaust duct cover was secured. The driver vent valve was closed, the driver was evacuated, if desired, and then the diaphragm was preloaded with helium. The dilution and purge air pressure regulator dome pressure was set, and the test cell ambient temperature was recorded. The system

was now ready for the flow to be initiated, and all subsequent operations were conducted in the control room. The pressure regulator dome pressures were set, and the blower was turned on. The following steps were performed in a fairly rapid sequence: The camera shutters were opened, the recorder paper drive was started, the exhaust duct dilution air flow was started, the hydrogen-oxygen flow switch was turned on, the automatic shutdown circuit was armed, the oscilloscope sweep circuits were armed, and then the diaphragm was broken by admitting additional helium. The automatic shutdown system was actuated by the shock wave. The nitrogen and air purge and dilution flows were stopped manually, the recorder was stopped, the camera shutters were closed, and all switches were returned to their pre-run positions. The pictures were then removed from the oscilloscope cameras, and were inspected to see if the instrumentation had operated properly. The oscillograph recording was also scrutinized in order to ascertain that all flow associated instrumentation had performed satisfactorily. Since a loud report was associated with every detonation wave, it was not necessary to look at the data to know whether detonation had occurred or not.

IV. RESULTS AND DISCUSSION

Results

Several experiments of a preliminary nature were made early in the experimental program. The primary result of these experiments was the evolution of the configuration of the experimental apparatus and instrumentation to that which has been described previously, and the determination of the friction factor (f) of the flowing gas section. The tube friction factors were .0048, .0041, and .0032 for near stoichiometric mixtures of hydrogen and oxygen flowing at exit Mach Numbers of approximately .2, .5, and .8, respectively. All of the remaining results presented in this section were obtained after the final modification had been made. As noted earlier, this set of apparatus involved a large number of components, all of which (including the operator) had to function correctly in order to produce a 100% successful run. As might be expected, the reliability of the overall system was not 100% -- there were many malfunctions of one sort or another during the experimental program. The component which malfunctioned most often was the heat transfer gage. Over 50 of these gages were expended during the entire program. The result of

the failure of one of the heat transfer gages to function properly during a run was that the transmitted shock wave speed was not available for that run. In order for a run to be considered partially successful it was necessary to obtain, as a minimum, steady state mass flow rate data, the incident shock wave speed, and audible (or ionization probe) evidence of whether there was a detonation or not. A run for which any of the above elements was missing was not considered further. Under this criteria a total of 66 partially to completely successful runs were made. Since the experimental results could be expected to depend somewhat on the mixture composition, an arbitrary hydrogen molar composition limit of 66.67 ± 2% was established. When this criteria was applied, it was found that the hydrogen composition of 3 of the above runs was not acceptable, leaving a total of 63 runs for which data are presented in this section. Of these 63 runs, seven were conducted with the flowing gas exit Mach Number (M_{Exit}) essentially 0, twenty-three with M_{Exit} at approximately .2, twenty-two with M_{Exit} at approximately .5, and eleven with M_{Exit} at approximately .8. Transition to detonation occurred on thirty-four of these runs.

Oscilloscope trace pictures typical of those obtained on a run during which detonation did not occur are presented in Figure 16. In these pictures the oscilloscope

sweep starts on the left (and at the bottom of the pictures showing the presentation of the raster trace). Note that when detonation does not occur there is no output from the ionization probes. Figure 17 presents typical pictures for a run in which detonation did occur.

The reduced data for the 63 acceptable runs are presented in Tables 1 through 4, for the flow exit nominal Mach Numbers of 0, .2, .5, and .8, respectively. These data are presented graphically in Figures 18-20.

Figure 18 is a graph of the incident shock wave Mach Number (M_{SI}) vs the Mach Number of the flowing mixture near the exit of the flowing section (M_{Exit}). The parameter M_{SI}, instead of M_{SE}, was chosen for the ordinate of this graph because it was more representative of the energy input to the flowing gas for the runs in which detonation occurred. This fact will be obvious after inspection of Figures 19 and 20, which will be presented next. Results from all 63 runs are included in Figure 18. The curve is drawn through the points representing the minimum incident shock wave Mach Numbers above which transition to detonation always occurred. There was some overlap in the data for the .2 Mach Number flow, but none was evident for the other flow conditions. The curve was extrapolated so as to intersect the ordinate ($M_{Exit} = 0$) at an incident shock wave Mach Number

of 2.93, the value reported by Belles and Ehlers [10] for a stationary stoichiometric mixture of hydrogen and oxygen. (Rigorously speaking, the incident shock wave Mach Number of 2.93 of Belles and Ehlers should be compared with M_{SE} instead of M_{SI}, since M_{SI} was based on the speed of sound in air, whereas the other two Mach Numbers were based on the speed of sound in the hydrogen-oxygen mixture; however, as noted below, M_{SI} did not differ appreciably from M_{SE} for the runs in which detonation did not occur.) This curve shows that the incident shock wave Mach Number required to produce a detonation wave in a flowing stoichiometric mixture of hydrogen and oxygen was considerably less than that required for a stationary mixture and, more significantly, that the minimum value required decreased as the flow Mach Number increased. No detonations were produced in the stationary mixture by incident shock waves having Mach Numbers up to 2.62, but detonation always occurred for incident shock wave Mach Numbers greater than 2.12 for the $M_{Exit} = .2$ flows; 1.75 for the $M_{Exit} = .5$ flows; and 1.56 for the $M_{Exit} = .8$ flows. Incident shock wave Mach Numbers greater than 2.62 could not be produced with the diaphragm materials available.

Comparison of M_{SI} and M_{SE} values listed in Tables 1-4 for runs in which detonation did not occur showed that the net effect of the exit diaphragm, the area change

in the transition section, and the change from stationary air to the flowing hydrogen-oxygen mixture was to decrease slightly the value of the wave Mach Number. The decrease ranged from 0% for Run 64 to a maximum of 10.1% for Run 30. For the runs in which detonation occurred, M_{SE} was affected by the detonation before the shock wave reached the location of the heat transfer gages, (except for Run 85 which is discussed separately), and thus M_{SE} was not representative of the initial energy input to the flowing gas for these runs. These results are illustrated in Figures 19 and 20.

In Figure 19 a graph of the Mach Number of the shock wave at the exit of the flowing section (M_{SE}) vs the Mach Number of the incident shock wave (M_{SI}) for $M_{Exit} = .2$ is presented. This graph shows that M_{SE} was always slightly less than M_{SI} unless detonation occurred, and that when detonation did occur, M_{SE} was transformed from the relatively low M_{SI} to a high value by the time the wave reached the speed measuring station, which was located 14 1/2 inches from the exit of the driver transition section. The maximum M_{SE} observed without detonation was 1.99. There was no intermediate value of M_{SE} between 1.99 and 5.32. For runs in which detonation occurred, M_{SE} increased to a maximum value of 6.11 for an M_{SI} of 2.12, and then decreased as M_{SI} was increased.

A graph of M_{SE} vs M_{SI} for M_{Exit} = .5 is presented in Figure 20. This graph shows that for the M_{Exit} = .5 flow, the maximum M_{SE} observed without detonation was 1.68. The sharp peak exhibited by M_{SE} when detonation occurred with M_{Exit} = .2 was not observed when M_{Exit} = .5; instead, the values seem to follow a general downward trend, although there was some scatter. The maximum M_{SE} observed was 5.87, which occurred for an M_{SI} = 1.77, which was just slightly greater than the minimum required to initiate detonation (1.75).

There was insufficient reliable heat transfer gage data obtained with M_{Exit} = 0, and .8, respectively, to warrant the preparation of graphs of M_{SE} vs M_{SI} for those cases.

Graphs showing the flow velocity and the detonation wave velocity vs position in the flowing gas section are presented in Figures 21-54. The abcissa scale located at the bottom of the graphs applies to both of the curves. The zero point on the abcissa coincides with the plane of the ionization probe nearest the exit of the flowing gas section, which was 12 1/2 inches from the driver transition section exit diaphragm. The speed of the transmitted shock wave relative to the flowing mixture at the exit station (V_{SE}), when available, was also shown in these graphs. These graphs are grouped according to M_{Exit}, and within a particular group they have

been arranged in a sequence of increasing M_{SI} in order to facilitate comparison. The hydrogen content of the mixture and the theoretical Chapman-Jouget detonation wave velocity (V_{C-J}), along with M_{Exit} and M_{SI} have been listed on each of the graphs. The flow velocity curve was obtained by joining the calculated values of flow velocity at five positions along the flowing gas section with a smooth curve. This curve was used to obtain the values of flow velocity at intermediate positi . in the flowing gas section which were added to the measured detonation wave velocity relative to the tube in order to convert it to a velocity relative to the flowing gas. The points plotted for the detonation wave velocities represent average values obtained by dividing the distance between two probes by the time it took the wave to move between them. The value so obtained was plotted at the midpoint between the appropriate probes. Thus, the line drawn in the vicinity of these points has no physical significance other than to indicate a possible trend among these discrete average values. When a definite up or down trend in the points was not apparent, a "best" straight line was located visually so as to minimize the distance of the maximum number of points from it.

A startling result obtained on 5 out of 12 of the initial runs attempted at the $M_{Exit} = .8$ flow condition

was that spontaneous detonation occurred. This phenomenon was also observed by McKenna [13] in some of his experiments at high subsonic flow Mach Numbers. These spontaneous detonations occurred during runs which were being conducted to determine a suitable material for the exit diaphragm for the $M_{Exit} = .8$ series of runs. Due to the nature of the tests being conducted, the wave speed instrumentation was not activated for the first two of these runs; however, it was activated on all later runs, and wave direction and speed data were obtained in three of the five cases. On these runs the ionization probe oscilloscope was set for internal triggering, and the sweep was triggered by the first ionization probe to give an output. In all three of these runs the data showed that the detonation wave passed the ionization probe nearest the flow exit first, and that it moved upstream from that point. On the first of these three runs, and on the two previous runs, the detonation occurred during the flow start transient before steady mass flow rate data was produced. In the last two of these five runs both wave speed and steady mass flow rate data were obtained. These two runs were designated 011 and 012. Pictures of the ionization probe output for these two runs are presented in Figure 55, and the reduced data for these runs is presented in Table 4, and in Figures 53 and 54. These figures show that in both runs the detonation wave

velocity was very unsteady as the wave moved through the tube. With but one exception (Figure 48) such unsteadiness in the detonation wave velocity was observed only when the transition to detonation was produced by incident shock waves which were close to the minimum strength required to cause detonation.

Thirteen runs were accomplished without spontaneous detonation after lengthening the flow starting transient and reducing the total mass flow rate from approximately .65 lb_m/sec to approximately .58 lb_m/sec, which resulted in a reduction of the flow Mach Number from approximately .8 to approximately .78.

Of all the runs conducted, Run 85 deserves special mention. Figure 56 contains the oscilloscope pictures obtained on this run. It is noted that M_{SE} was quite low (1.49), but the ionization probe output shows that a detonation occurred. Analysis of these pictures showed that the detonation wave did not reach the first ionization probe until 434.9 microseconds after the shock wave passed the first heat transfer gage, which was located essentially in the same plane. Assuming a constant shock wave speed during this time, the shock wave was 6.2 inches ahead of the reaction zone at the time it (the reaction zone) reached the first ionization probe. This run was the only one in which detonation produced by the incident shock wave had not accelerated the transmitted shock wave

to a Mach Number greater than 5 before the shock wave had reached the heat transfer gage speed measuring station. Figure 49 contains a plot of the detonation wave velocity for this run. Note that the initial velocity of the wave was 10,600 ft/sec (compared to a V_{C-J} of 9514 ft/sec), and that the incident shock Mach Number was 1.56, the lowest M_{SI} at which a detonation was produced (excluding the runs in which spontaneous detonation occurred, in which M_{SI} was 0). This same M_{SI} occurred on Run 87 (Figure 50) with quite ordinary results.

Discussion

It is felt that the most significant results obtained in this investigation are those contained in Figure 18, which shows the effect of the flow Mach Number on the strength of the incident shock wave required to produce a detonation wave in a flowing stoichiometric mixture of hydrogen and oxygen. All other results obtained, which will be discussed first, are of the nature of supporting evidence.

First of all, Figures 21-54 present conclusive evidence that a detonation wave was formed in the flowing mixture during the experimental runs for which the data apply. In all cases the reaction zone velocity, as determined from the ionization probes and the calculated flow

velocity, reached over 9000 ft/sec with respect to the combustible gas ahead of the wave. The sequence in which the ionization probes became conductive (shown on the picture of the oscillograph trace) demonstrated conclusively that the detonation waves always formed downstream of the ionization probe nearest the exit of the flowing gas section, and that the wave then moved upstream into the flowing combustible mixture which was flowing at velocities ranging from 340 to more than 1300 ft/sec. These flow velocities are higher than any yet reported in which a true detonation wave has been initiated by any means. Comparison of the characteristics of the detonation waves produced in the flowing mixture reveals that they possess many of the characteristics of detonation waves produced in stationary gases. For example, Berets, Greene, and Kistiakowski [21] reported that the experimentally determined steady detonation velocities in stationary stoichiometric mixtures of hydrogen and oxygen were found to be 1 to 2% less than the theoretical Chapman-Jouget velocity, depending on the diameter of the detonation tube. Many of the aforementioned figures, for example, Figures 22, 24, 25, 26, ..., show that steady detonation velocities were achieved which are within the experimental error of these reported values. In addition to the wave velocity, the detonation waves produced in this investigation exhibit the same

characteristics reported by Berets, Greene, and Kistiakowski [6] when the strength of the initiating shock wave was varied. That is, relatively weak shock waves produce detonation waves which have an unsteady velocity (see Figures 21-24, 34, 35, 49, 50, and 51; note that Figures 32 and 33 are exceptions), whereas stronger shock waves tend to produce steadier detonation waves (see Figures 25-31, 36-47, and 52; note Figure 48 is an exception).

Another feature noted in these results is the difference between the speed of the shock wave at the first speed measuring station (the velocity used in calculating M_{SE}) and that of the reaction zone at the same location. These two speeds were approximately equal for both the weaker and for the stronger incident shock waves, but the shock wave speed was considerably higher than the reaction zone speed for intermediate incident shock speeds. This trend is easily observed for both the $M_{Exit} = .2$ and .5 flow conditions, by examining Figures 21-45. This feature is undoubtedly due to the nature of the detonation initiation process. A possible explanation is as follows. A shock wave strength which was only slightly greater than the minimum required to initiate detonation probably produced a small reaction zone initially which existed in an environment which was not sufficiently activated by the weak shock wave

to permit a rapid growth of the reaction zone. As a result, the reaction zone grew in size so slowly that a gradual acceleration of the shock wave occurred. (It is noted later that several of the detonation waves formed with weak incident shock waves required longer induction distances than those formed with stronger incident shock waves.) As the shock strength was increased, the initial reaction zone was larger, grew faster, and caused a larger volume of the gas behind the wave to react in a sufficiently short time period to impulsively accelerate the shock wave to an excessively high velocity. The stronger incident shock waves probably caused the mixture to react so rapidly that a large volume of shock processed gas could not accumulate behind the wave prior to reaction. That is, in this case the shock wave and the reaction zone were probably closely coupled very soon after the incident shock wave emerged from the driver transition section.

Another detonation parameter which has received much attention is the so called "induction distance", which is the distance between the ignition source and the point at which a detonation wave is formed. Bollinger, Fong, and Edse [22] found that the minimum induction distance for a non-flowing stoichiometric mixture of hydrogen and oxygen at an initial temperature and pressure of 100 F and 1 atmosphere, respectively, was approximately

29 inches when the ignition source was a melting copper wire. The induction distance for shock induced detonation waves in a flowing mixture would be expected to be considerably less than that obtained with normal ignition of stationary mixtures for two reasons. First, much of the induction distance involved with normal ignition is required for the pre-detonation shock wave to be formed from pressure waves given off by the burning mixture, whereas, in shock induced detonations, the shock wave is formed either before, or very quickly after, it enters the combustible mixture. Secondly, the turbulence level in the flowing gas is much greater than that in an initially stationary mixture which has been disturbed only by an advancing flame front; therefore, an initially small reaction zone produced by the shock wave would be expected to grow in size much more rapidly, and become coupled with the shock wave sooner, in the flowing mixture. Review of the data presented in Figures 21-54 reveals that in all but 5 of the runs the average detonation wave velocity measured by the first two ionization probes was equal to, or exceeded, the steady state value achieved later, or else the Chapman-Jouget velocity, if a steady velocity was not attained by the wave. The term induction distance cannot be applied to these waves with its usual meaning because the point at which ignition first occurred in the mixture cannot be determined from

the data. However, if one chooses the location of the driver transition section exit diaphragm as the earliest possible point at which ignition could occur, then a statement can be made concerning the maximum possible induction distance for all of the detonation waves observed. The first point at which the speed of the detonation wave could be observed was the midpoint between the first two ionization probes, which was located 14 1/2 inches from the exit diaphragm. Thus, for the majority of the runs the induction distance was less than 14 1/2 inches. In Run 46 (Figure 22) the reaction zone velocity was less than the steady state value at the first probe station. The time increment from the second to the third probe (second measuring station) was not obtained because the oscilloscope trace reversed direction between the signals from these two probes, making it impossible to obtain an accurate measurement from the picture. Thus, it cannot be definitely determined just when the detonation velocity reached its steady value, but it had done so by the time the wave passed the third measuring station. Therefore, the maximum induction distance for this run was between 14 1/2 and 22 1/2 inches. In Run 44 (Figure 24) the maximum induction distance was 18 1/2 inches, although the transmitted shock wave speed was greater than the Chapman-Jouget velocity at the first measuring station.

It is noted that in both of these runs the incident shock wave speed was in the marginal region where some shocks of equal or greater strength than these did not produce detonation. In Run 87 (Figure 50) the maximum induction distance appears to be about 15 inches based on the near steady value of the velocity reached near the upstream end of the flowing gas section. In this case $M_{SI} = 1.56$, the minimum value required to produce detonation at this flow condition. The other two runs in which the induction distance seems to be greater than 14 1/2 inches are the runs in which spontaneous detonation occurred (Figures 53 and 54). Both of these waves were very unsteady, but both seem to accelerate to, or above, the Chapman-Jouget velocity before slowing down. The maximum induction distance for the wave in Run 012 was about 30 inches, and in Run 011, it was about 51 inches. Thus, it would seem that the disturbance which caused the spontaneous detonations was a weak one, i.e., weaker than that caused by an $M_{SI} = 1.56$ shock wave, but stronger than that caused by an $M_{SI} = 1.49$ shock wave. These two values of M_{SI} appear in Table 4 and are the values which did, and did not, respectively, cause a transition to detonation at this nominal flow condition.

The discussion must now turn to the results illustrated in Figure 18, which shows that incident shock waves with quite low Mach Numbers were sufficient to

cause initiation of detonation in the flowing stoichiometric mixtures of hydrogen and oxygen. The data in Table 2 (for runs with $M_{Exit} = .2$) show that the maximum transmitted shock wave Mach Number (M_{SE}) for a run in which detonation did not occur was produced in Run 45, in which M_{SI} was 2.10 and M_{SE} was 1.99. In Run 40, M_{SI} was 2.12, and detonation occurred. Furthermore, detonation occurred in all runs for which M_{SI} was greater than 2.12. Thus, it can be assumed that the transmitted shock wave in Run 45 produced a temperature in the flowing mixture which was only slightly less than the ignition temperature for the prevailing conditions. Similarly, for the $M_{Exit} = .5$ flow, the data in Table 3 shows that the maximum M_{SE} without detonation occurred in Run 54, in which M_{SI} was 1.69 and M_{SE} was 1.68. The next highest M_{SI} was 1.75, which produced a detonation in Run 52. Thus, it can be assumed that the temperature produced by the transmitted shock wave in Run 54 was slightly less than the ignition temperature for the conditions existing during that run. The data in Table 4 for the $M_{Exit} = .8$ flow, show that in Run 85, in which M_{SI} was 1.56, M_{SE} was 1.49, and that delayed detonation occurred. Therefore, it can be assumed that the temperature produced by this shock wave was quite close to the minimum ignition temperature required by the mixture under the existing conditions. The data from Runs 45, 54, and 85

were chosen for further analysis in order to determine approximate values for the ignition temperatures and for the maximum induction times available for ignition for the respective flow Mach Numbers.

Figures 57, 58, and 59 contain x - t diagrams for Runs 45, 54, and 85, respectively. In constructing these diagrams it was assumed that the transition section area change and exit diaphragm could be replaced by a constant area section with only a stationary contact surface separating the hydrogen-oxygen mixture and the air in the inert section. Experimental values of the incident and transmitted shock wave speeds relative to the tube were plotted. These shock waves were assumed to form instantaneously upon rupture of the main diaphragm, and upon arrival of the incident shock wave at the hydrogen-oxygen-air contact surface, respectively. The shock waves were also assumed to be one dimensional waves which propagated with constant velocities. The Mach Numbers of the waves relative to the medium in which each was propagating were used in conjunction with the normal shock tables contained in [23] in order to determine the change in properties across each wave. These wave diagrams illustrate two important points. First, it is noted that the transmitted shock waves had sufficient strength in Runs 45 and 54 (Figures 57 and 58) to cause a reversal of the flow direction. In both of these

runs the particle velocity behind the transmitted shock waves is toward the upstream end of the tube. Figure 59 shows that in Run 85 the transmitted shock wave did not possess sufficient strength to overcome the high flow velocity, and the particle velocity behind the wave was directed downstream toward the exit. In all runs in which detonation occurred, the reaction was initiated downstream of the first ionization probe and then moved upstream. This fact was used in conjunction with the wave diagrams to arrive at values for the maximum time available for ignition of the mixture, i.e., since ignition was always indicated first by the first ionization probe, then ignition had to occur before the contact surface separating the combustible mixture and the air reached the position of the first ionization probe. The time interval during which ignition could occur began with the formation of the transmitted shock wave at the stationary contact surface. In Runs 45 and 54, this time interval was approximately 600 and 1500 microseconds, respectively. Since the contact surface did not move toward the ionization probes in Run 85, a much longer time interval was available for ignition; however, the detonation wave reached the first ionization probe approximately 1300 microseconds after the formation of the transmitted shock wave. Thus, the time available for ignition increased with the flow velocity. Experiments

with other types of ignition sources have shown that, within limits, longer induction times permit ignition to be accomplished with lower ignition temperatures [1]. Extension of these results to the present experiments indicates that ignition could be accomplished at lower temperatures, i.e., with weaker shock waves, at the higher flow Mach Numbers, in agreement with the experimental observations.

The second important point illustrated by Figures 57-59 is that the reflected expansion wave associated with the production of the incident shock wave was not a factor in the ignition process. The driver section was of such length that the leading edge of the expansion wave did not reach the end of the driver until after the contact surface had passed the location of the first ionization probe in Run 45, and inspection of the diagrams for Runs 54 and 85 shows that the reflected wave could not have arrived at this location in time to affect the ignition process for the flow conditions represented by these runs.

The temperatures theoretically available for ignition of the combustible mixtures in Runs 45, 54, and 85 were calculated using several assumed models for the calculations, and the results are all included in Figure 60. The model used in Case 1 assumed that the incident shock wave travelling at M_{SI} through stationary air encountered

a stationary contact surface separating the air and the combustible mixture. The pressure was assumed to be ambient on both sides of the contact surface. The air temperature was assumed to be the ambient temperature, and the mixture temperature was assumed to be the stagnation temperature of the flowing gas. The strength of the transmitted shock wave was calculated using the equations listed by Glass [24] which pertain to the interaction of a normal shock wave and a contact surface. The one dimensional shock tables [23] were then used to find the temperature behind the transmitted shock wave. The temperatures determined in this manner were 435 K, 370 K and 369 K for Runs 45, 54, and 85, respectively.

In Case 2 the temperature behind the transmitted shock wave was calculated using the experimentally determined value of M_{SE} and the static temperature of the flowing mixture. The temperatures determined in this manner were 469 K, 381 K, and 340 K for Runs 45, 54, and 85, respectively. The explosion limit temperatures at the pressures existing behind the transmitted shock waves of Case 2 were obtained from [1]. These temperatures were 770 K, 788 K, and 793 K for Runs 45, 54, and 85, respectively. These values are also plotted in Figure 60.

In Case 3 it was assumed that the transmitted shock wave, having a Mach Number equal to the experimentally

determined M_{SE}, formed instantaneously in the stagnation region adjacent to the exit diaphragm. In this case the reference temperature was the stagnation temperature of the flowing mixture, rather than its static temperature at a location where the full flow velocity existed. In this case the calculated temperatures were 471 K, 400 K, and 383 K for Runs 45, 54, and 85, respectively.

In Case 4 the effect of the velocity profile in the flowing mixture was considered. Since the Reynolds Numbers for all three of the runs being considered were in excess of 10^5, the flow was turbulent in each case. For fully developed turbulent flow in circular pipes the average one dimensional flow velocity is approximately .8 times the maximum velocity existing in the flow [25]. To account for this effect a new Mach Number was calculated using the experimentally determined transmitted shock wave velocity with respect to the tube plus the calculated maximum velocity of the flow. The static temperature of the flowing gas was used to calculate the speed of sound in the mixture. The post-shock temperatures calculated under these conditions were 480 K, 406 K, and 374 K for Runs 45, 54, and 85, respectively.

In Case 5 it was assumed that the transmitted shock wave did not reach its final velocity instantaneously upon encountering the combustible mixture, but that it retained the velocity of the incident shock wave with

respect to the tube until after it had moved into the flowing mixture. The Mach Number of this assumed shock wave was calculated using the velocity of the incident shock wave with respect to the tube plus the maximum velocity on the velocity profile of the flowing mixture, divided by the speed of sound in the mixture based on the static temperature of the flowing mixture. The post-shock temperatures calculated in this manner were 391 K, 393 K, and 443 K for Runs 45, 54, and 85, respectively.

Reference to Figure 60 shows that the temperatures calculated according to the various assumptions listed above are considerably less than the ignition temperatures predicted by the thermal explosion limit theory. Furthermore, all of the models considered, except Case 5, resulted in a decrease in temperature with an increase in flow velocity. The assumptions of Case 5 resulted in the maximum calculated temperature for Run 85 (443 K) in which ignition occurred; however, Cases 2, 3, and 4 resulted in higher temperatures for Run 45, in which ignition did not occur.

In summary, application of one dimensional normal shock wave theory resulted in maximum calculated temperatures in the flowing mixture which were 290 K, 382 K, and 350 K less than the respective ignition temperatures predicted by the thermal explosion limit theory for Runs 45, 54, and 85. The temperatures produced in Runs 45

and 54 were only slightly less than those actually required for ignition, and ignition occurred in Run 85.

The question naturally arises, what is the explanation for this low temperature ignition phenomena? In answering this question, the first thing that should be noted is that there is no a priori reason to suspect that the thermal explosion limit ignition temperature results should apply to the experiments conducted in this investigation, because the experimental conditions are quite different. The thermal explosion limit experiment is conducted in a closed quartz bulb of a specified size and surface coating, and the heating of the gas is accomplished relatively slowly through the walls of the container. The reaction is termed a heterogeneous reaction because the walls and size of the container play such a prominent role in the results. On the other hand, in a shock tube, or detonation tube, experiment the size and geometry of the reaction vessel are different, the heating is applied essentially instantaneously, and directly to the body of the gas by the shock wave, and the influence of the wall is so slight that the reaction is called a homogeneous reaction. Nevertheless, numerous shock tube experiments have been conducted in which stationary stoichiometric mixtures of hydrogen and oxygen have been ignited by both incident and reflected shock waves, and the minimum temperatures required behind the

shock waves have agreed well with the predictions of the thermal explosion limit theory. Of course, the ignition of stationary mixtures in a shock tube is still far removed from the conditions existing in the present experiments, because these mixtures are not in motion prior to the arrival of the shock wave. Therefore, these shock tube results (which Belles and Ehlers [10] classify as fortuitous) do not necessarily apply to the present experiments any more than do those obtained with the quartz bulb.

In continuing the search for an explanation for the "low temperature ignitions" experienced, the next item that comes to mind is the results obtained by Shepherd and by Fay, which have been mentioned in the Introduction. These experimenters obtained very low ignition temperatures when their test gases were next to the diaphragm. Fay observed no change in the shock strength required to produce ignition when he used a buffer section terminated with a weak cellophane diaphragm, between the main diaphragm and the test gas. Later experimenters [9] used buffer sections not requiring the second diaphragm, and obtained results in agreement with the thermal explosion limit theory; however, the initial pressures ahead of the shock waves were of the order of 200 mm Hg, or less. They explained the discrepancy by blaming "non-one dimensional effects" associated with

the diaphragm opening process. The experimental apparatus used in this investigation employed an air filled "inert section" between the main diaphragm and the test gas. As discussed previously, preliminary experiments showed the necessity for a diaphragm at the driver transition section exit, and so one was used. Thus, based on the results mentioned above, the likelihood that such "non-one-dimensional" effects might play a significant role in the observed phenomena must be considered. Actually, it is noted that even more pronounced "non-one-dimensional" effects are associated with the opening of this diaphragm than is the case in a normal shock tube, due to the abrupt area increase experienced by the shock wave as it leaves the driver transition section and enters the flowing gas section transition section. Experiments conducted by numerous investigators [26, 27, 28, 29] have shown that this configuration results in the emerging shock wave taking on a spheroidal shape. The sides of this expanding wave soon contact the walls of the container and reflect back toward the center where they intersect to form a "focus" [27, 28].

In order to determine the magnitude of the effects of possible reflected shock waves in the transition section, another series of calculations was performed using the data from Runs 45, 54, and 85. In this series of calculations it was assumed that a shock wave, having a

Mach Number equal to the experimental value of M_{SE}, impinged normally on a solid wall and was reflected. The gas properties ahead of the wave were taken to be the properties of the flowing mixture. This model neglects the fact that the strength of the expanding wave would actually decrease as the wave expands and, therefore, the temperatures obtained using this model should exceed those produced by the reflection of the actual wave by the walls of the transition section. The strength of the reflected shock wave was determined using the appropriate equations in [24], and then the temperature behind the wave was determined using the normal shock tables [23]. The temperatures resulting from these calculations were 692 K, 516 K, and 431 K for Runs 45, 54, and 85, respectively. These values are referred to as Case 6 in Figure 60. The temperatures resulting from this reflected shock wave model are higher than those calculated using any of the other models for Runs 45, and 54; however, the value of 431 K calculated for Run 85 is slightly less than the 443 K calculated in Case 5. The fact that the temperatures calculated for Runs 45 and 54 (in which ignition did not occur) are so much higher than the temperature calculated for Run 85 (in which ignition did occur) is a good reason to doubt the validity of the model and therefore, the existence of the resulting high temperatures for Runs 45 and 54.

One final set of calculations was performed using the data of Run 45. In these calculations it was assumed that the pressure ratio existing across the experimentally observed transmitted shock wave was effective in producing two normal shock waves moving perpendicular to the axis of the transition section, i.e., the properties behind the transmitted shock wave were assumed to be driver conditions leading to the formation of two new shock waves which moved in opposite directions and transverse to the flow. The walls of the transition section were assumed to be parallel to the centerline of the tube. The gas properties in front of the transversely moving shock waves were taken to be the properties of the flowing mixture. The shock waves were assumed to be reflected back toward the centerline by the walls of the transition section. Enroute to the centerline, the reflected shock waves were assumed to encounter the contact surfaces associated with their formation, and then later on they were assumed to interact with the reflected rarefaction waves also associated with their formation. Due to symmetry considerations the equations used [24] showed that the centerline of the tube could be considered equivalent to a solid wall, and it was necessary to make the calculations for only one of the transversely moving shock waves. When this shock wave arrived at the centerline, it was assumed to be reflected

a second time and the temperature behind this twice reflected wave was calculated. The resulting temperature was found to be 491 K, which was 20 K higher than the temperature initially assumed behind the transmitted shock wave. The temperature rise attainable with this model is limited by the fact that the reflected shock wave must interact with contact surfaces and reflected expansion waves, and these interactions become more numerous as time goes on. On subsequent cycles the shock wave strength is progressively diminished by these interactions and by non-adiabatic conditions existing at the walls of the tube. The temperature rise resulting from similar wave reflections in Runs 54 and 85 would be less than that calculated for Run 45, since the transmitted shock waves were weaker, and thus the pressures available for the production of the transverse waves were lower.

In summary, the last two sets of calculations show that, under the assumptions used, reflected shock waves caused by the abrupt area change in the transition section could result in an increase in temperature beyond that produced by a simple normal shock wave moving into the flowing mixture; however, the real significance of these reflected shock waves cannot be deduced from the data now available. The importance of such effects can be determined only by conducting additional experiments

in which temperatures in the transition section are measured, or in which transition sections having different geometrical configurations are used.

Since the actual ignition temperatures under the conditions produced in the present experiments are not known or theoretically predictable, a priori, one can only list the calculated temperatures, along with the assumptions used. There is no definite basis for choosing any one of the models as the one which gives the most accurate prediction of the actual ignition temperature.

At the present time it is not felt that reflected shock waves in the transition section played a significant role in the ignition process. At any rate, if one accepts this mechanism as the explanation for the apparently low ignition temperatures observed, how does he then explain the fact that no ignition was obtained with incident shock wave Mach Numbers up to 2.62 with $M_{Exit} = 0$, and that as M_{Exit} was increased (which also reduced the flow static temperature at the exit), progressively weaker shock waves were sufficient to initiate detonation? Going one step further, how are the spontaneous detonations to be explained? In the case of the spontaneous detonations, no shock wave was injected into the transition section. Furthermore, after these spontaneous detonations were observed, Edse [30] conducted experiments using a flowing mixture of hydrogen

and oxygen in a simple constant area tube containing no surface irregularities, instrumentation access holes, or diaphragms. In these experiments spontaneous detonation occurred repeatedly during the flow starting transient. It is felt that any explanation of the other phenomena observed must also explain the occurrence of these spontaneous detonations, because it is believed that their occurrence is due to a further increase of the same effect which causes a reduction in the minimum shock strength required to produce detonation as the flow velocity is increased.

One possible explanation of the observed low ignition temperatures can be based on the work of Lewis [31], who reported that a mixture containing 40 mm of Hg of ozone and 100 mm of Hg of hydrogen exploded at a temperature of 358 K, and that mixtures of these gases that ordinarily react at a moderate rate can be made to explode by previously exposing the walls of the container to hydrogen atoms. If a mechanism should exist in the present experiments by which a portion of the flowing oxygen was converted into ozone, such that the amount of ozone increased with the flow velocity, then it could be expected that lower ignition temperatures would be observed as the flow velocity was increased. Since the existence of such a mechanism for ozone production has

not yet been reported, it is felt that this explanation of the observed phenomena is too speculative.

A further search of the literature yielded information upon which a more plausible explanation of the observed phenomena can be based. Finch and Cowen [32] conducted experiments in which they studied the ignition of stoichiometric mixtures of hydrogen and oxygen by passing a direct-current electrical discharge between two electrodes spaced up to 15 mm apart in the combustible mixture. The results showed that the minimum igniting current was of the order of a few milliamperes and that it varied with the pressure of the mixture over a considerable range in a hyperbolic manner. They concluded that in these experiments ignition was determined solely by the attainment in some portion of the gas transversed by the discharge of a certain definite concentration of suitable ions or electrically charged particles. The question now becomes, is there a source of ionization in the experimental apparatus used in this investigation? The ionization probes themselves might be considered a source of ionization; but this source must be insignificant, because no voltage was applied to the ionization probes on the first two runs in which spontaneous detonation occurred, and such probes were not even installed in the apparatus used by Edse [30]. Therefore, another source of ionization was sought.

The final evidence was provided by Guest [33], who summarized the work of Pothmann and of Nusselt, which was reported in 1922. Both of these investigators conducted experiments with hydrogen flowing in a tube and exiting into the atmosphere. In Pothmann's experiments, various amounts of water were aspirated into the flowing hydrogen. Observation of the flow as it left the end of the tube revealed that a pale blue glow was present in the flow. When the pressure was increased (which increased the mass flow rate), the intensity and extent of the glow increased. By a suitable arrangement of electrodes, one of which was insulated and placed in the gas stream, and the other was attached to the tube, sparks were produced which ignited the hydrogen in the presence of atmospheric air. Nusselt discovered that hydrogen gas often carried minute particles of iron oxide which were picked up from the storage cylinders, and that hydrogen containing these particles exhibited a pale blue glow upon exiting from a small orifice. He found that a sharp-pointed copper wire placed directly in the path of the gas, and grounded, reduced the glow to a small point. When the wire was moved to the side of the gas stream, the glow reappeared and ignition followed.

These two sets of experiments showed that hydrogen, containing either small quantities of water or iron

oxide, becomes electrically charged, i.e., ionized, when it flows through a tube, and that such a degree of ionization can be developed that sparking and ignition (when oxygen is present) result.

It is quite likely that technical grade hydrogen, which is presently supplied and stored in steel high pressure bottles, or in compressed gas trailers, could entrain minute particles of rust from these containers when the gas is delivered directly from these containers to an experimental apparatus at high mass flow rates. It is even more likely that such particles could be found in the oxygen, which is supplied in the same type containers. The hydrogen and oxygen used in the present investigation were technical grade gases, and they were delivered from their high pressure storage containers directly to the gas flow control and metering system without further purification or filtration; therefore, the gases used in this investigation could be expected to contain any impurities normally present in such gases. The fact that Edse also encountered spontaneous detonations in a different experimental facility is a strong indication that the phenomenon is not peculiar to the test facility being used, but instead, that it is a characteristic associated with flowing mixtures of the gases used.

Based on the above observations, it is believed that the major results observed in this investigation can be explained in the following way. When mixtures of hydrogen and oxygen are flowing through an apparatus with an appreciable velocity, a certain amount of ionization occurs in the mixture, due to frictional effects, possibly aided by the presence of impurities, either solid or liquid, which are normally contained in the gases, or form after they are mixed. The amount of ionization increases as the flow velocity increases until, finally, there is a sufficient amount present to result in a chain branching reaction, i.e., a spontaneous ignition of the mixture. At lower velocities the ionization present in the flowing stream makes it more sensitive to ignition than is a stationary mixture, and as the velocity is increased, less and less additional energy is required for ignition. In other words, a relatively weak shock wave would be sufficient to cause ignition of a flowing mixture, and as the flow velocity is increased, weaker and weaker shock waves would be sufficient.

It is realized that the above explanation of the data presented in Figure 18 may be somewhat speculative, but the explanation does account for all aspects of the phenomena which have been observed, and no more plausible explanation can be offered at this time. It is felt that

neither verification nor rejection of the explanation can be accomplished without further experiments specifically directed toward the determination of the electrical properties of flowing hydrogen and oxygen, individually, and mixed. In the meantime, the possibility of unexpected or spontaneous ignition of flowing mixtures of hydrogen and oxygen should not be overlooked.

CONCLUSIONS

The results obtained in this investigation led to the following conclusions:

1. Shock induced detonation waves were initiated for the first time in flowing stoichiometric mixtures of hydrogen and oxygen with flow Mach Numbers up to approximately .8. The minimum incident shock wave Mach Number above which detonation always occurred was 2.12 for $M_{Exit} = .2$; 1.75 for $M_{Exit} = .5$; and 1.56 for $M_{Exit} = .8$.

2. There was a high probability of the occurrence of spontaneous detonation waves (first reported by McKenna) when the flow Mach Number exceeded .8.

3. The temperatures behind the shock waves which were just sufficiently strong to initiate detonation were far below the ignition temperatures predicted by the thermal explosion limit theory.

4. The low temperature ignition phenomena can possibly be accounted for by an increase in the degree of ionization of the flowing mixture

with flow velocity, due to frictional effects and possible impurities normally present in the gases.

5. Additional experimentation is required in order to determine the extent of ionization present in flowing hydrogen, oxygen, and mixtures thereof.

TABLE 1

EXPERIMENTAL RESULTS WITH THE FLOW EXIT MACH NUMBER AT APPROXIMATELY 0

Run No.	H_2 Percentage	T_{Exit} K	P_{Exit} Atm.	M_{SI}	M_{SE}	Number and Thickness of Diaphragms	
						No.	Thickness
68	67.37	286	.970	1.75	-a	1	.002 in
69	67.01	286	.970	1.89	1.78	2	.002 in
70	67.43	286	.970	2.14	2.06	3	.002 in
71	67.01	281	.961	2.28	1.39[b]	2	.005 in
72	67.26	281	.968	2.28	-c	2	.005 in
73	66.82	279	.969	2.62	3.86[b,d]	3	.005 in
74[e]	66.62	281	.975	2.00[f]	2.02	4	.005 in

a - Heat transfer gage No. 2 did not operate.

b - Unreliable value - suspect heat transfer gage No. 2 circuit actuated prematurely.

c - Heat transfer gage No. 2 circuit actuated prematurely.

d - There was no indication of ignition by the ionization probes.

e - Heat transfer gage amplifier sensitivities reset and operation checked prior to this run.

f - Suspect poorly formed incident shock wave due to poor opening of the multi-layered diaphragm.

TABLE 2

EXPERIMENTAL RESULTS WITH THE FLOW EXIT MACH NUMBER AT APPROXIMATELY .2

Run No.	Mass Flow Rate lb_m/sec	H_2 Percentage	T_{Exit} K	P_{Exit} Atm.	M_{Exit}	M_{SI}	M_{SE}
26	.155	67.23	271	.981	.212	1.74	1.60
27	.153	67.75	271	.981	.210	1.75	1.63
28	.153	67.5[illegible]	271	.981	.210	1.91	1.74
29	.154	67.42	271	.971	.212	1.86	1.76
30	.154	67.42	271	.971	.212	2.07	1.88
31	.155	67.49	271	.972	.215	2.08	5.75
32	.153	67.53	276	.970	.215	1.91	1.75
33	.152	68.33	276	.970	.215	1.87	1.78
34	.154	67.39	275	.970	.216	2.10	1.94
35	.153	66.73	276	.964	.213	2.04	5.70
36	.152	66.79	276	.963	.212	2.09	1.92
40	.154	64.86	276	.958	.212	2.12	6.11
41	.155	65.[illegible]7	275	.959	.214	2.15	6.00
42	.153	65.84	276	.962	.212	1.99	5.52
43	.151	65.44	276	.966	.207	1.97	1.81
44	.149	66.36	279	.958	.210	2.06	5.58
45	.149	66.06	279	.963	.208	2.10	1.99
46	.148	66.83	279	.964	.208	2.00	--a
47	.146	65.94	279	.963	.203	2.18	--a
48	.148	66.45	279	.966	.207	2.23	5.92
49	.148	66.58	279	.965	.208	2.19	--a
75	.143	68.09	281	.975	.203	2.34	5.67
76	.143	68.14	281	.974	.203	2.60	5.32

a - Detonation occurred

TABLE 3

EXPERIMENTAL RESULTS WITH THE FLOW EXIT MACH NUMBER AT APPROXIMATELY .5

Run No.	Mass Flow Rate lb_m/sec	H_2 Percentage	T_{Exit} K	P_{Exit} Atm.	M_{Exit}	M_{SI}	M_{SE}
50	.338	68.00	263	.924	.512	1.89	5.75
51	.337	67.12	264	.937	.496	1.89	5.86
52	.337	66.52	265	.947	.487	1.75	5.76
53	.336	66.74	264	.940	.490	1.76	5.74
54	.337	66.89	264	.934	.497	1.69	1.68
55	.341	68.11	263	.924	.517	1.69	1.66
56	.335	66.86	278	.928	.510	1.91	5.84
57	.339	66.51	277	.924	.516	1.97	5.58
58	.334	66.75	278	.928	.508	1.93	5.68
59	.332	67.03	278	.929	.506	2.06	5.60
60	.334	67.70	278	.929	.506	2.17	5.61
61	.338	66.32	278	.930	.509	2.18	5.59
62	.338	66.91	273	.925	.511	1.51	--a
63	.337	66.39	272	.931	.503	1.54	1.51
64	.337	66.39	273	.937	.499	1.52	1.52
65	.341	66.58	269	.934	.505	1.77	5.87
66	.336	66.70	270	.941	.495	2.21	5.70
67	.338	66.82	269	.943	.498	1.81	5.76
78	.330	67.49	279	.931	.506	2.18	5.58
79	.340	66.78	278	.936	.512	2.44	--b
80	.339	66.61	278	.934	.511	2.52	--b
81	.338	66.92	278	.929	.515	2.47	--b

a - No detonation

b - Detonation occurred

TABLE 4

EXPERIMENTAL RESULTS WITH THE FLOW EXIT MACH NUMBER AT APPROXIMATELY .8

Run No.	Mass Flow Rate lb_m/sec	H_2 Percentage	T_{Exit} K	P_{Exit} Atm.	M_{Exit}	M_{SI}	M_{SE}
011	.654	67.28	252	1.179	.808	--a	--b
012	.571	67.02	258	1.088	.764	--a	--b
82	.584	66.75	258	1.097	.772	2.08	-b,e
83	.583	67.31	257	1.092	.779	1.47	-c,f
84	.585	66.66	256	1.082	.784	1.67	5.96
85	.554	67.78	259	1.044	.784	1.56	1.49[d]
86	.587	67.59	258	1.092	.792	1.49	-b,f
87	.592	66.33	258	1.095	.784	1.56	-b,e
88	.586	66.51	260	1.111	.764	1.65	-b,e
89	.589	66.22	260	1.111	.765	1.65	-b,e
90	.566	66.43	262	1.082	.759	1.69	-b,e

a - Spontaneous detonation occurred

b - Heat transfer gages not installed

c - No output from either heat transfer gage

d - Delayed detonation

e - Detonation occurred

f - Detonation did not occur

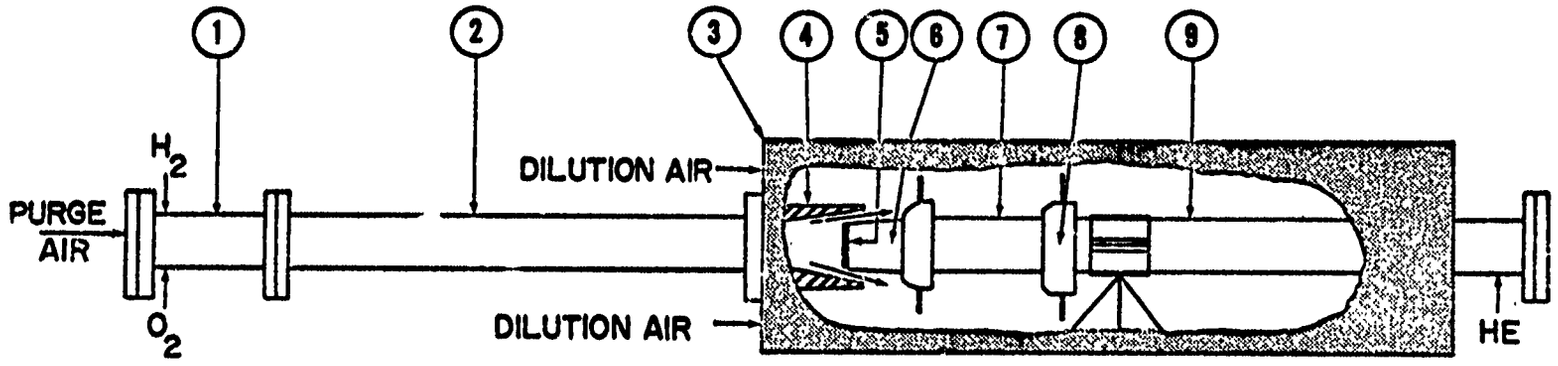

LEGEND

1. MIXING SECTION
2. FLOWING GAS SECTION
3. EXHAUST DUCT
4. TRANSITION SECTION
5. EXIT DIAPHRAGM
6. DRIVER TRANSITION SECTION
7. INERT SECTION
8. MAIN DIAPHRAGM
9. DRIVER

Figure 1 Schematic Diagram of the Detonation System

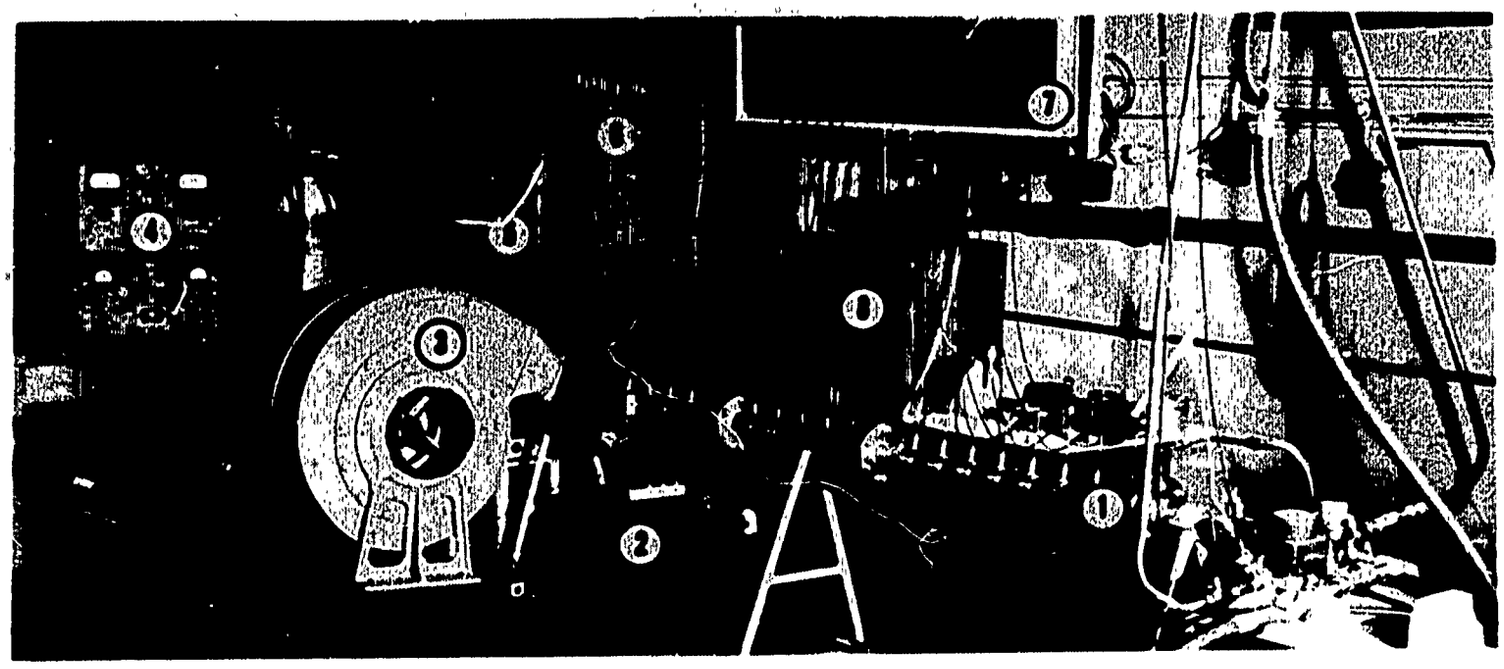

1. Flowing Gas Detonation Tube
2. 24 Volt Battery
3. Blower
4. Ionization Probe Power Supply
5. Driver Helium Supply
6. Manometer Bank
7. Ionization Probe Circuitry
8. Heat Transfer Gage Amplifier Cabinet

Figure 2 Overall View of Experimental Apparatus

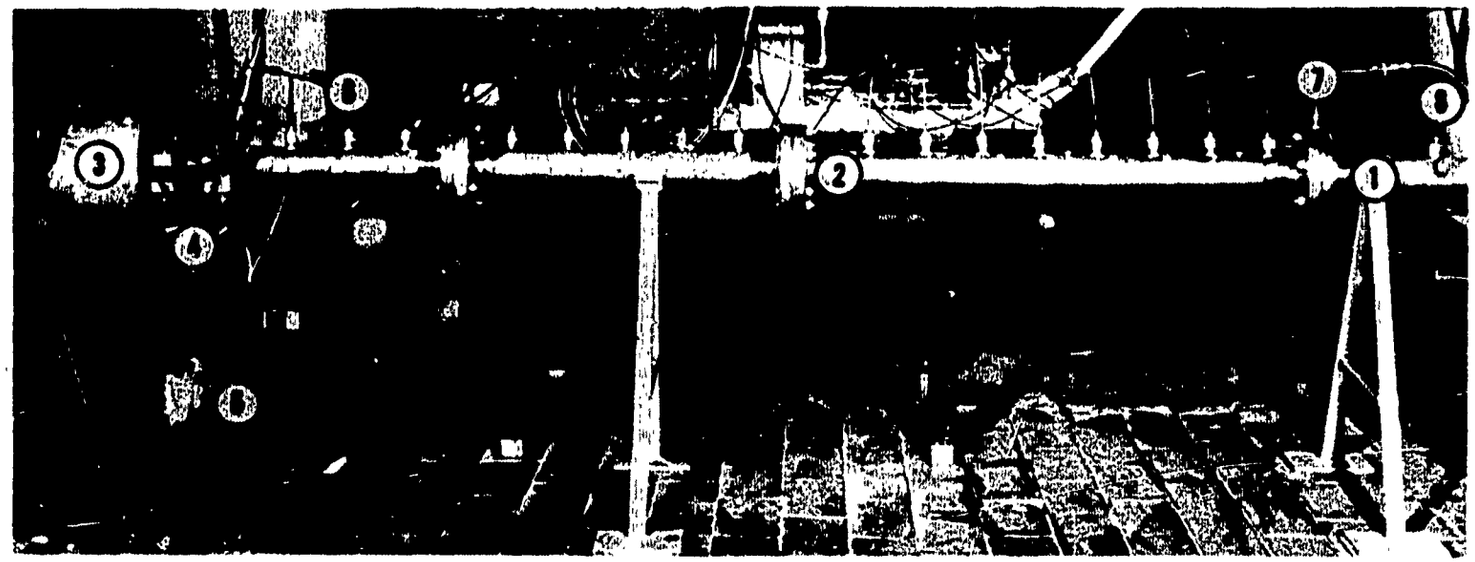

1. Gas Mixing Section
2. Flowing Section
3. Exhaust Duct
4. Heat Transfer Gages
5. 24 Volt Battery
6. Ionization Probe (Total of 18)
7. Flowing Gas Static Pressure Tap
8. Thermocouple for Automatic Shutdown

Figure 3 The Flowing Gas Detonation Tube and Instrumentation

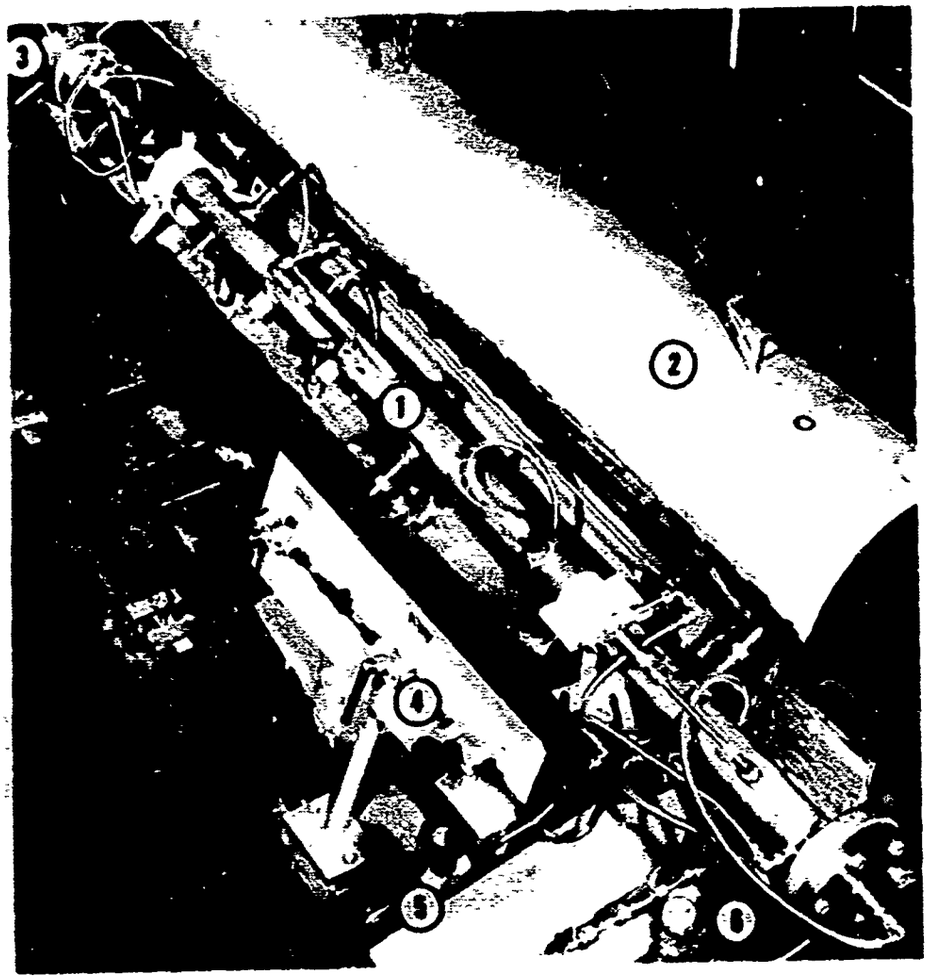

1. Driver Section
2. Exhaust Duct Cover
3. Main Diaphragm Station
4. Driver Evacuation Valve
5. Manometer Valve
6. Helium Fill Valve

Figure 4 The Driver Section Mounted in the Exhaust Duct

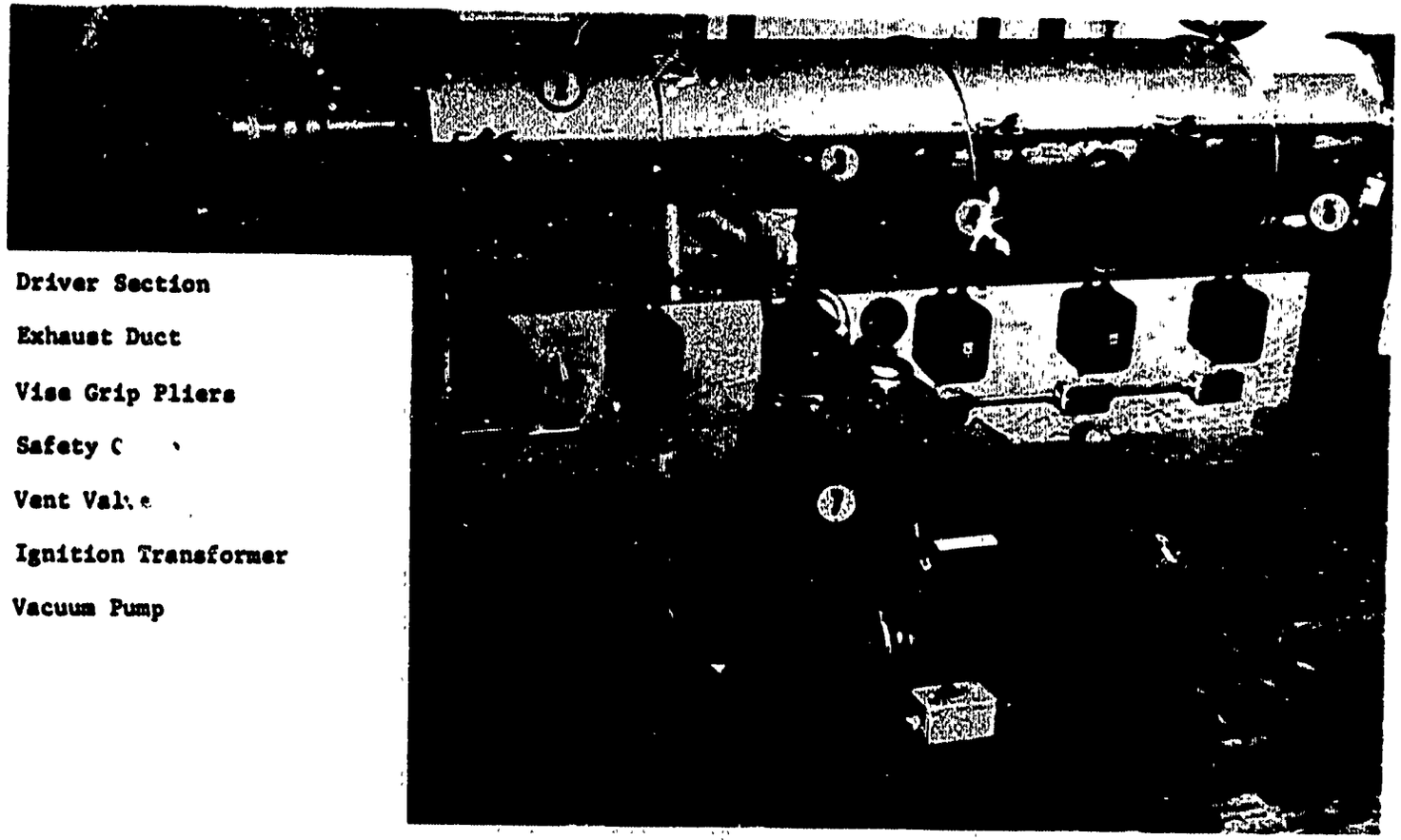

1. Driver Section
2. Exhaust Duct
3. Vise Grip Pliers
4. Safety C
5. Vent Valve
6. Ignition Transformer
7. Vacuum Pump

Figure 5 Driver Section and Exhaust Duct in Run Configuration

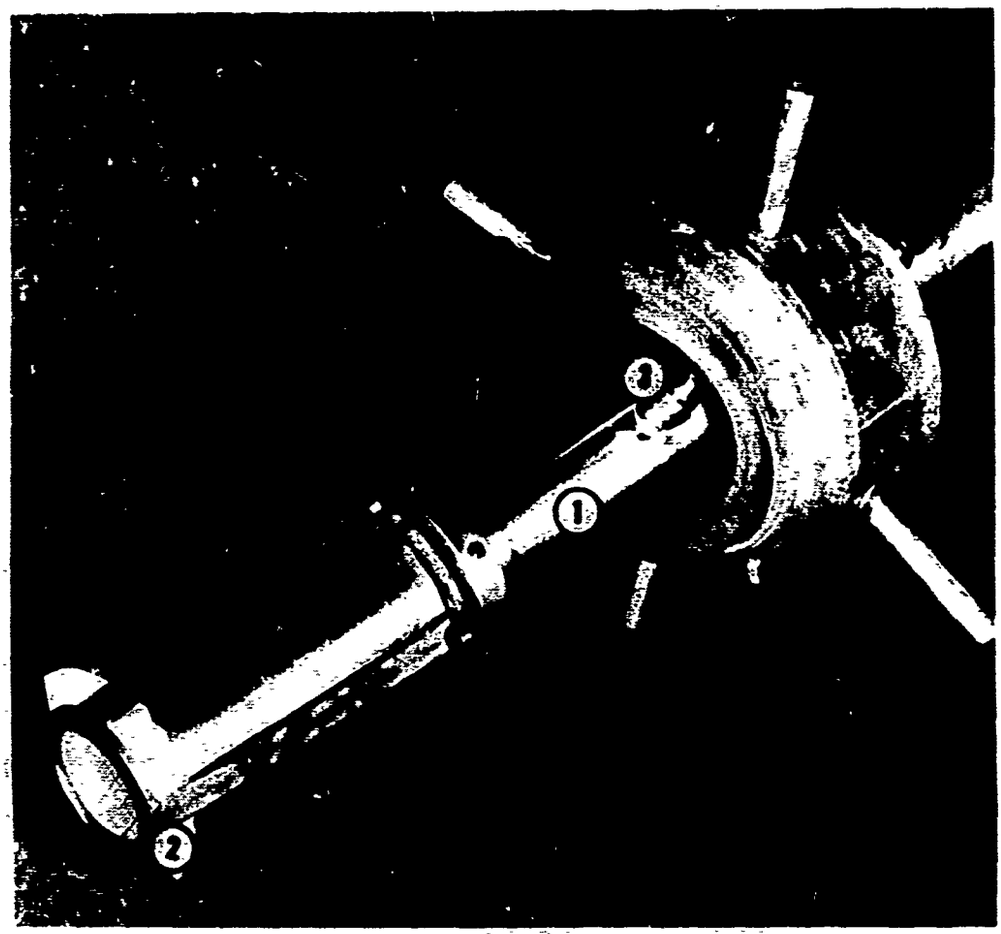

1. Driver Transition Section
2. Exit Diaphragm and Retaining Mechanism
3. Kistler Pressure Transducer Mounting Adapter

Figure 6 Shock Wave Exit End of the Driver Transition Section

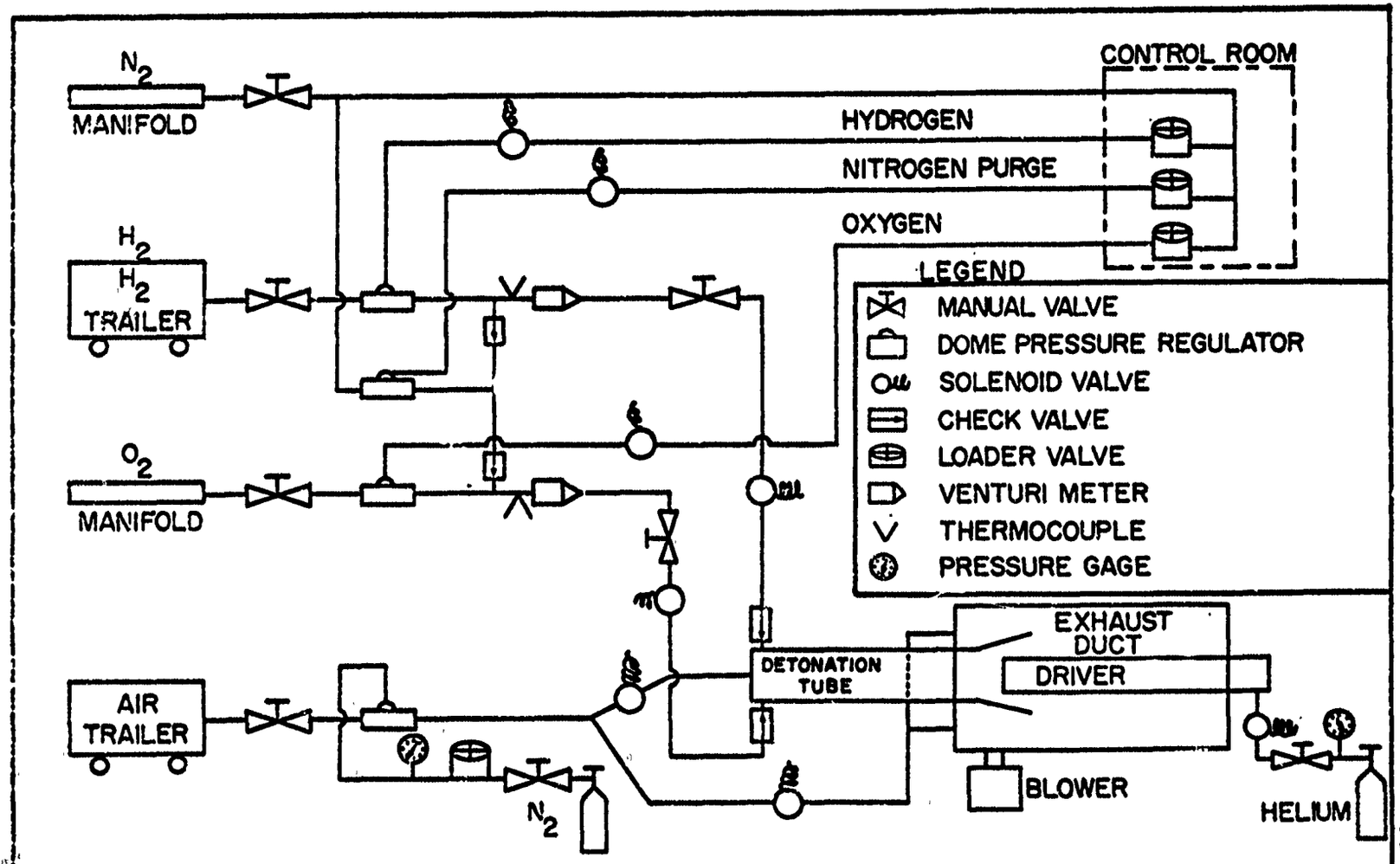

Figure 7 Schematic Diagram of Gas Supply, Control, and Metering System

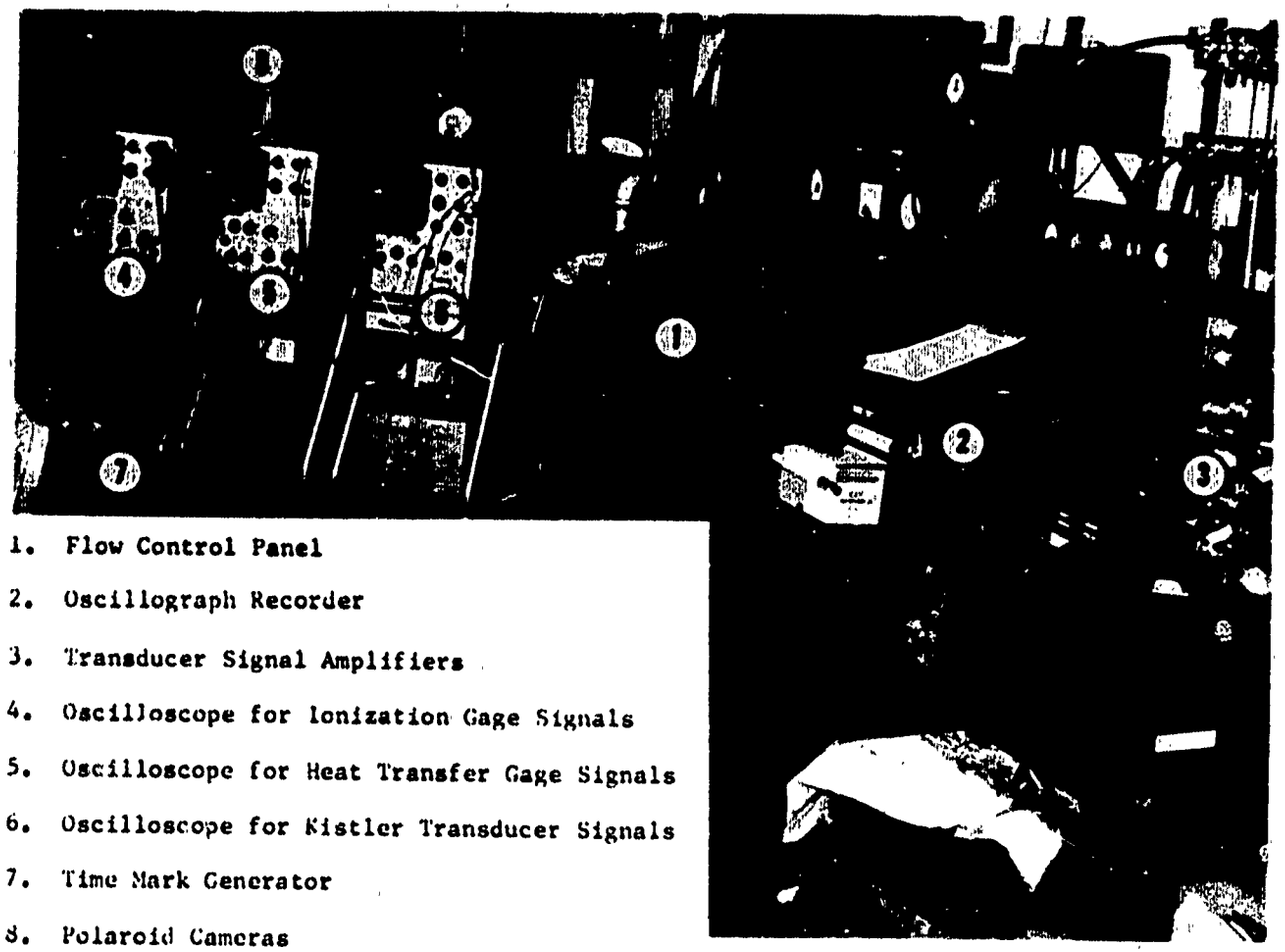

1. Flow Control Panel
2. Oscillograph Recorder
3. Transducer Signal Amplifiers
4. Oscilloscope for Ionization Gage Signals
5. Oscilloscope for Heat Transfer Gage Signals
6. Oscilloscope for Kistler Transducer Signals
7. Time Mark Generator
8. Polaroid Cameras

Figure 8 Control Room and Data Recording Equipment

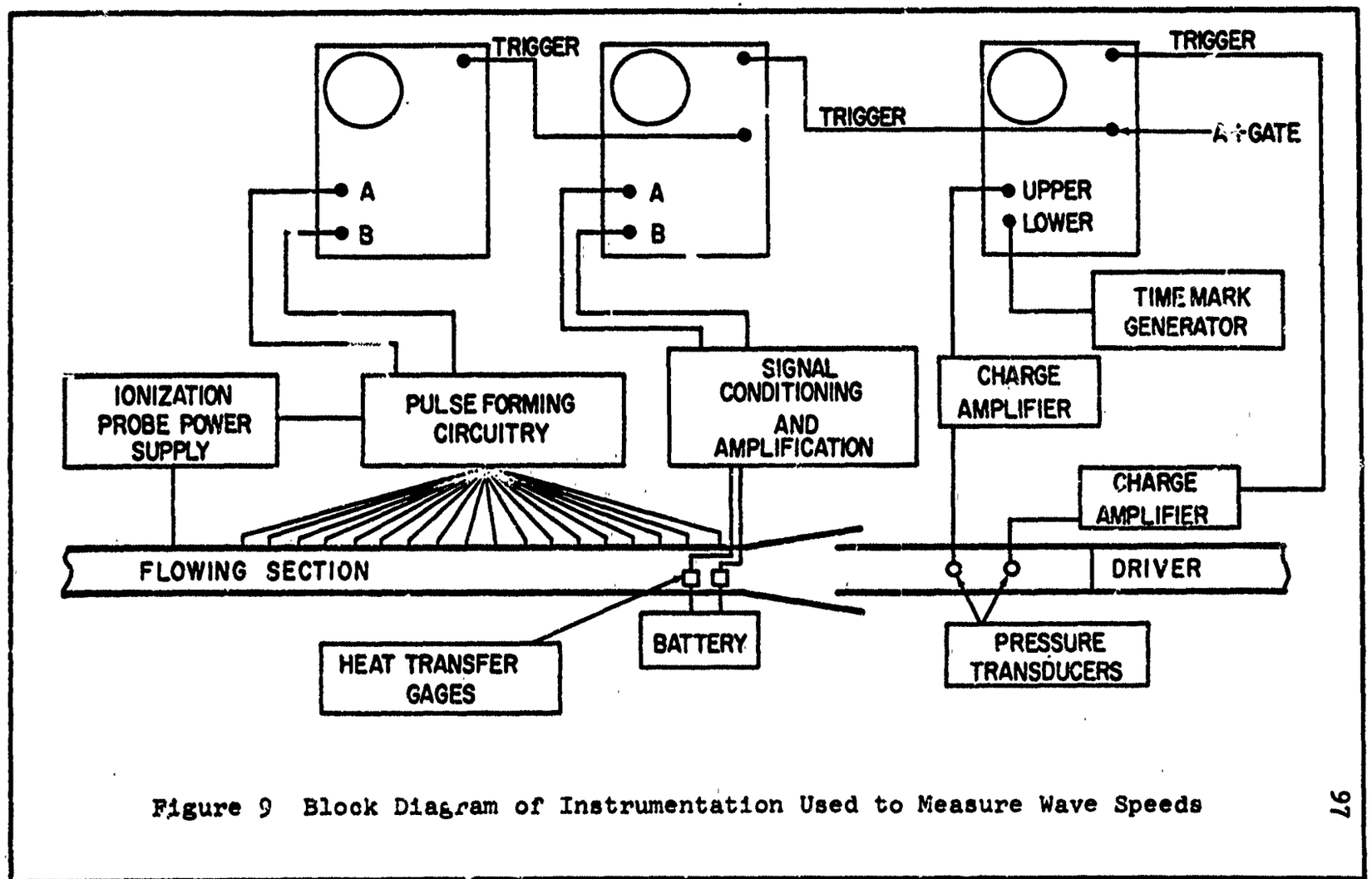

Figure 9 Block Diagram of Instrumentation Used to Measure Wave Speeds

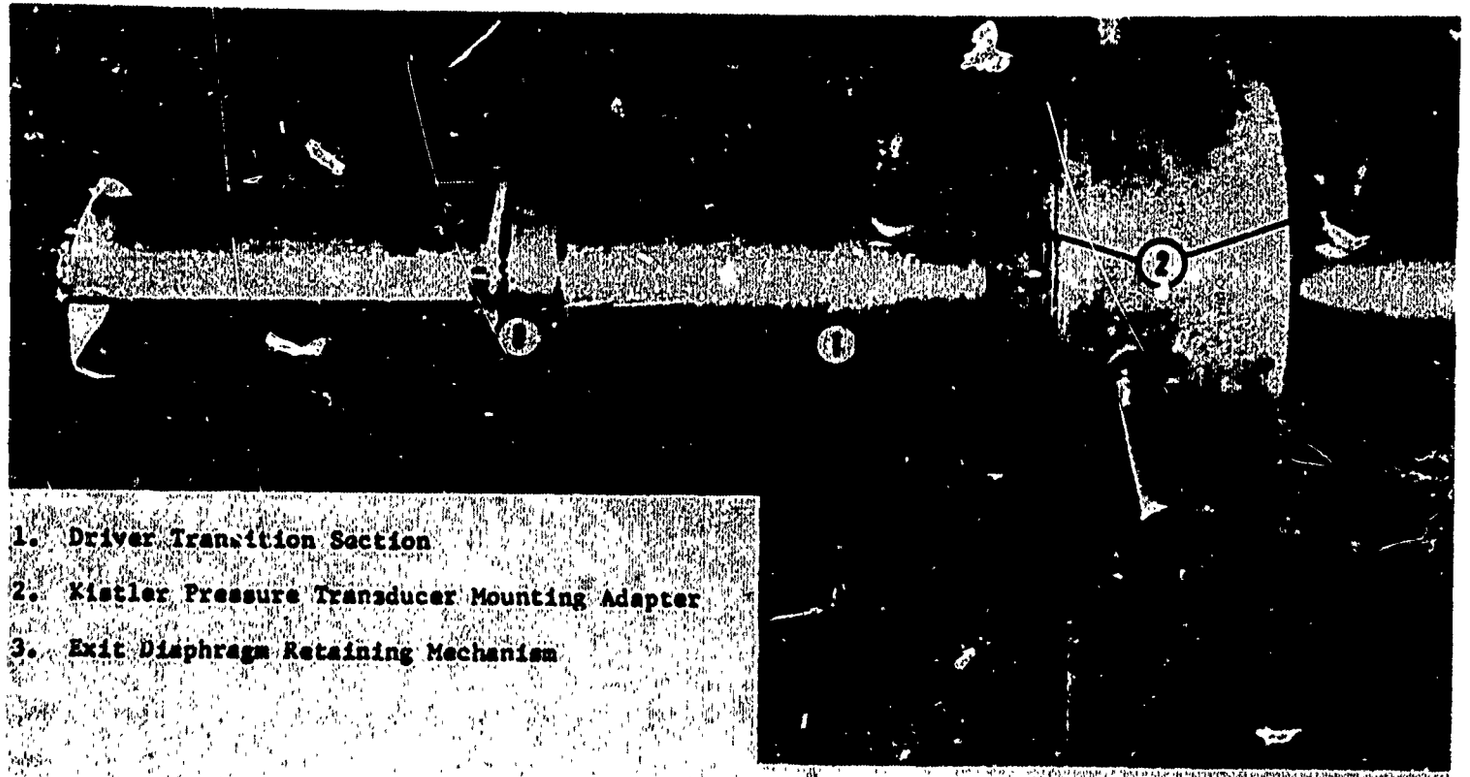

1. Driver Transition Section
2. Kistler Pressure Transducer Mounting Adapter
3. Exit Diaphragm Retaining Mechanism

Figure 10 The Driver Transition Section Showing the Incident Shock Wave Speed Measuring Station

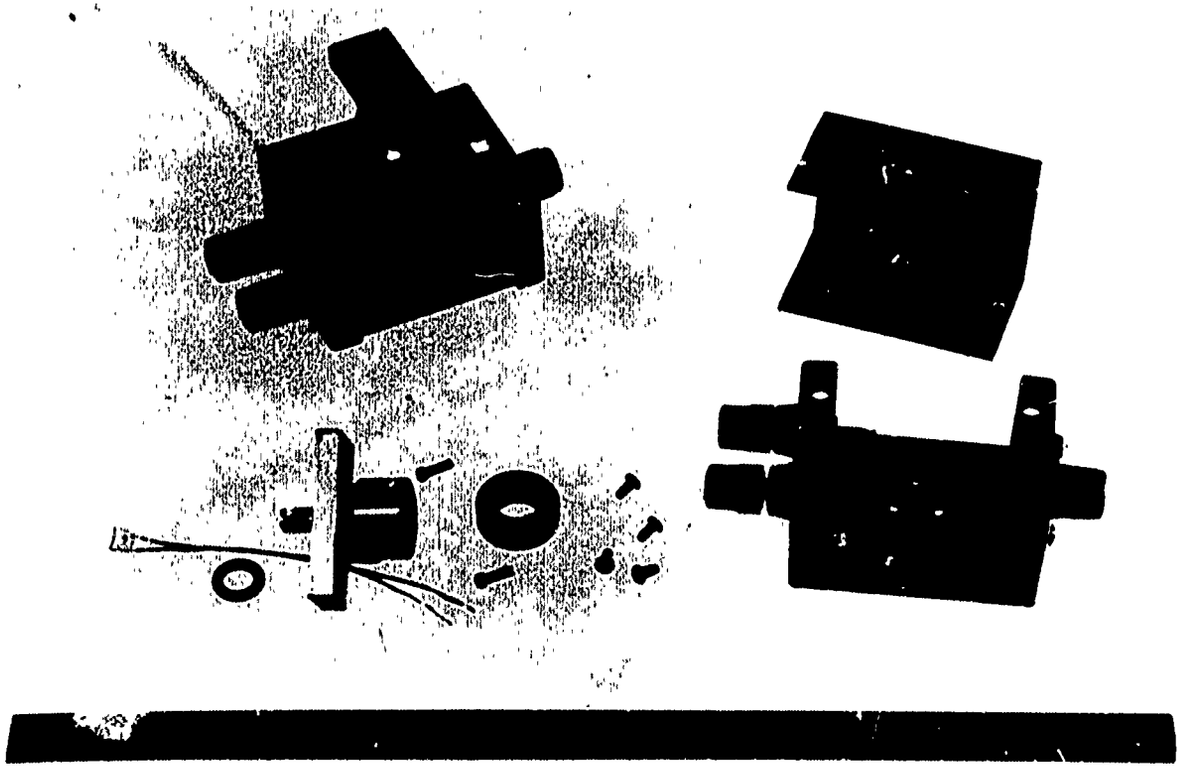

Figure 11 Exploded and Assembled View of the Thin Fi' .eat Transfer Gage

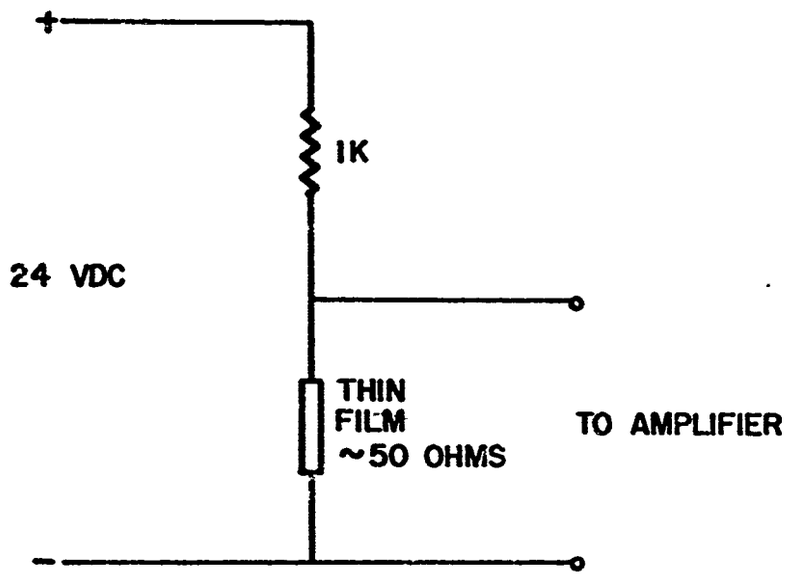

Figure 12 Schematic Diagram of the Heat Transfer Gage Circuit

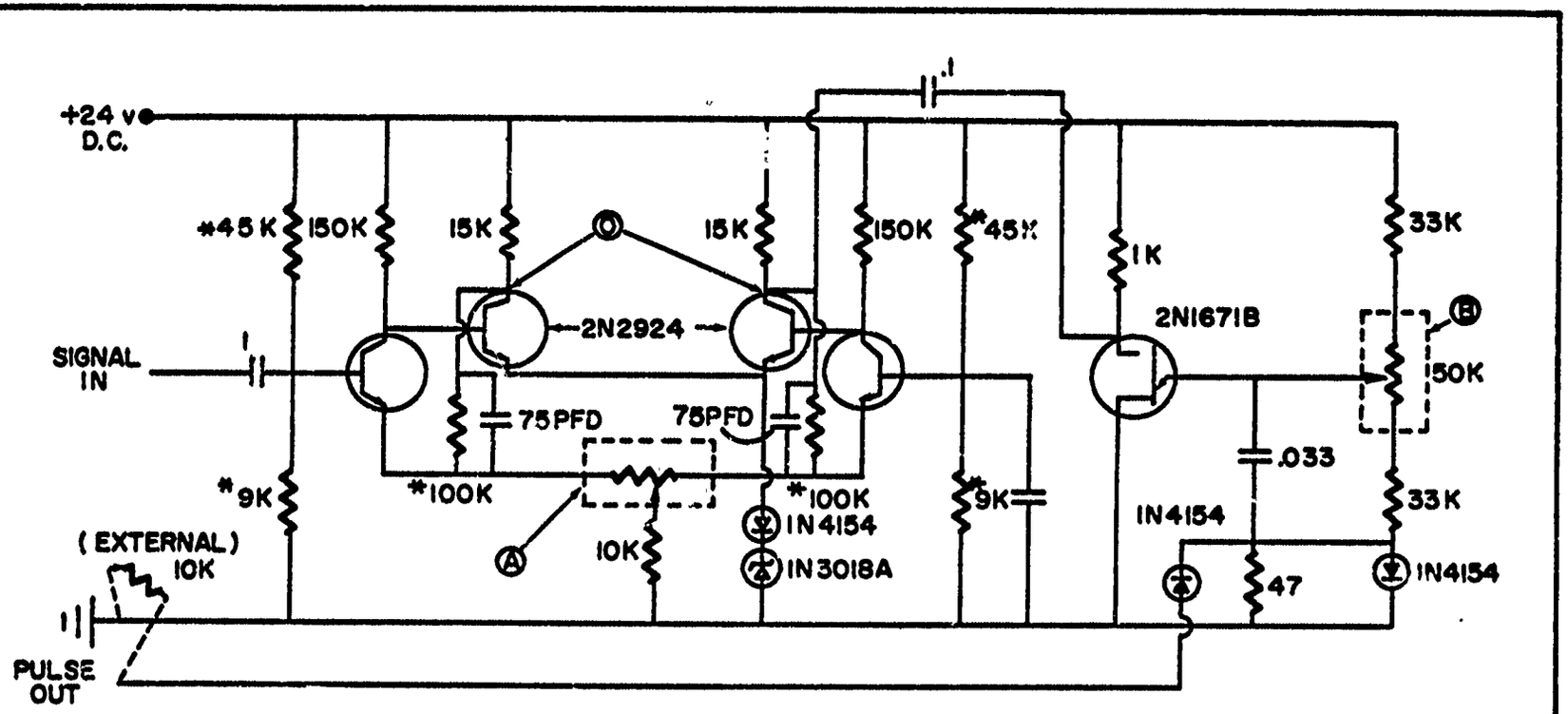

TRANSISTORS NOT IDENTIFIED ABOVE ARE 2N2924's
(A)– ADJUST FOR MINIMUM VOLTAGE BETWEEN POINTS (O)
(B)– INPUT SENSITIVITY ADJUSTMENT
*– 1% PRECISION, TEMPERATURE COMPENSATING RESISTORS

Figure 13 Circuit Diagram for Heat Transfer Gage Signal Amplifier

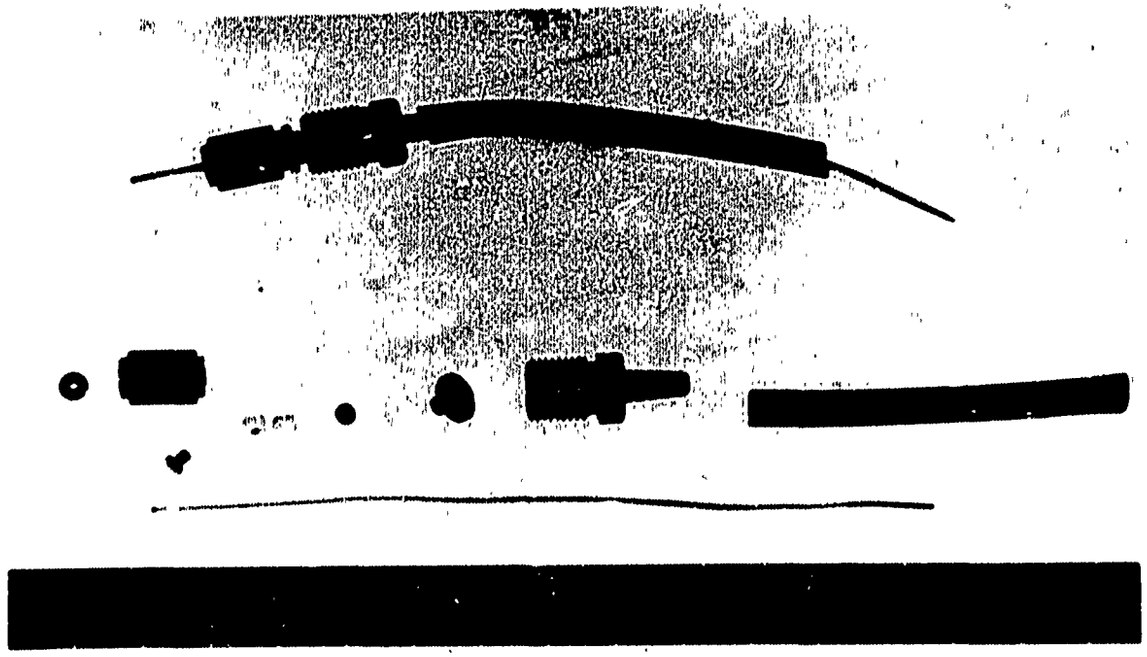

Figure 14 Exploded and Assembled View of the Ionization Probe

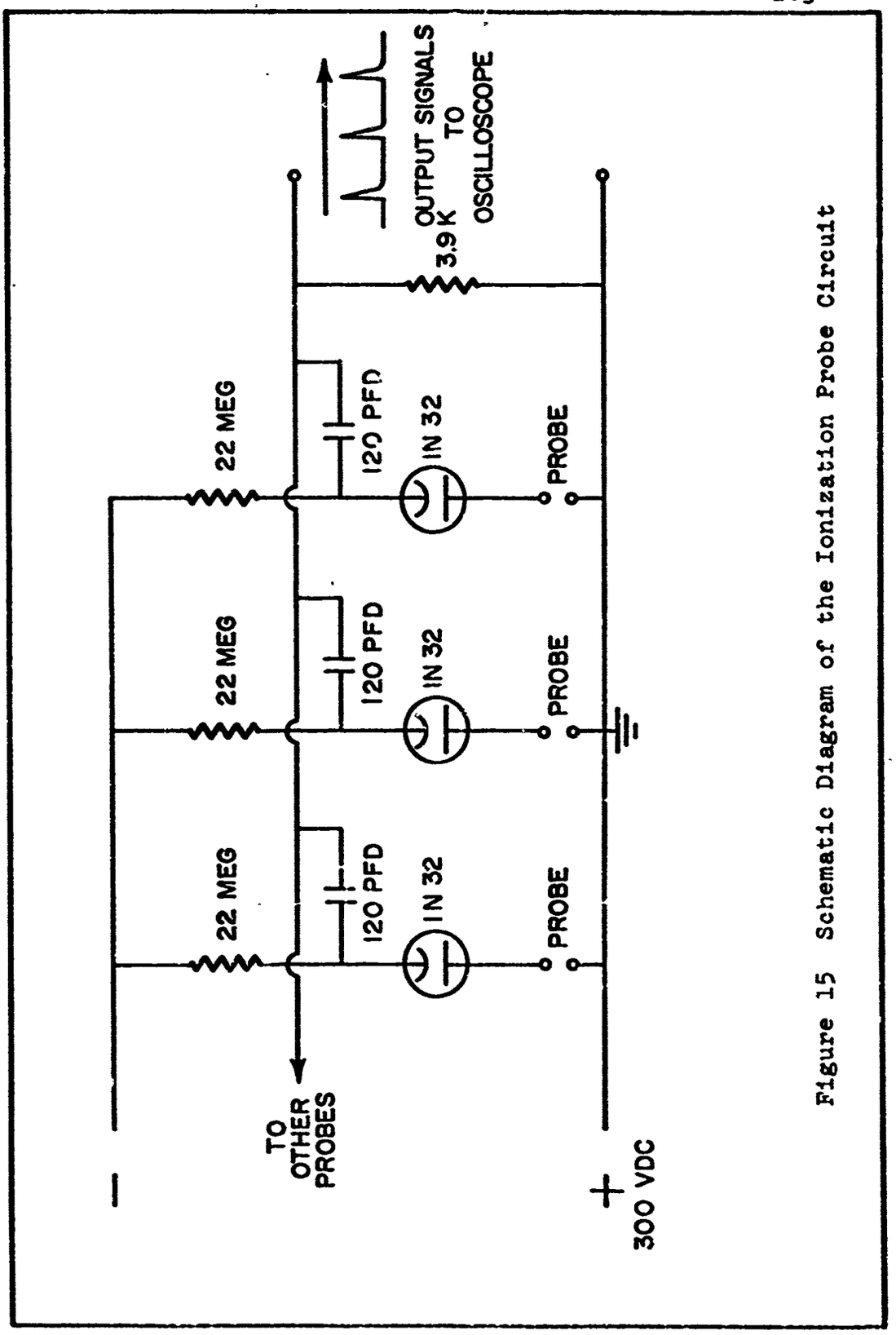

Figure 15 Schematic Diagram of the Ionization Probe Circuit

Upper Trace - Kistler Transducer Output Upon the Passage of the Incident Shock Wave

Lower Trace - Time Mark Generator Output

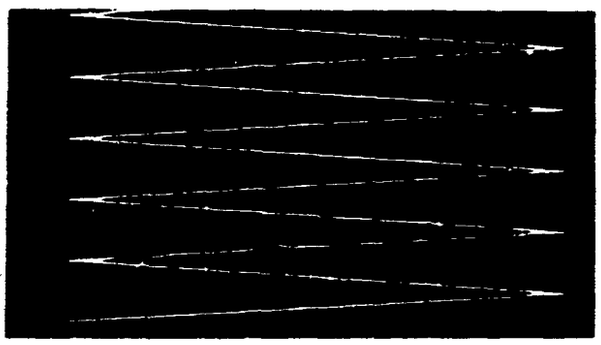

Output of the Two Heat Transfer Gages Upon the Passage of the Transmitted Shock Wave

Ionization Probe Output - No Output Due to the Absence of Ionization

Figure 16 Pictures of Oscilloscope Traces for a Typical Run in Which Detonation Did Not Occur

Upper Trace - Kistler Transducer Output Upon the Passage of the Incident Shock Wave

Lower Trace - Time Mark Generator Output

Output of the Two Heat Transfer Gages Upon the Passage of the Transmitted Shock Wave

Output From the 18 Ionization Probes

Figure 17 Pictures of Oscilloscope Traces for a Typical Run in Which Detonation Occurred

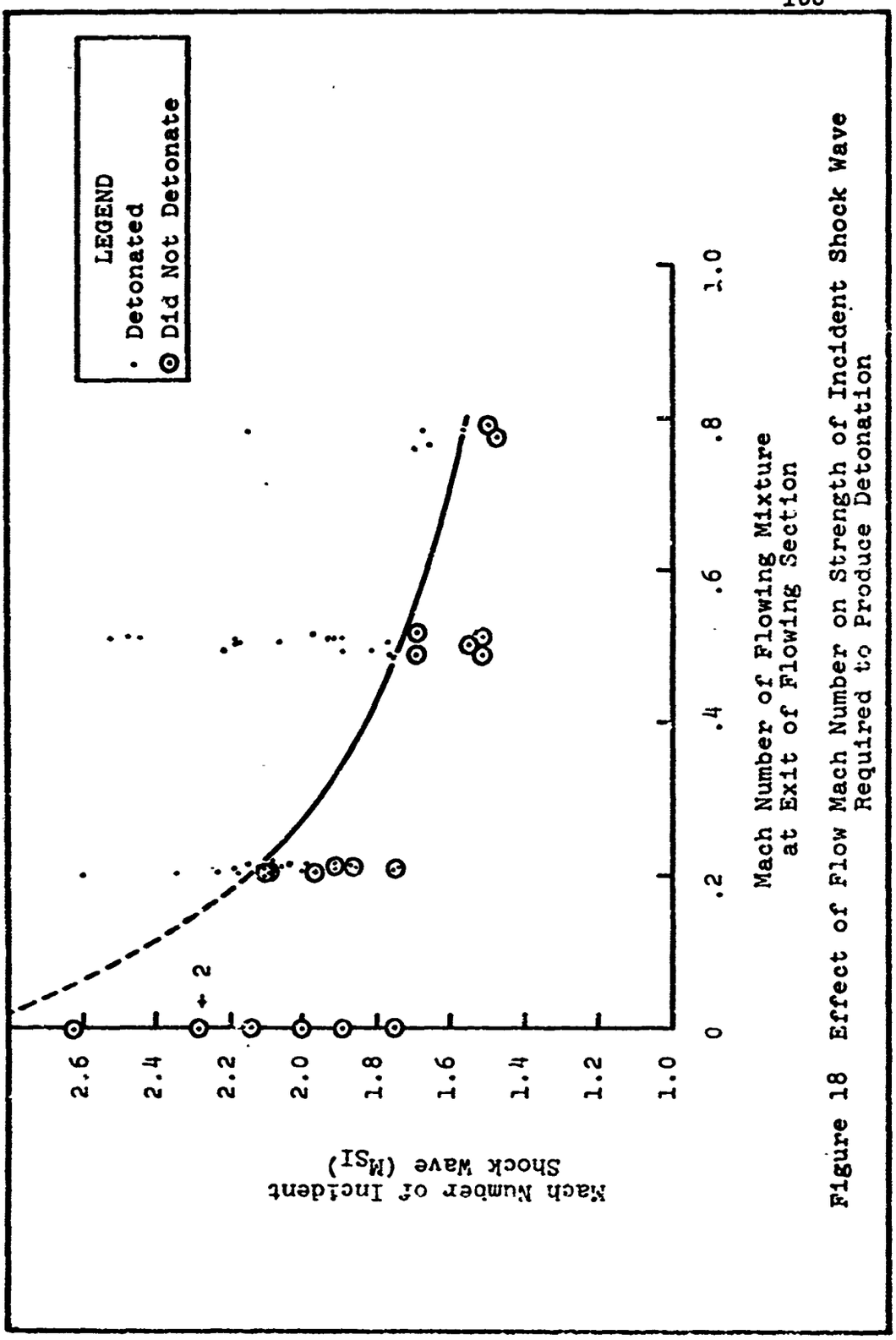

Figure 18 Effect of Flow Mach Number on Strength of Incident Shock Wave Required to Produce Detonation

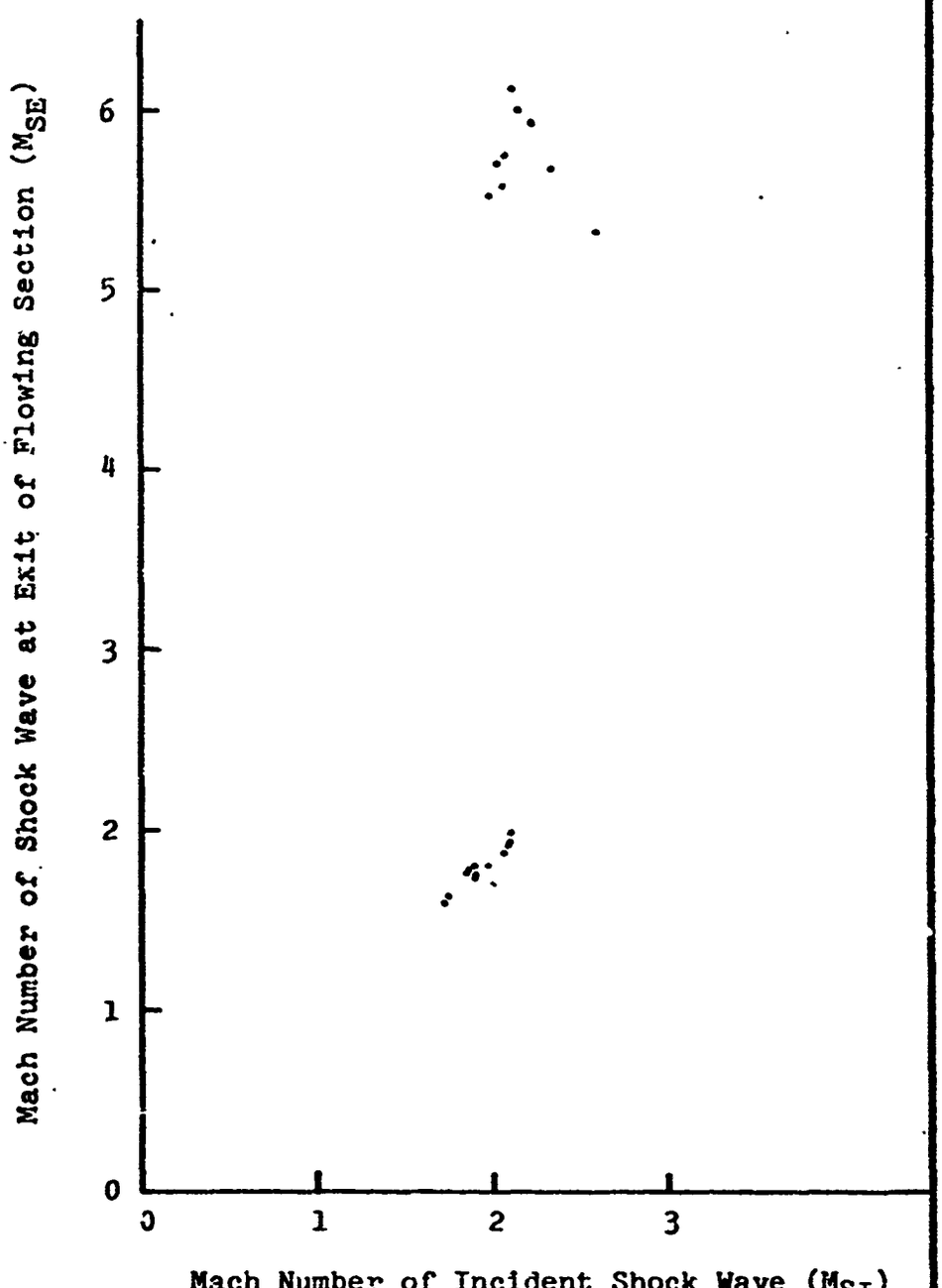

Figure 19 Mach Number of Transmitted Shock Wave Showing Effect of Transition to Detonation with a Flow Exit Mach Number of Approximately .2

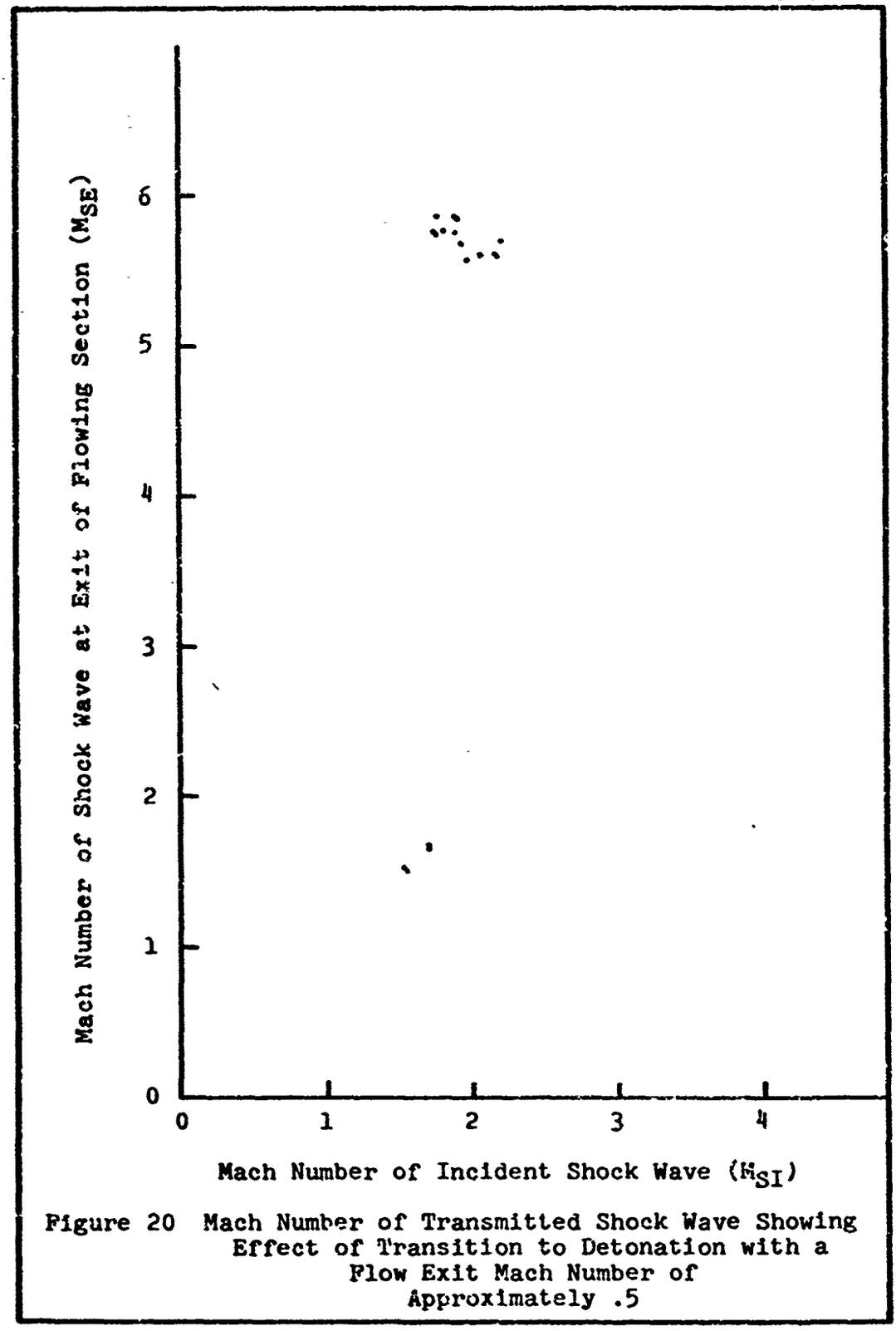

Figure 20 Mach Number of Transmitted Shock Wave Showing Effect of Transition to Detonation with a Flow Exit Mach Number of Approximately .5

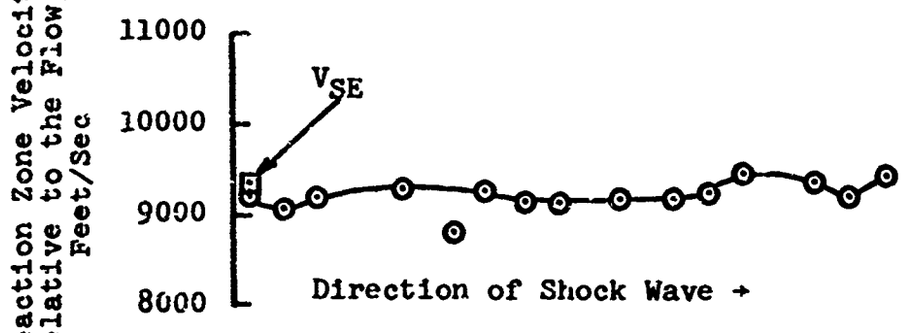

M_{Exit} = .212

M_{SI} = 1.99

H_2 Percentage = 65.84

V_{C-J} = 9242 Ft/Sec

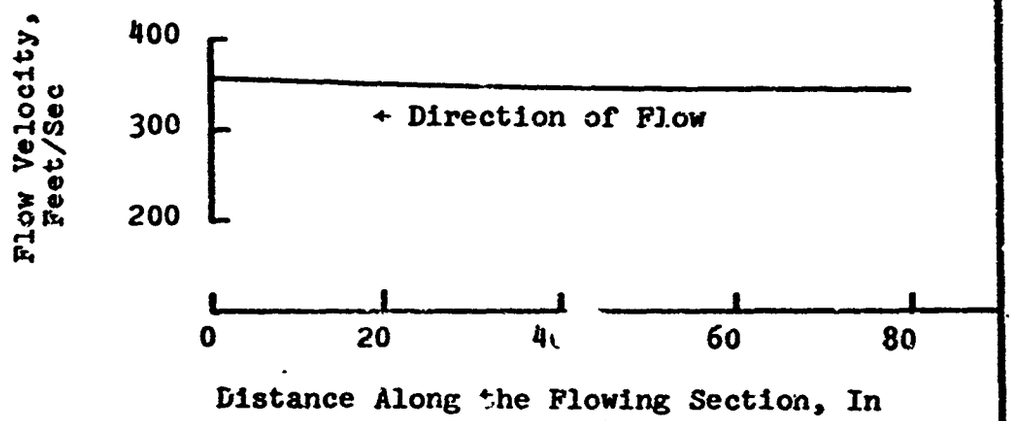

Figure 21 Flow and Reaction Zone Velocities in the Flowing Section, Run 42

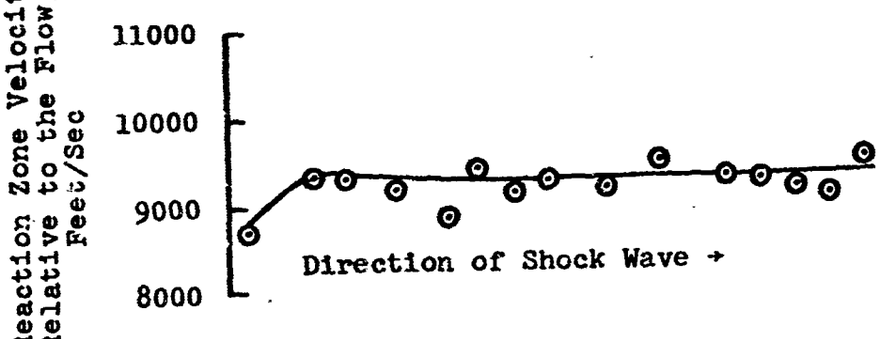

M_{Exit} = .208

M_{SI} = 2.00

H_2 Percentage = 66.83

V_{C-J} = 9360 Ft/Sec

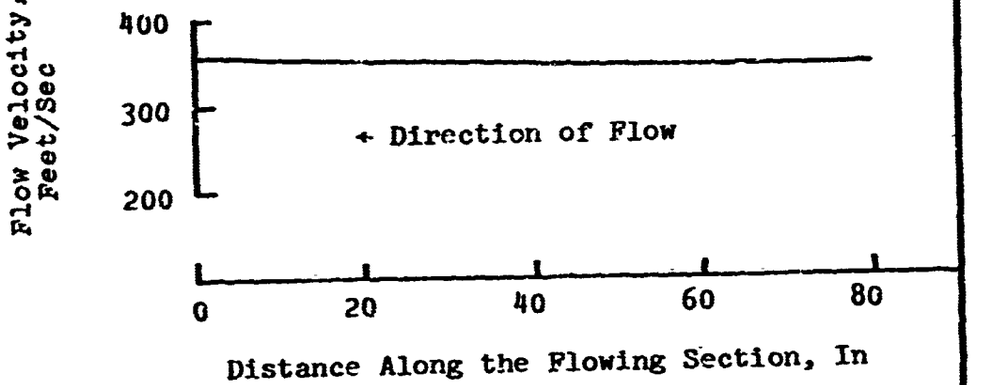

Figure 22 Flow and Reaction Zone Velocities in the Flowing Section, Run 46

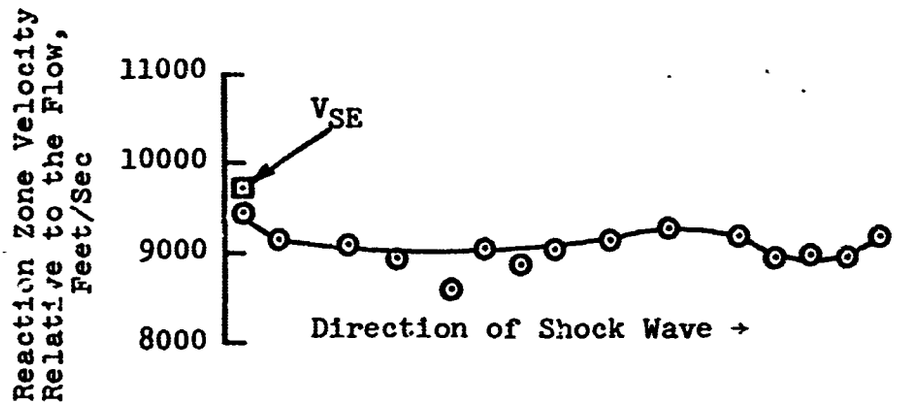

M_{Exit} = .217

M_{SI} = 2.04

H_2 Percentage = 66.73

V_{C-J} = 9350 Ft/Sec

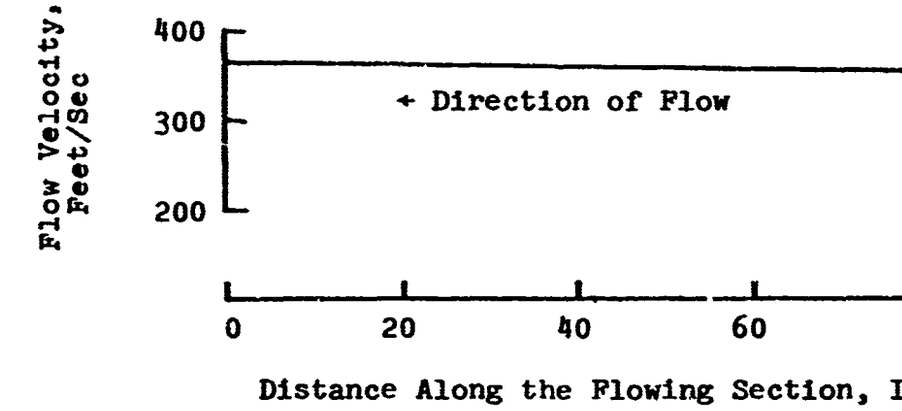

Figure 23 Flow and Reaction Zone Velocities in the Flowing Section, Run 35

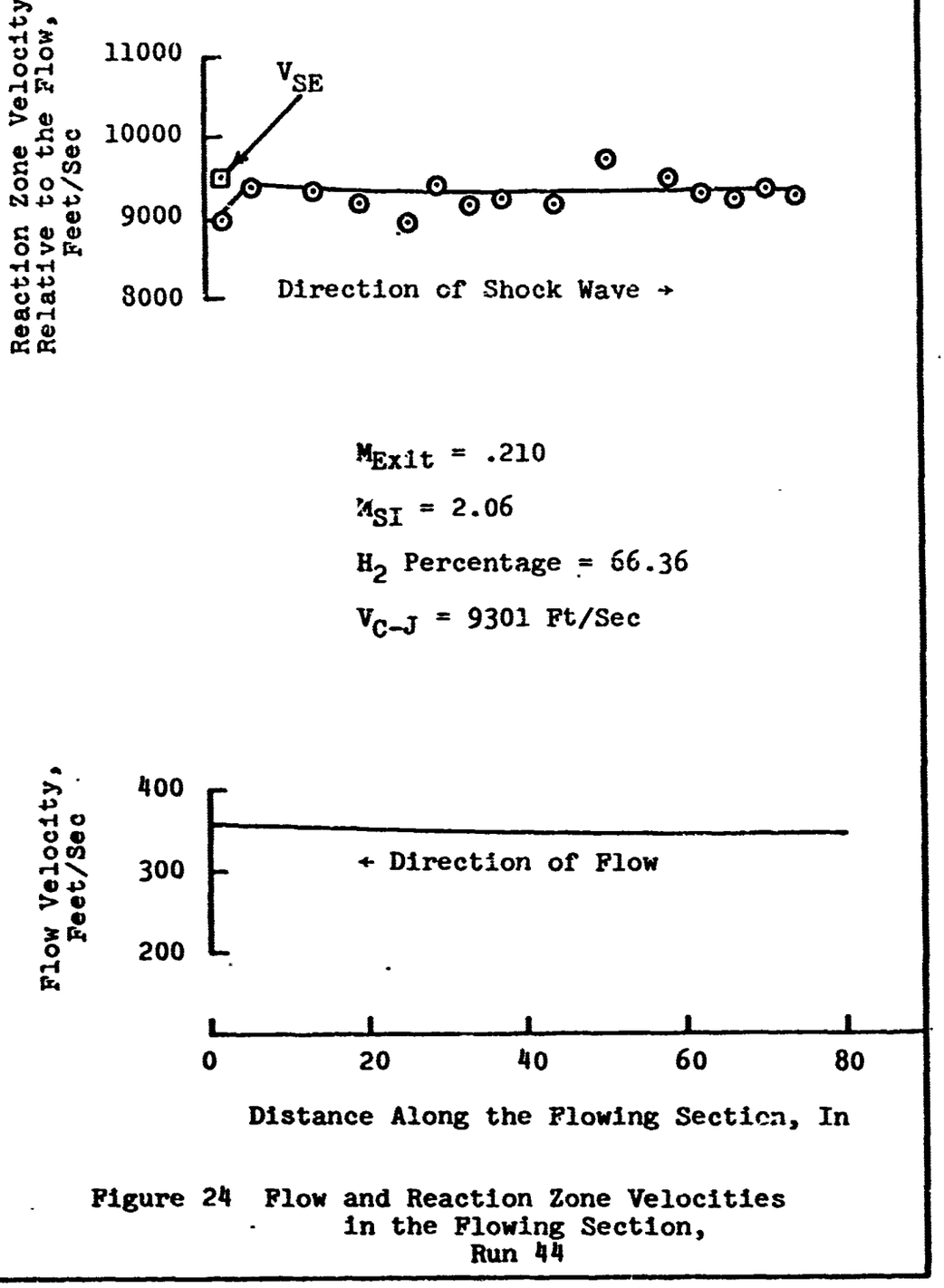

Figure 24 Flow and Reaction Zone Velocities in the Flowing Section, Run 44

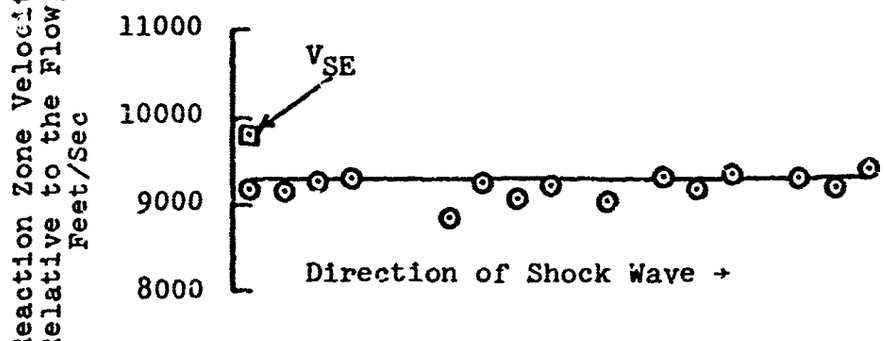

M_{Exit} = .215

M_{SI} = 2.08

H_2 Percentage = 67.49

V_{C-J} = 9452 Ft/Sec

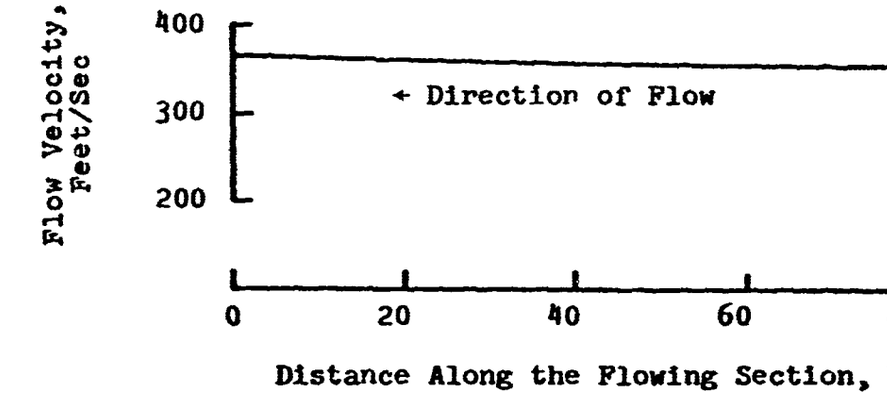

Figure 25 Flow and Reaction Zone Velocities in the Flowing Section, Run 31

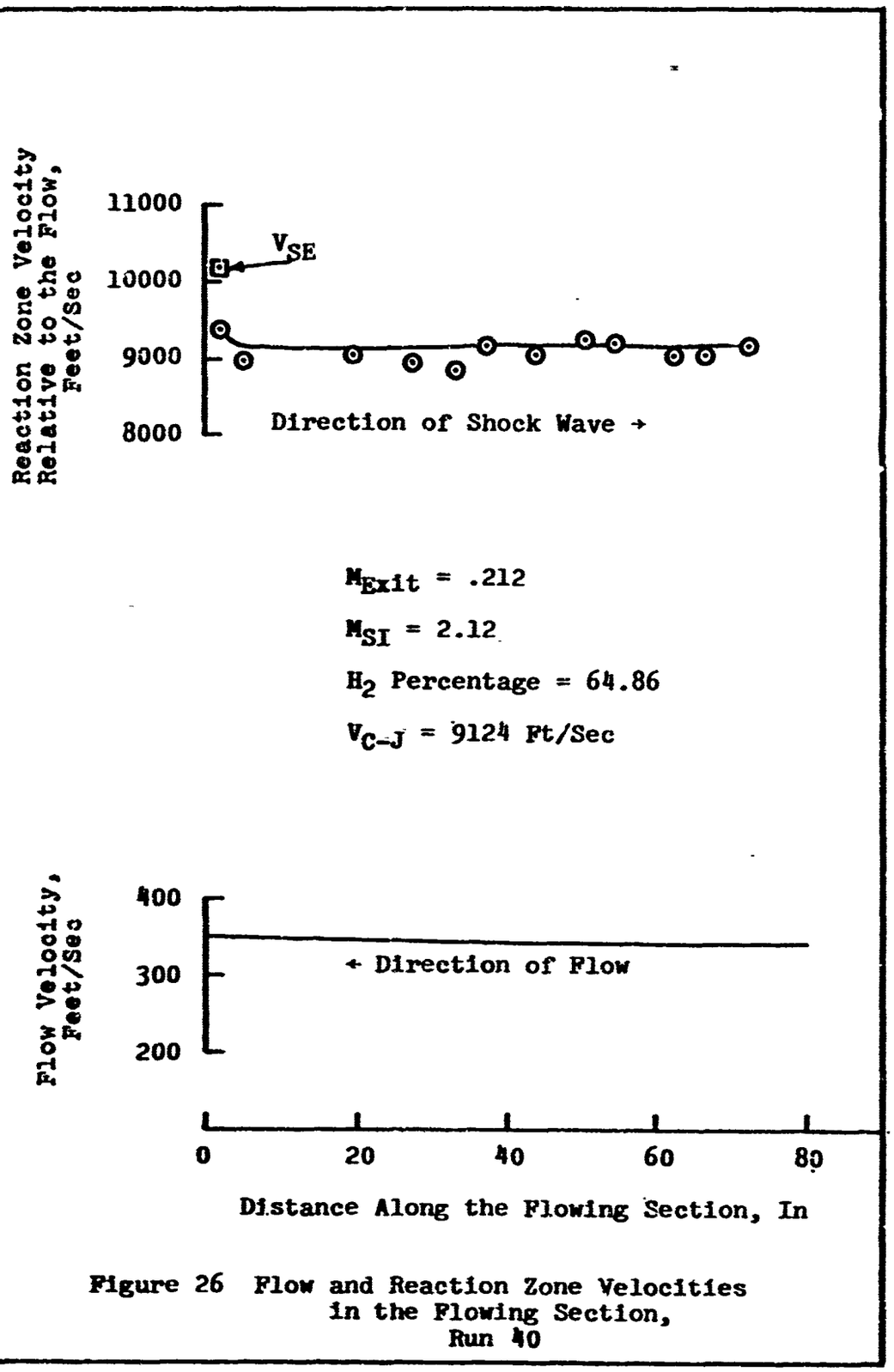

Figure 26 Flow and Reaction Zone Velocities in the Flowing Section, Run 40

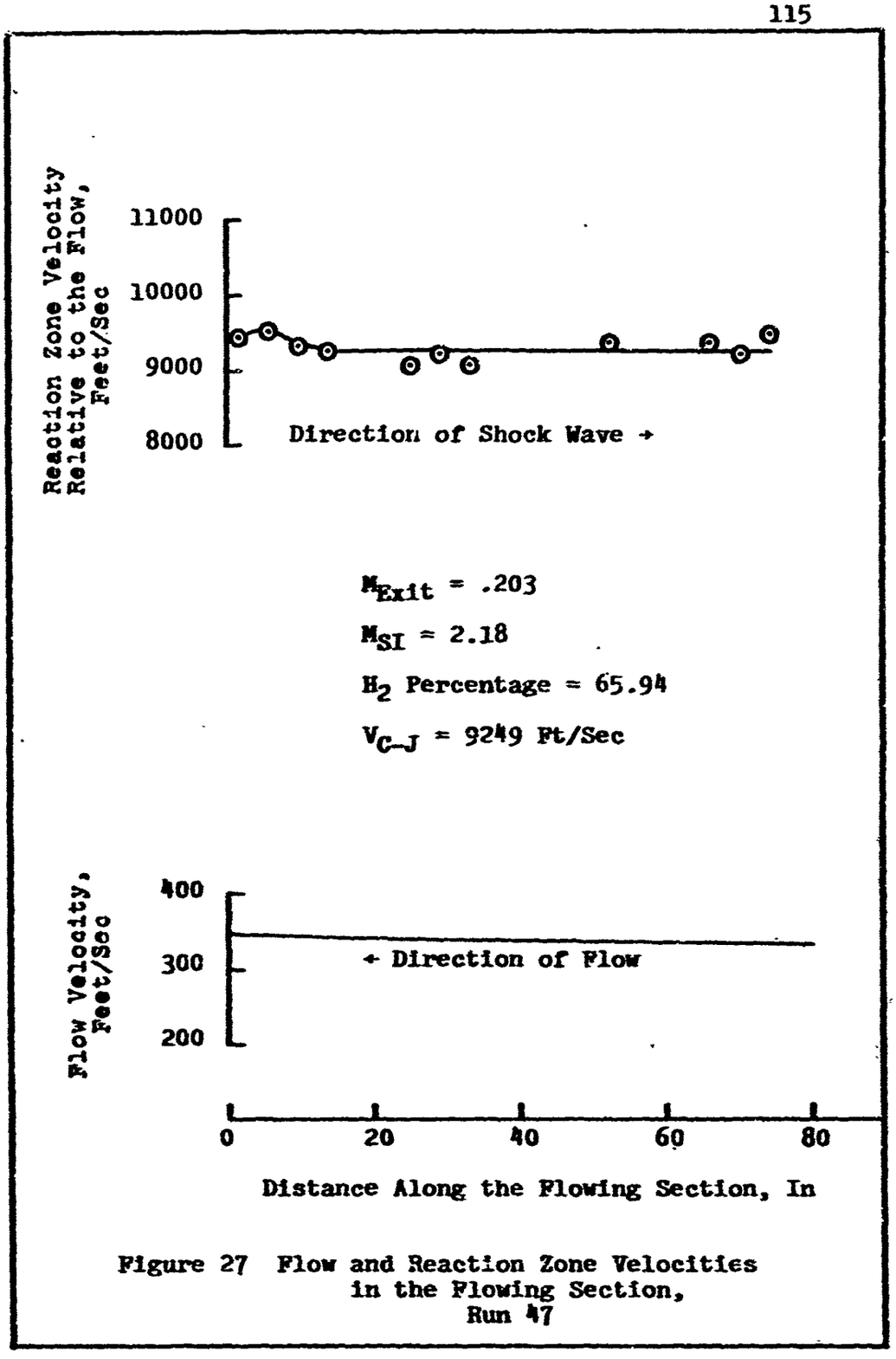

Figure 27 Flow and Reaction Zone Velocities in the Flowing Section, Run 47

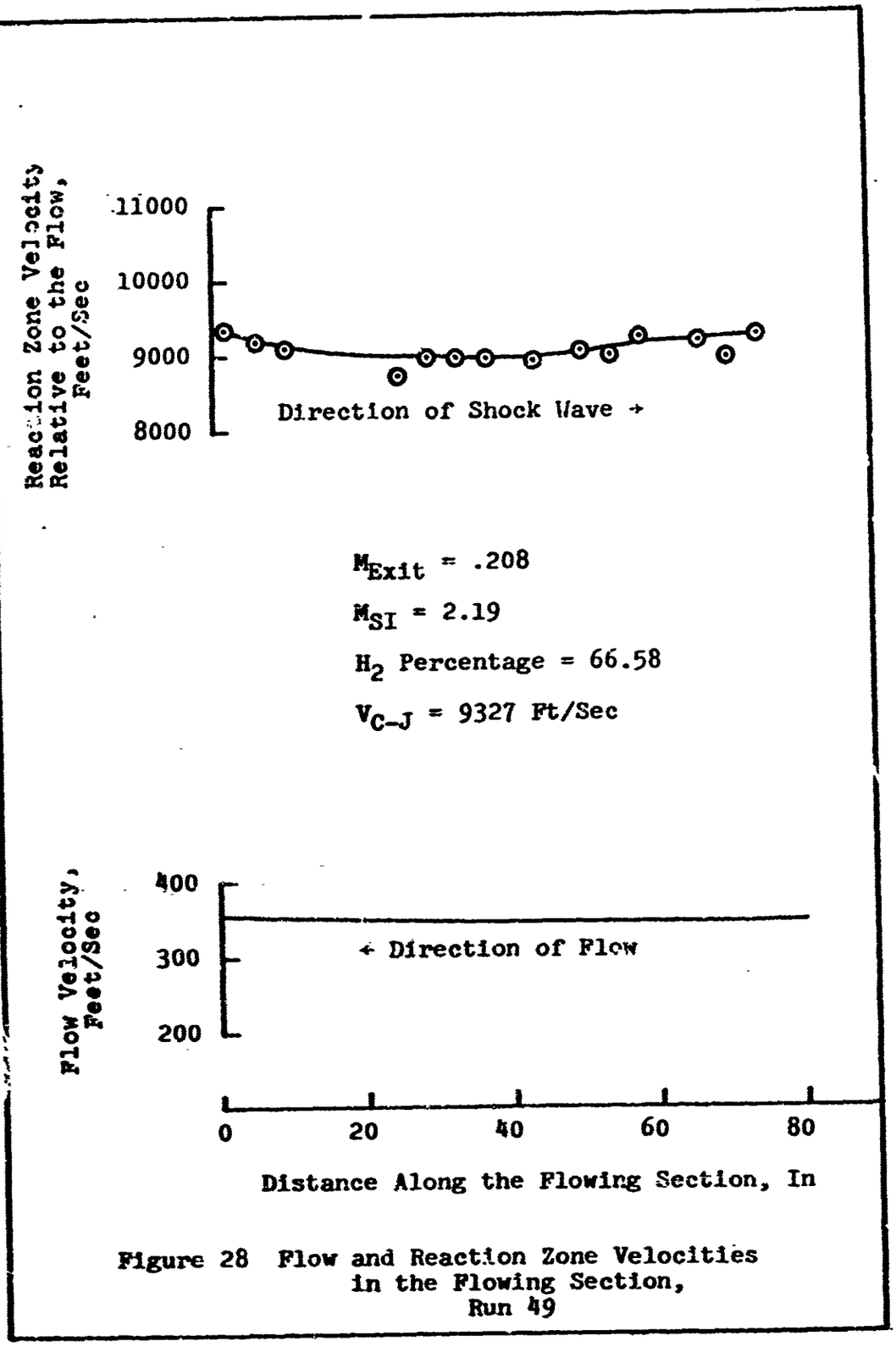

Figure 28 Flow and Reaction Zone Velocities in the Flowing Section, Run 49

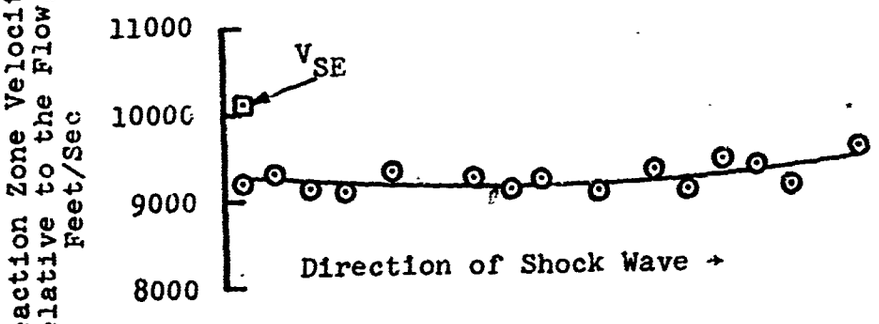

M_{Exit} = .207

M_{SI} = 2.23

H_2 Percentage = 66.45

V_{C-J} = 9314 Ft/Sec

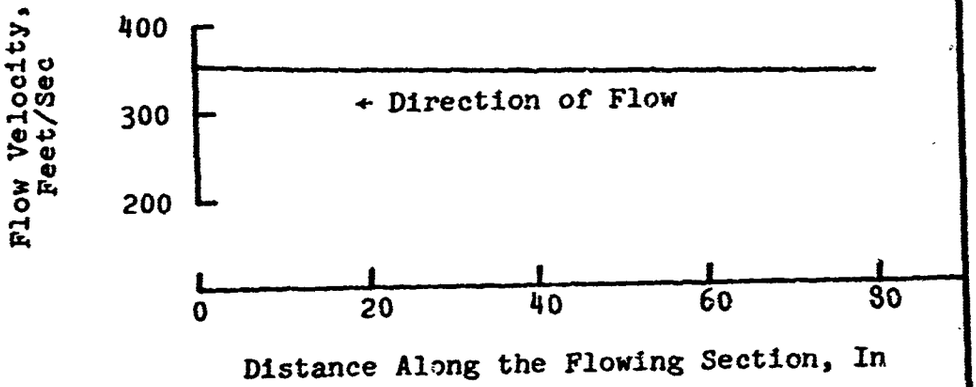

Figure 29 Flow and Reaction Zone Velocities in the Flowing Section, Run 43

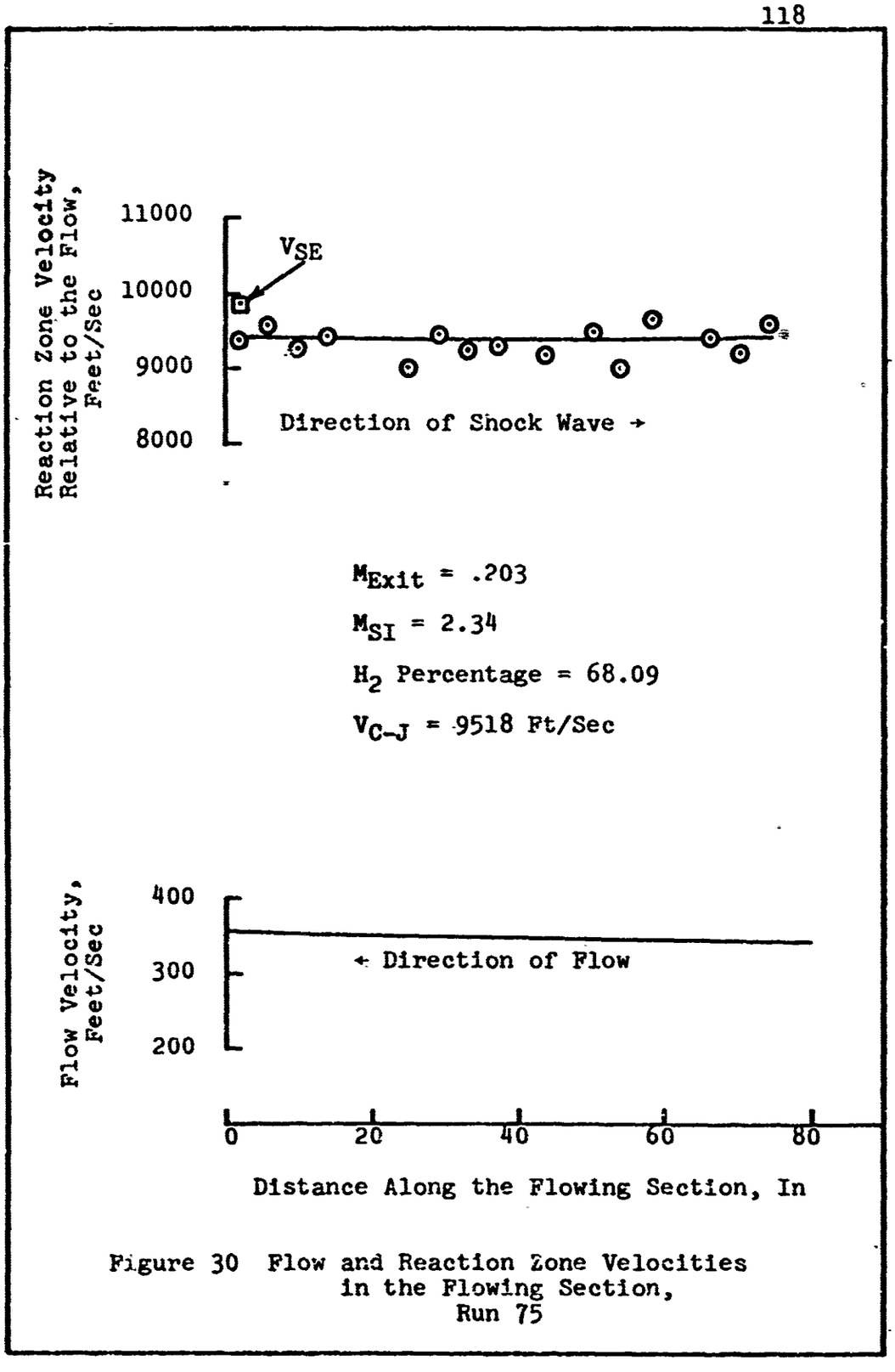

Figure 30 Flow and Reaction Zone Velocities in the Flowing Section, Run 75

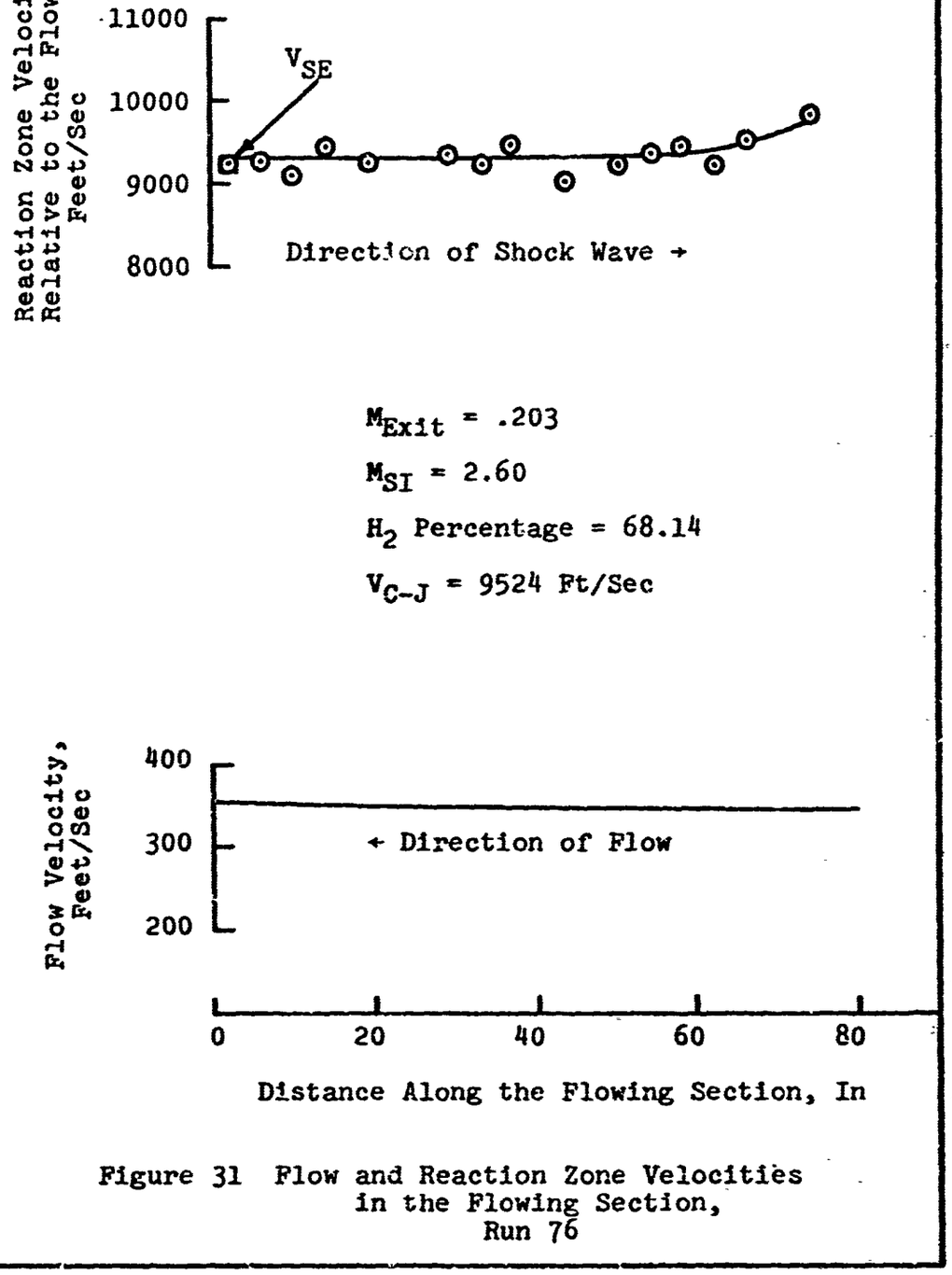

Figure 31 Flow and Reaction Zone Velocities in the Flowing Section, Run 76

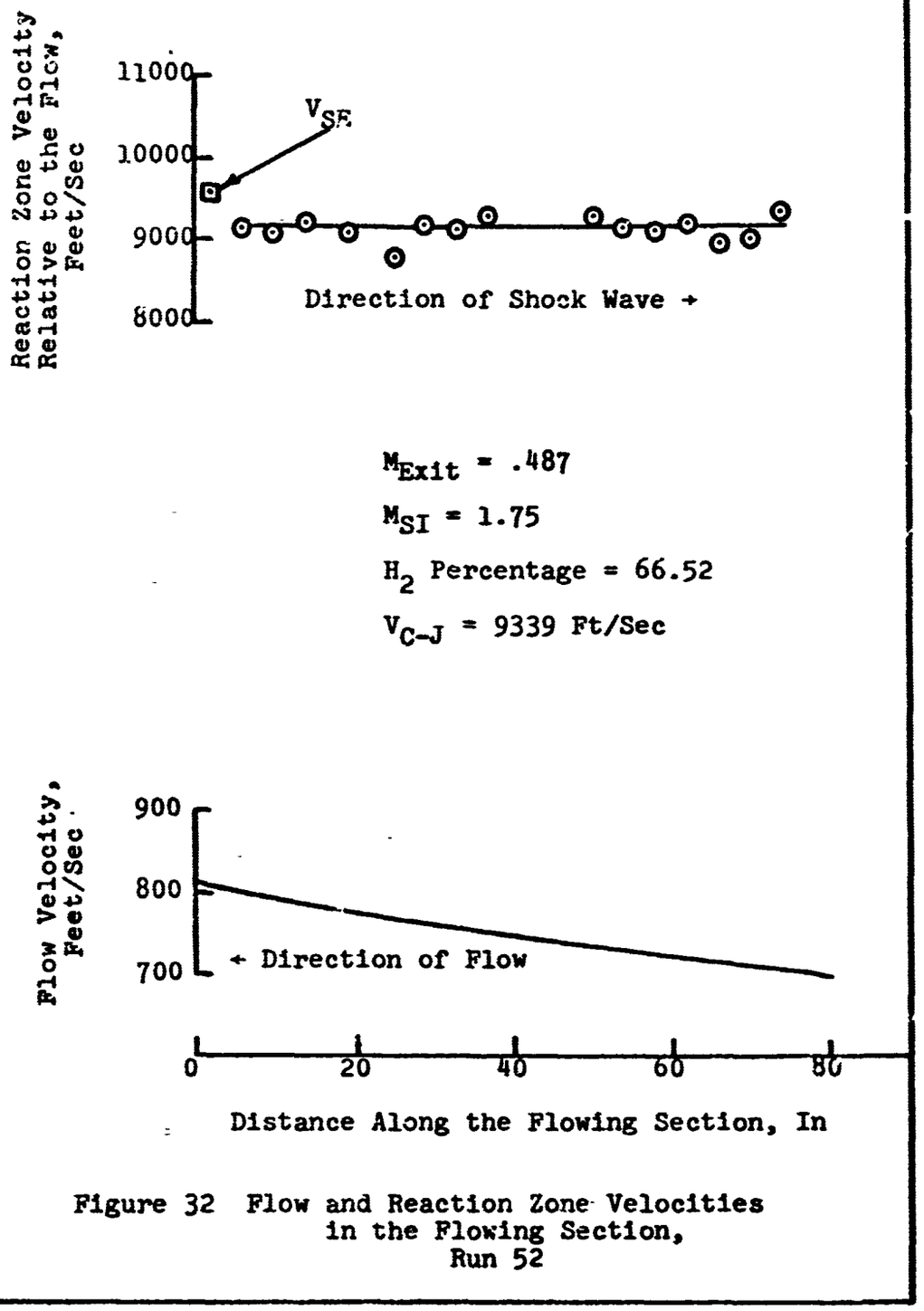

Figure 32 Flow and Reaction Zone Velocities in the Flowing Section, Run 52

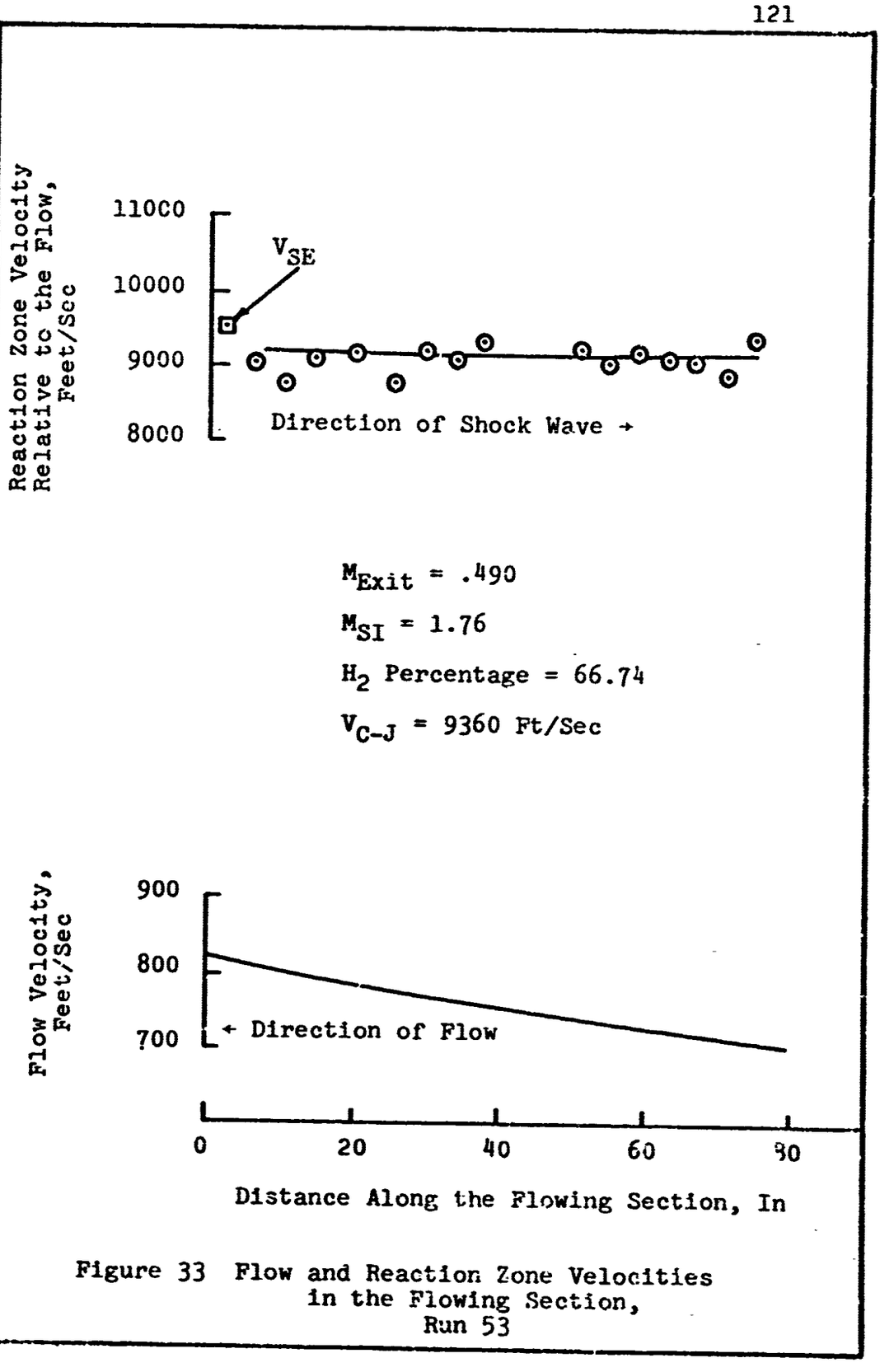

Figure 33 Flow and Reaction Zone Velocities in the Flowing Section, Run 53

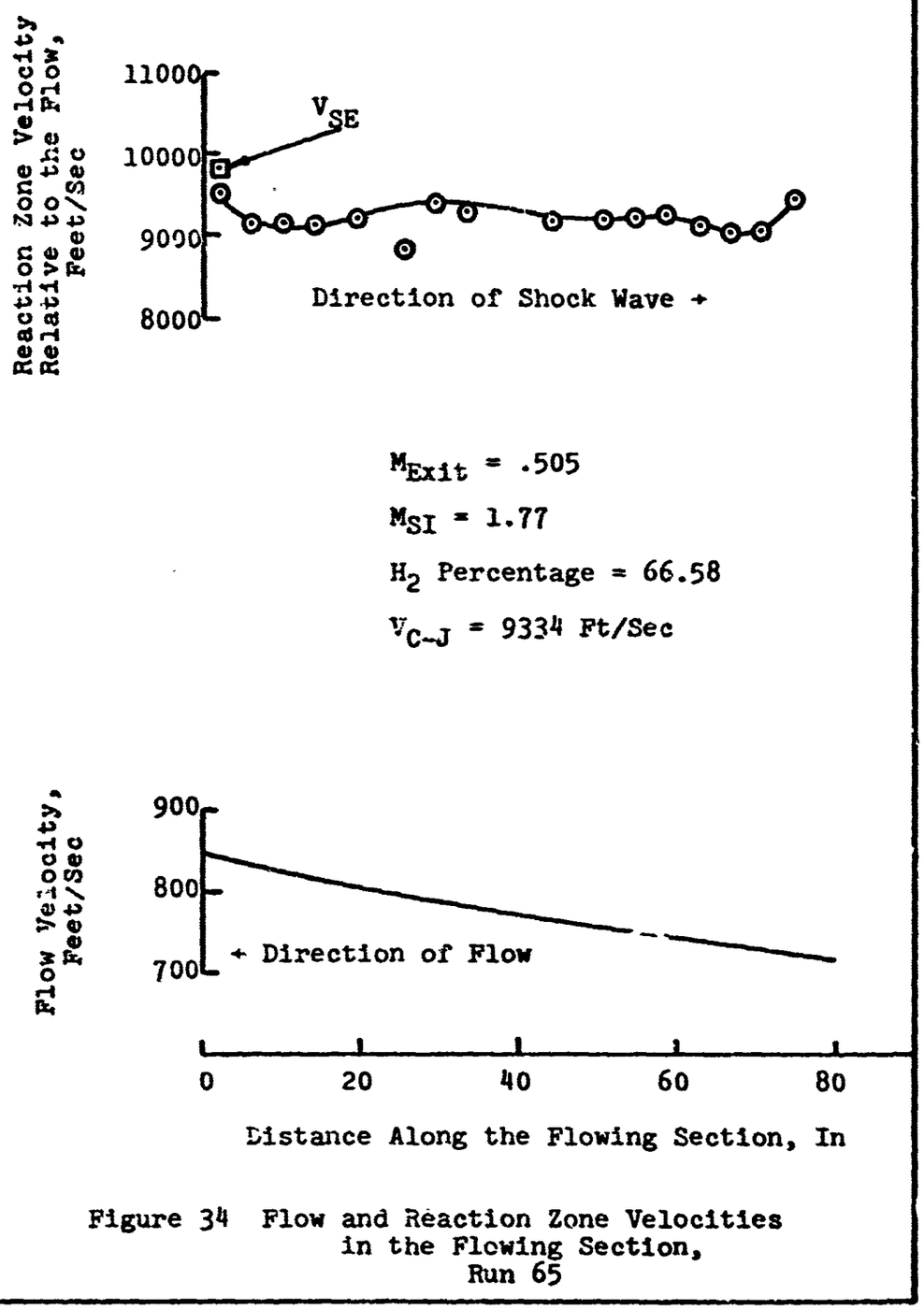

Figure 34 Flow and Reaction Zone Velocities in the Flowing Section, Run 65

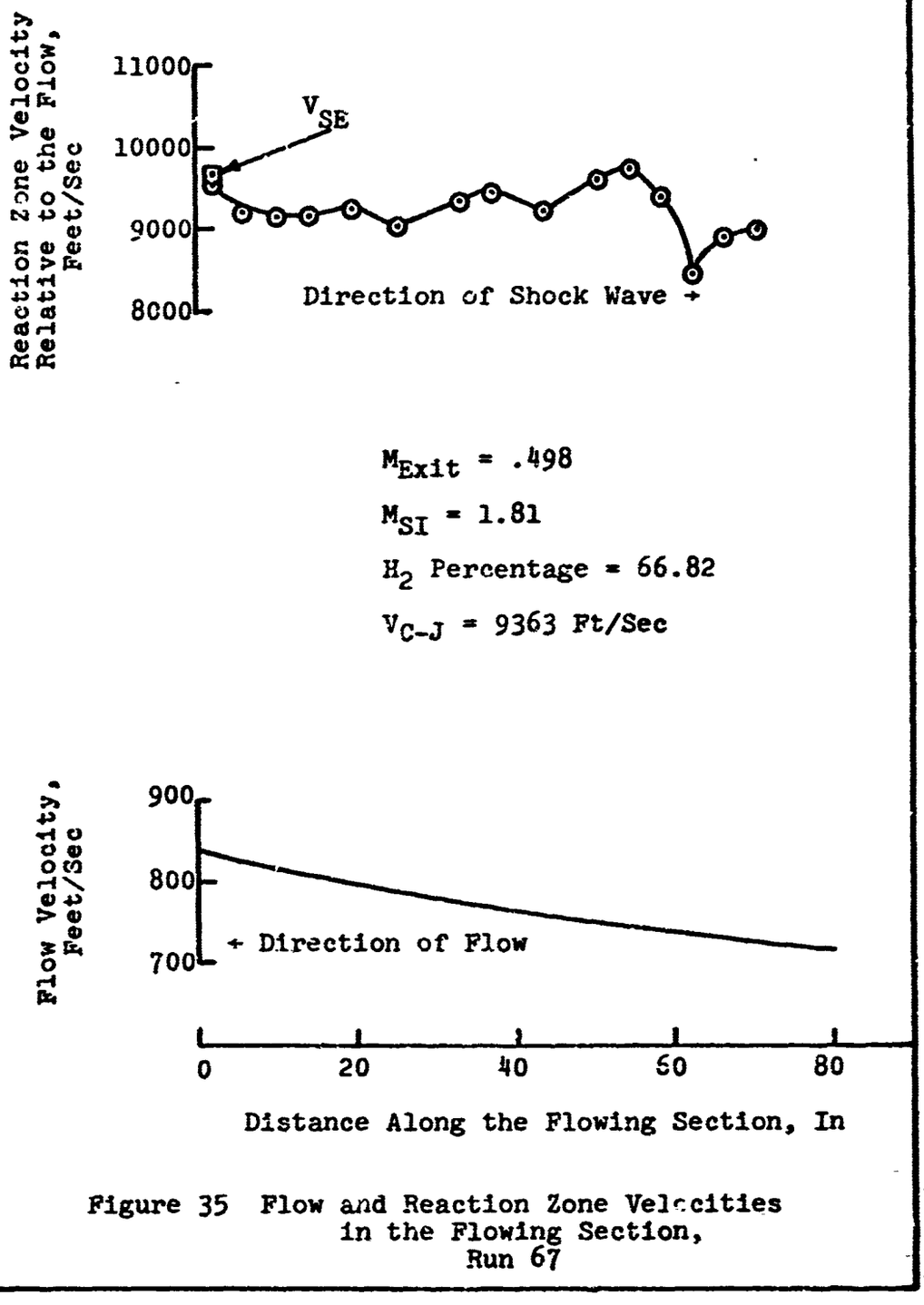

Figure 35 Flow and Reaction Zone Velocities in the Flowing Section, Run 67

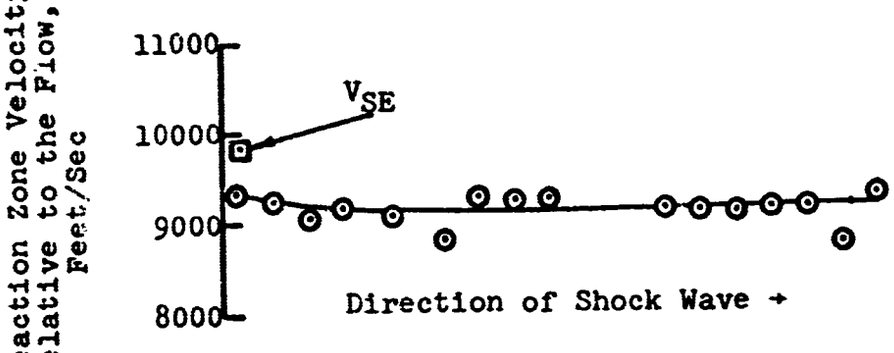

M_{Exit} = .496

M_{SI} = 1.89

H_2 Percentage = 67.12

V_{C-J} = 9406 Ft/Sec

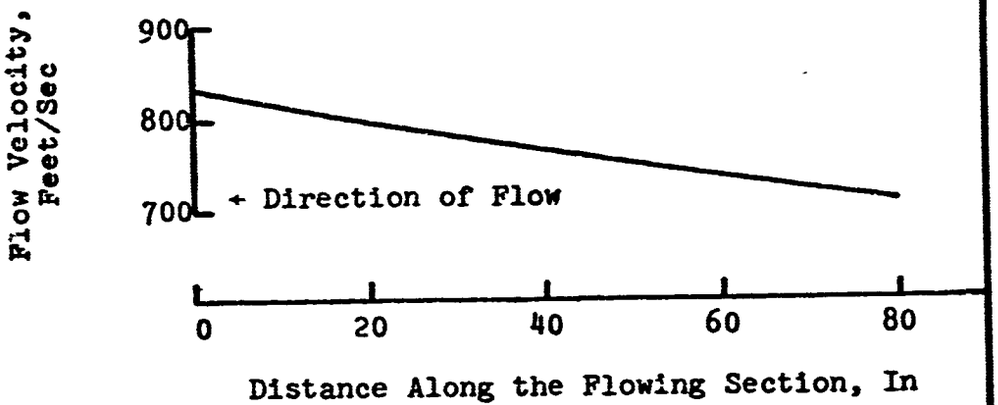

Figure 36 Flow and Reaction Zone Velocities in the Flowing Section, Run 51

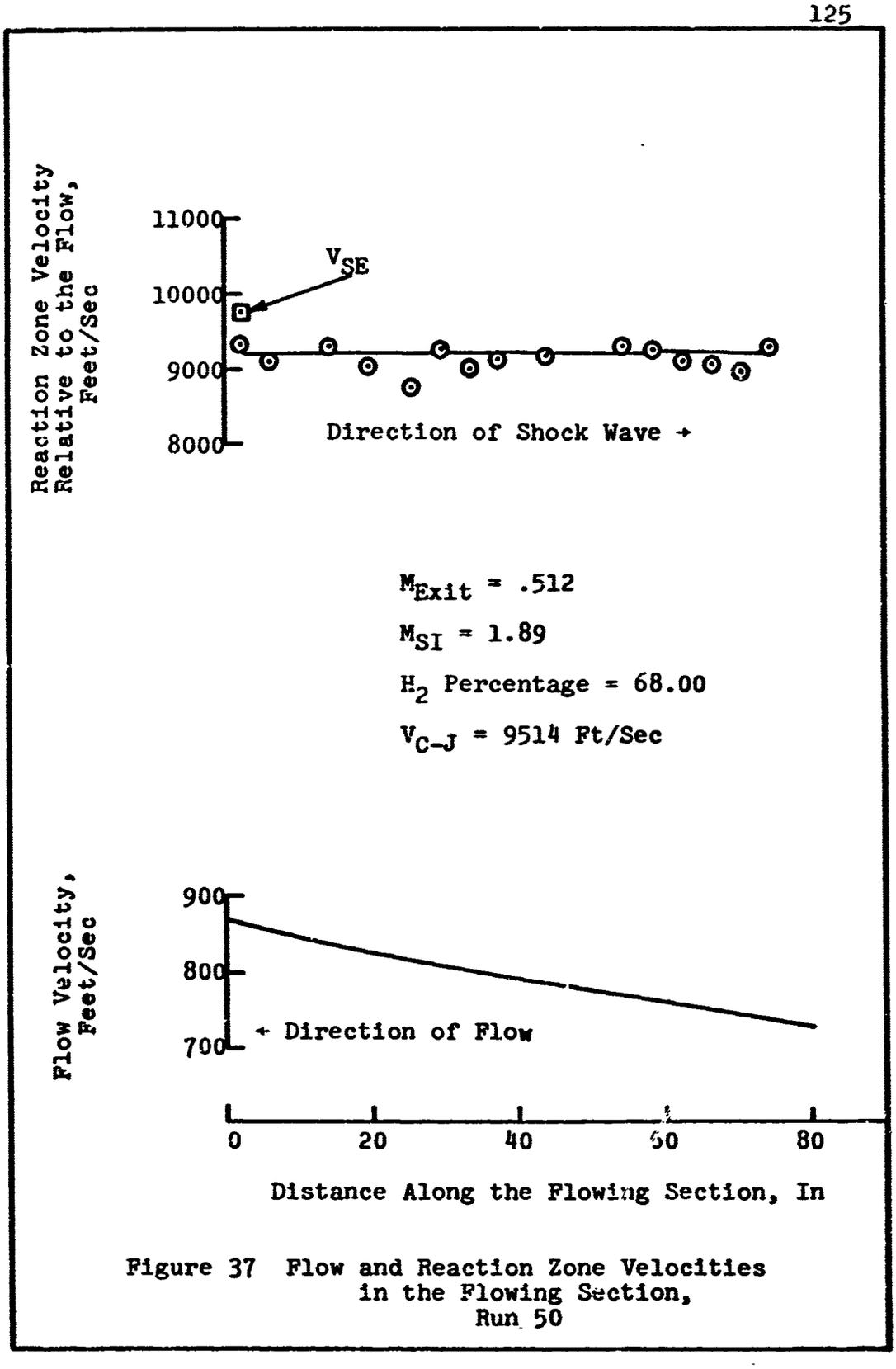

Figure 37 Flow and Reaction Zone Velocities in the Flowing Section, Run 50

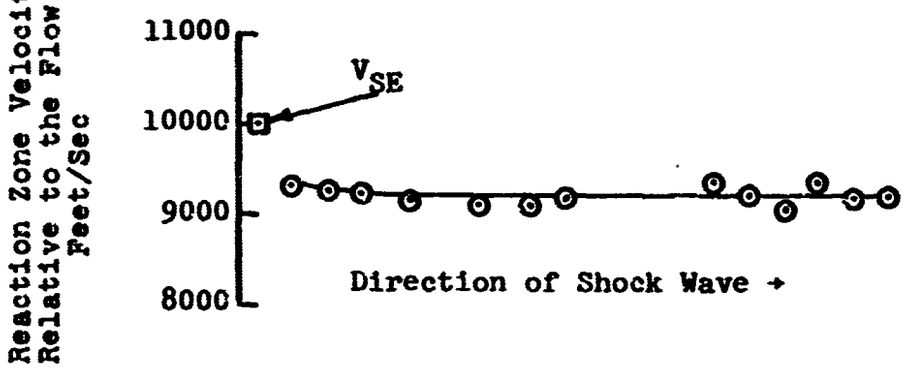

M_{Exit} = .510

M_{SI} = 1.91

H_2 Percentage = 66.86

V_{C-J} = 9357 Ft/Sec

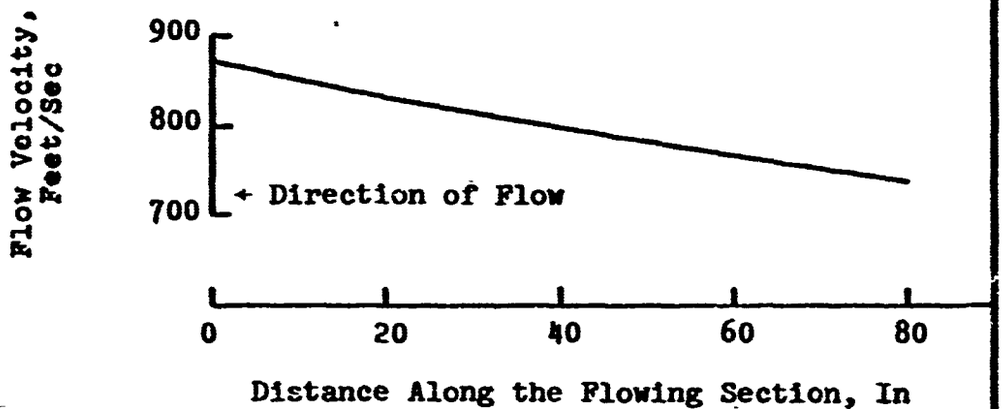

Figure 38 Flow and Reaction Zone Velocities in the Flowing Section, Run 56

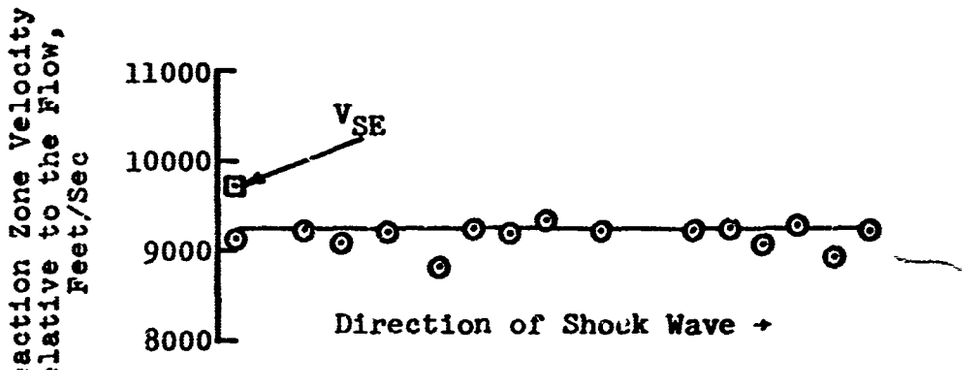

M_{Exit} = .508

M_{SI} = 1.93

H_2 Percentage = 66.75

V_{C-J} = 9344 Ft/Sec

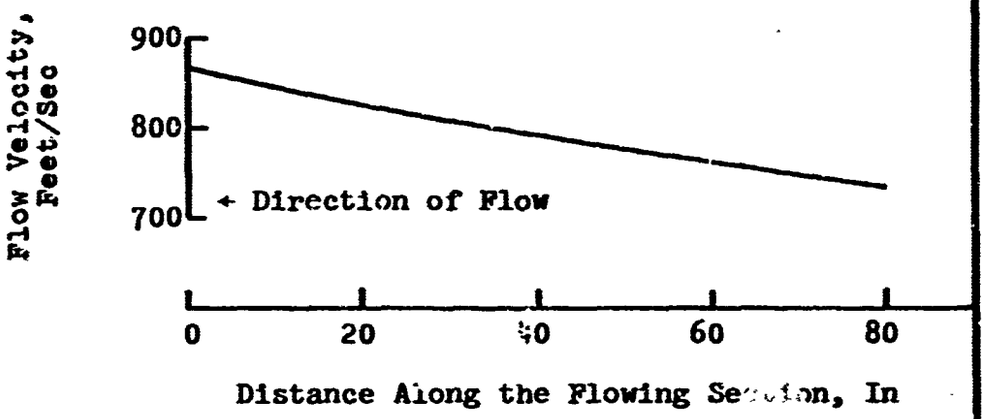

Figure 39 Flow and Reaction Zone Velocities in the Flowing Section, Run 58

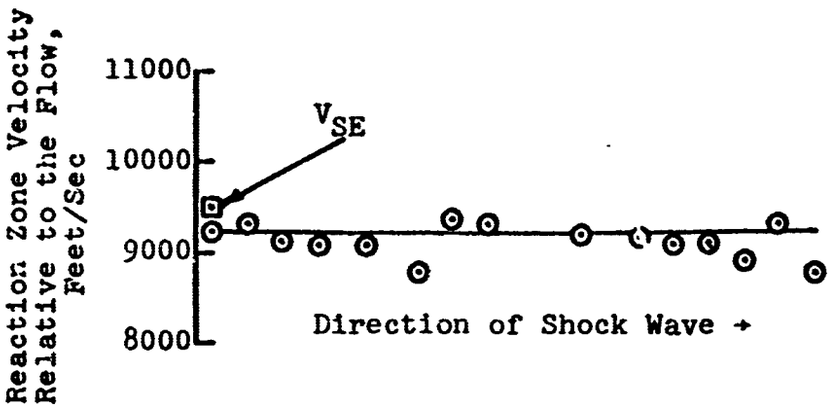

M_{Exit} = .516

M_{SI} = 1.97

H_2 Percentage = 66.51

V_{C-J} = 9341 Ft/Sec

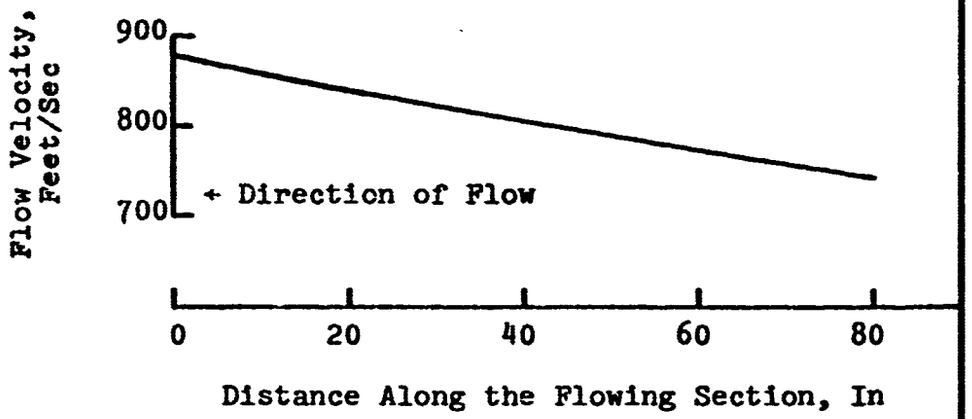

Figure 40 Flow and Reaction Zone Velocities in the Flowing Section, Run 57

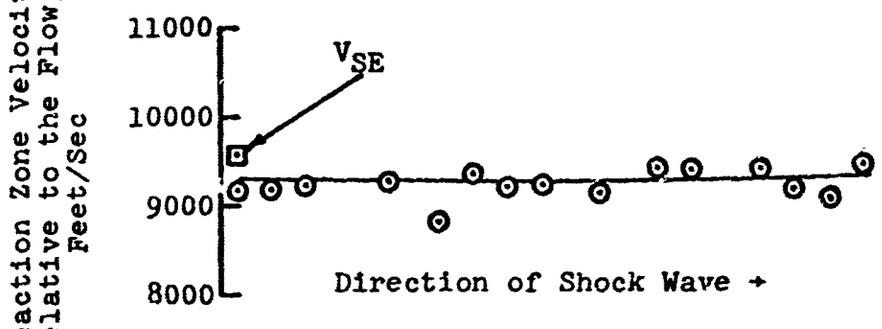

M_{Exit} = .506

M_{SI} = 2.06

H_2 Percentage = 57.03

V_{C-J} = 9376 Ft/Sec

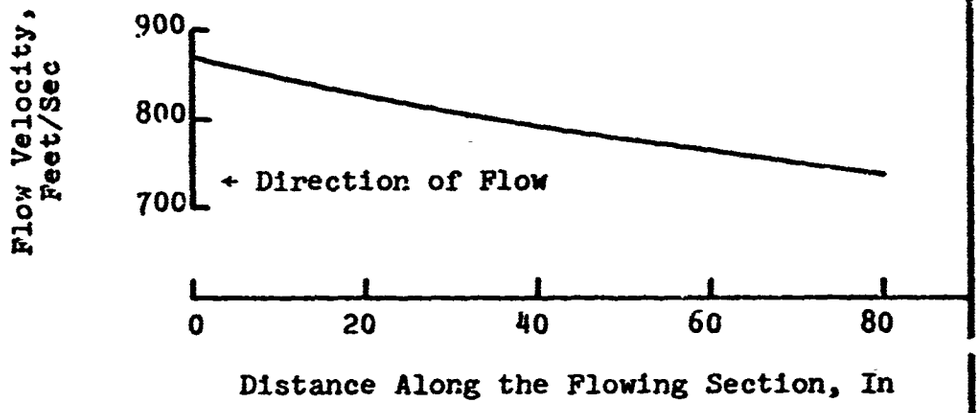

Figure 41 Flow and Reaction Zone Velocities in the Flowing Section, Run 59

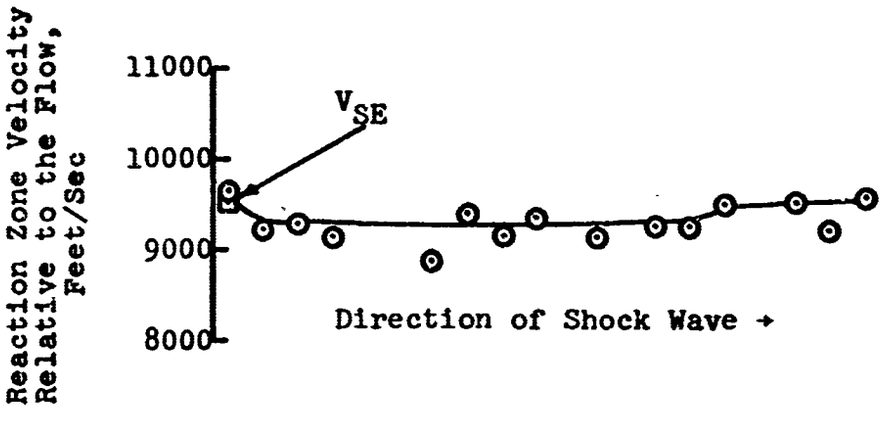

M_{Exit} = .506

M_{SI} = 2.17

H_2 Percentage = 66.70

V_{C-J} = 9337 Ft/Sec

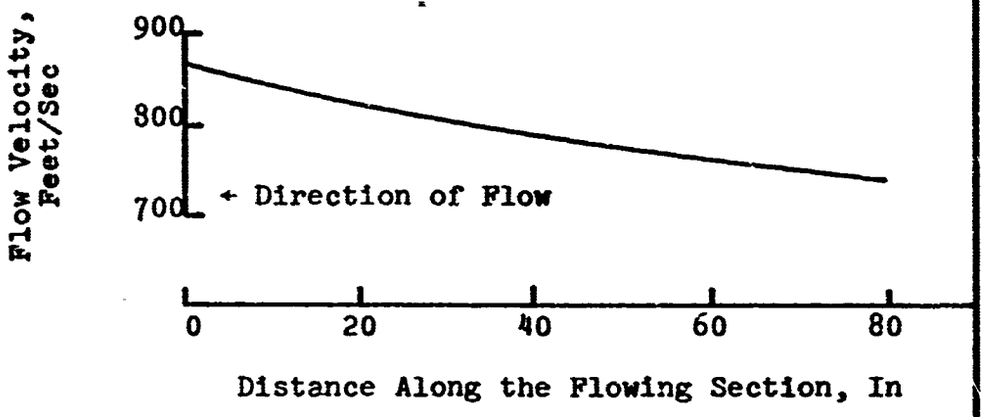

Figure 42 Flow and Reaction Zone Velocities in the Flowing Section, Run 60

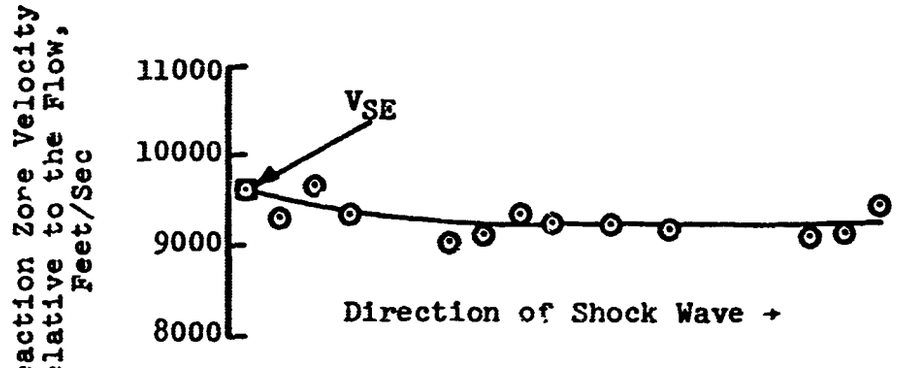

M_{Exit} = .506

M_{SI} = 2.18

H_2 Percentage = 67.49

V_{C-J} = 9436 Ft/Sec

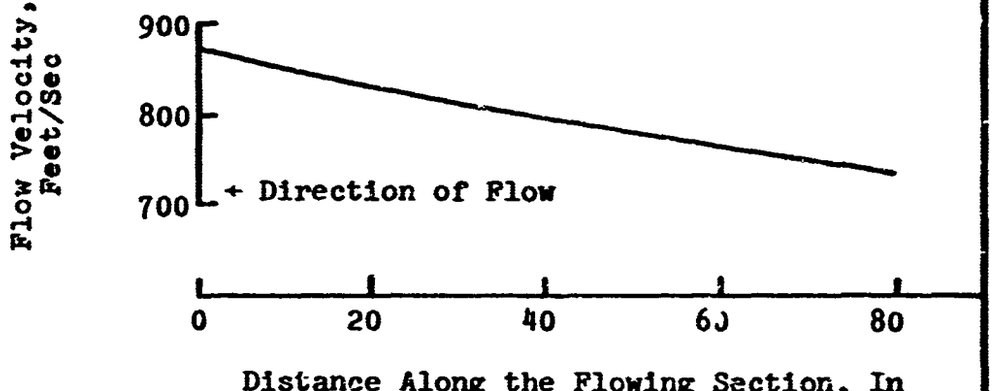

Figure 43 Flow and Reaction Zone Velocities in the Flowing Section, Run 78

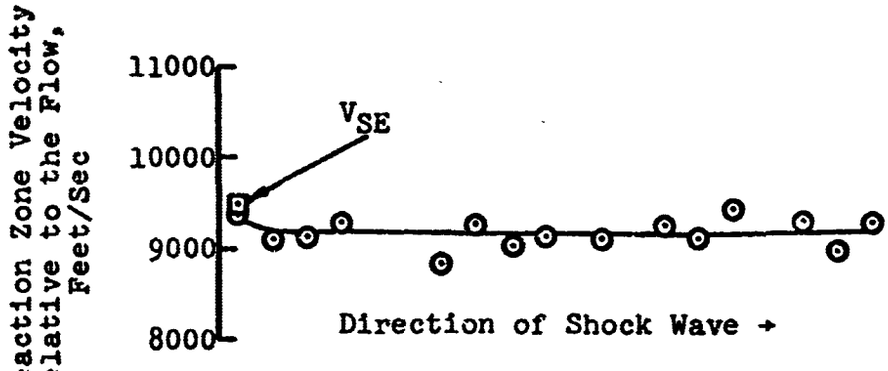

M_{Exit} = .509

M_{SI} = 2.18

H_2 Percentage = 66.32

V_{C-J} = 9291 Ft/Sec

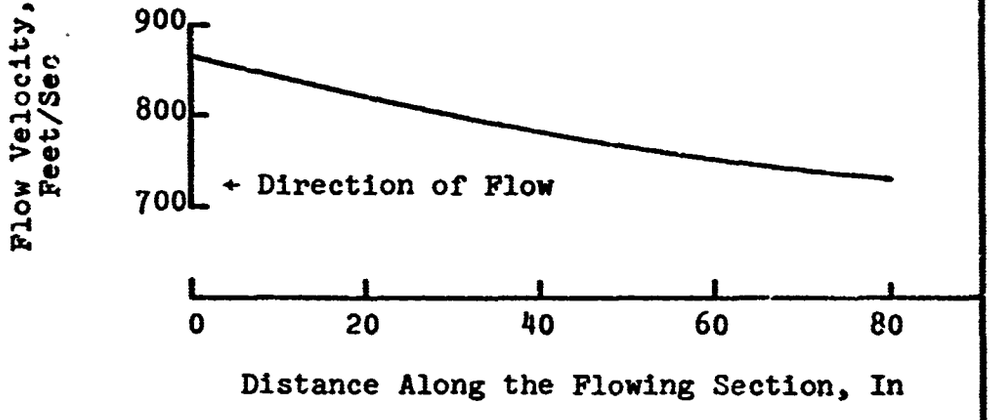

Figure 44 Flow and Reaction Zone Velocities in the Flowing Section, Run 61

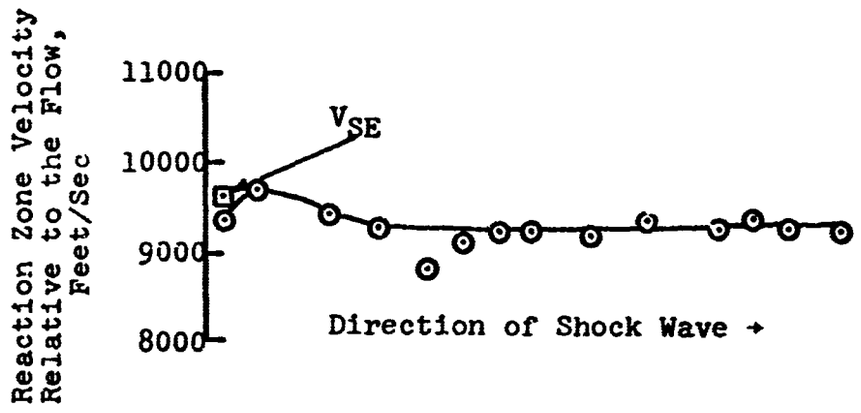

M_{Exit} = .495

M_{SI} = 2.21

H_2 Percentage = 66.70

V_{C-J} = 9347 Ft/Sec

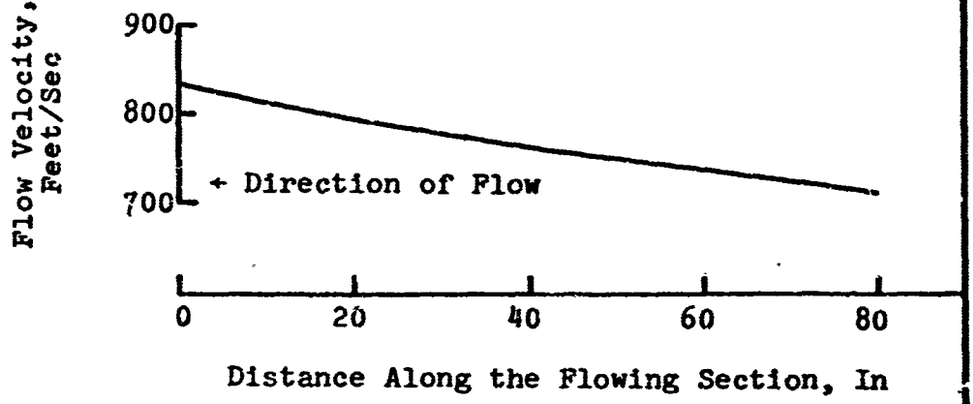

Figure 45 Flow and Reaction Zone Velocities in the Flowing Section, Run 66

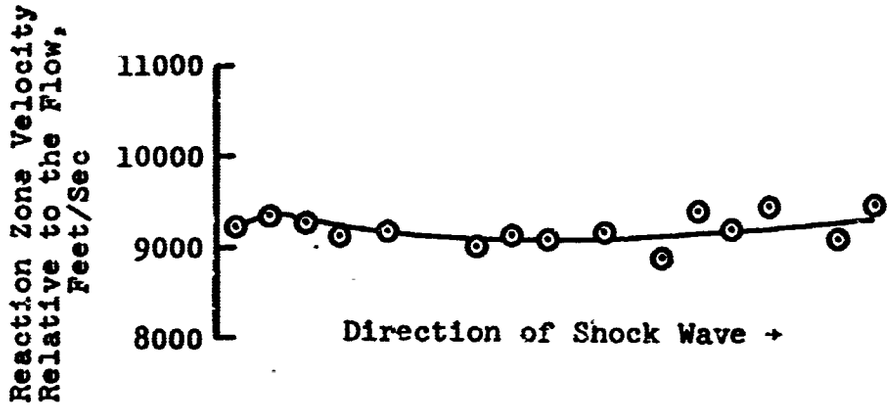

M_{Exit} = .512

M_{SI} = 2.44

H_2 Percentage = 66.78

V_{C-J} = 9347 Ft/Sec

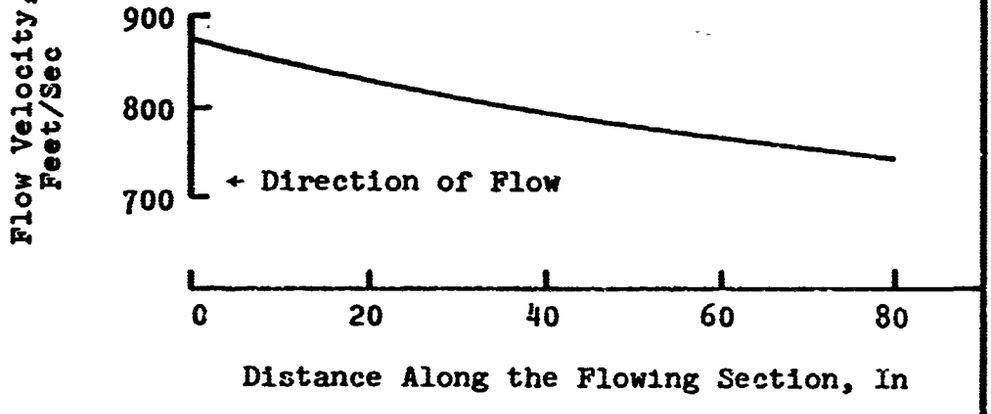

Figure 46 Flow and Reaction Zone Velocities in the Flowing Section, Run 79

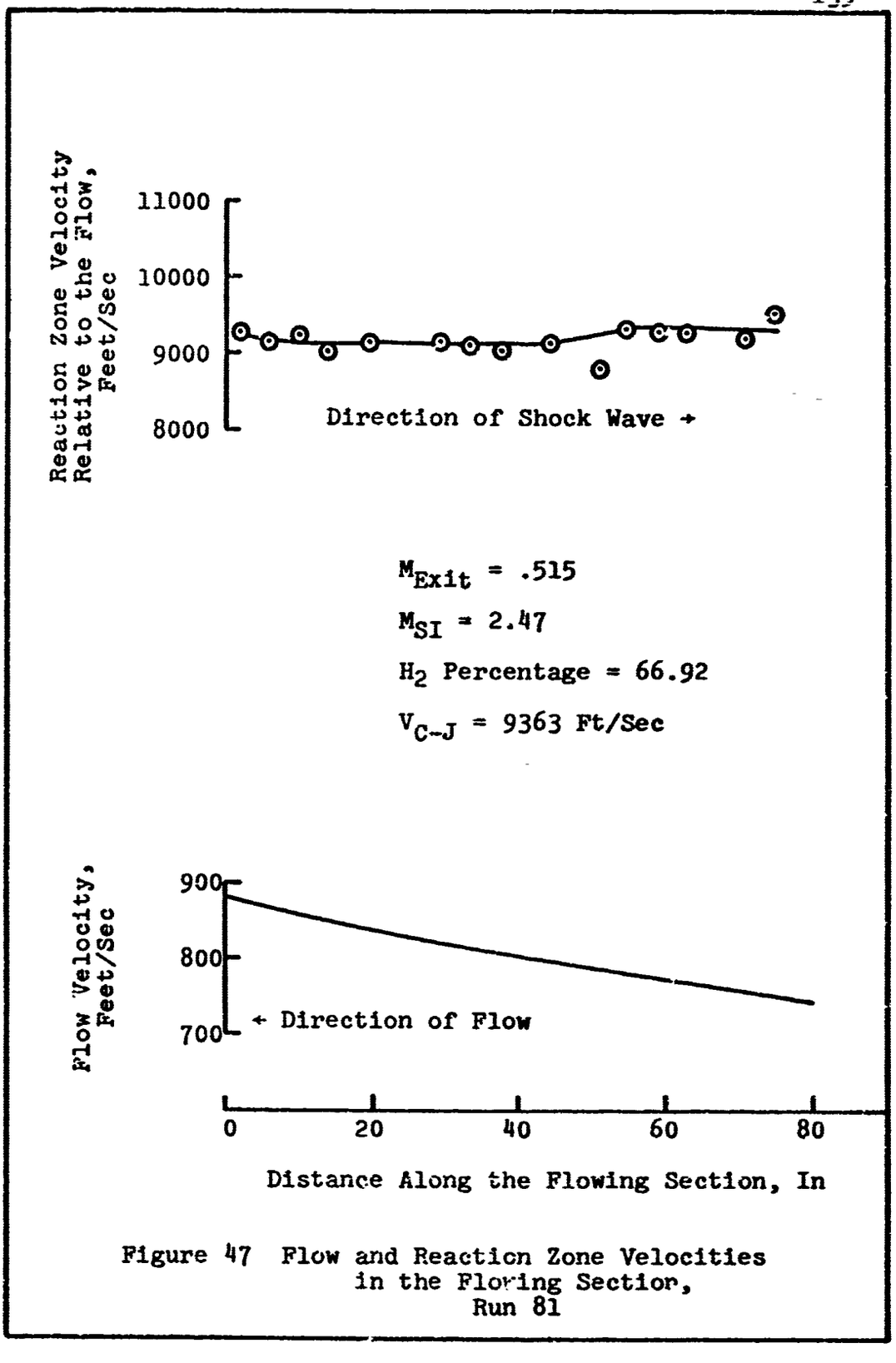

Figure 47 Flow and Reaction Zone Velocities in the Flowing Section, Run 81

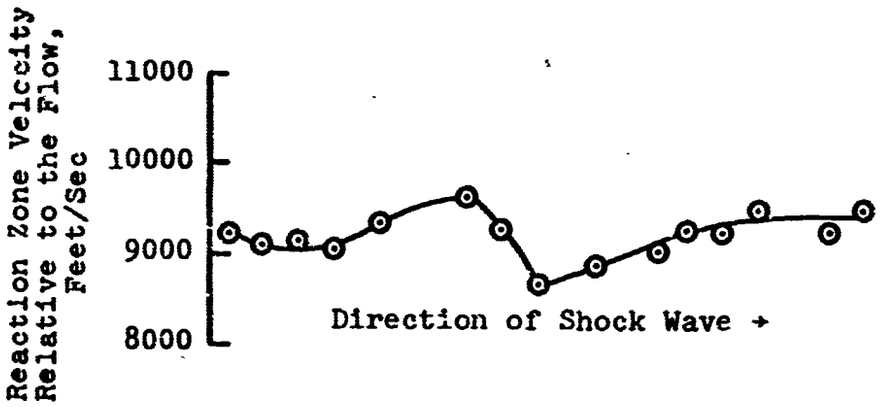

M_{Exit} = .511

M_{SI} = 2.52

H_2 Percentage = 66.61

V_{C-J} = 9327 Ft/Sec

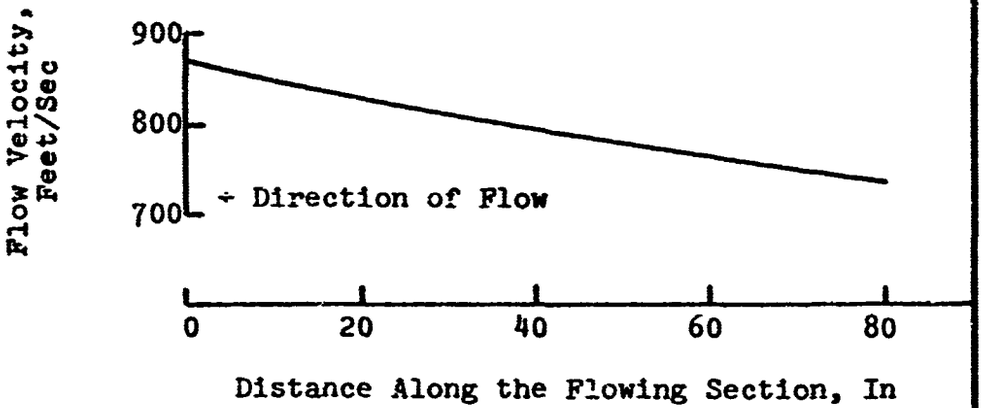

Figure 48 Flow and Reaction Zone Velocities in the Flowing Section, Run 80

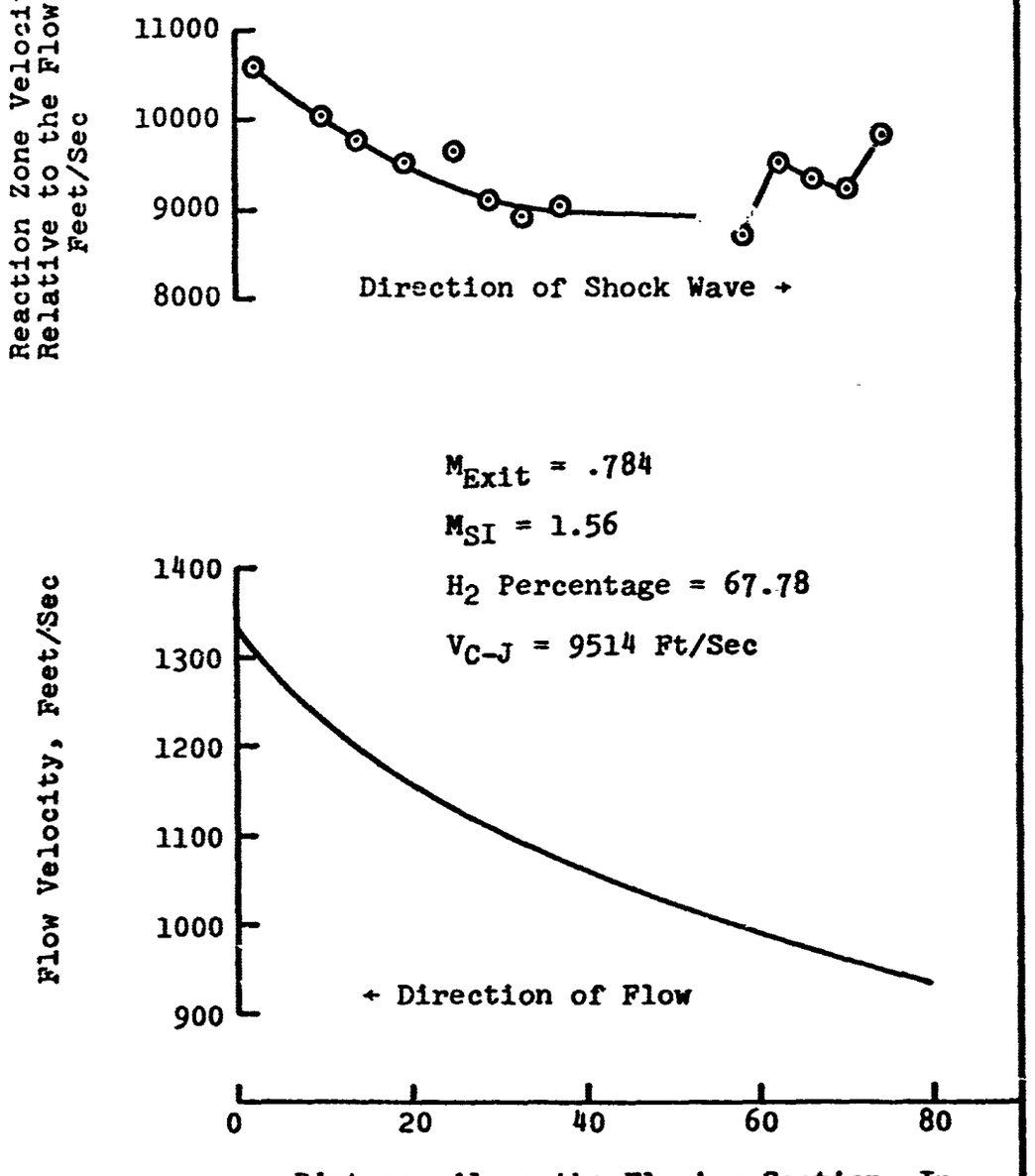

Figure 49 Flow and Reaction Zone Velocities in the Flowing Section, Run 85

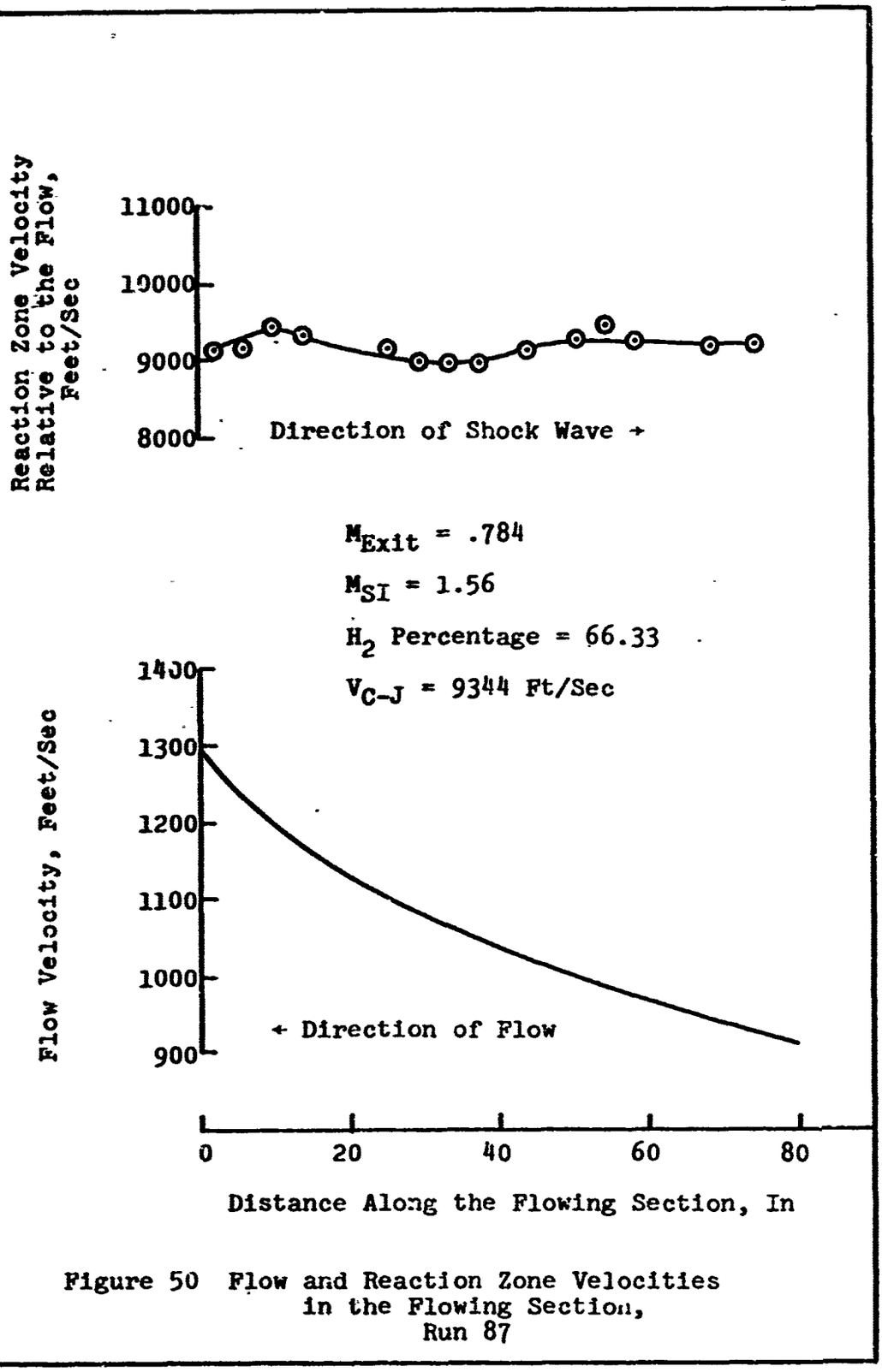

Figure 50 Flow and Reaction Zone Velocities in the Flowing Section, Run 87

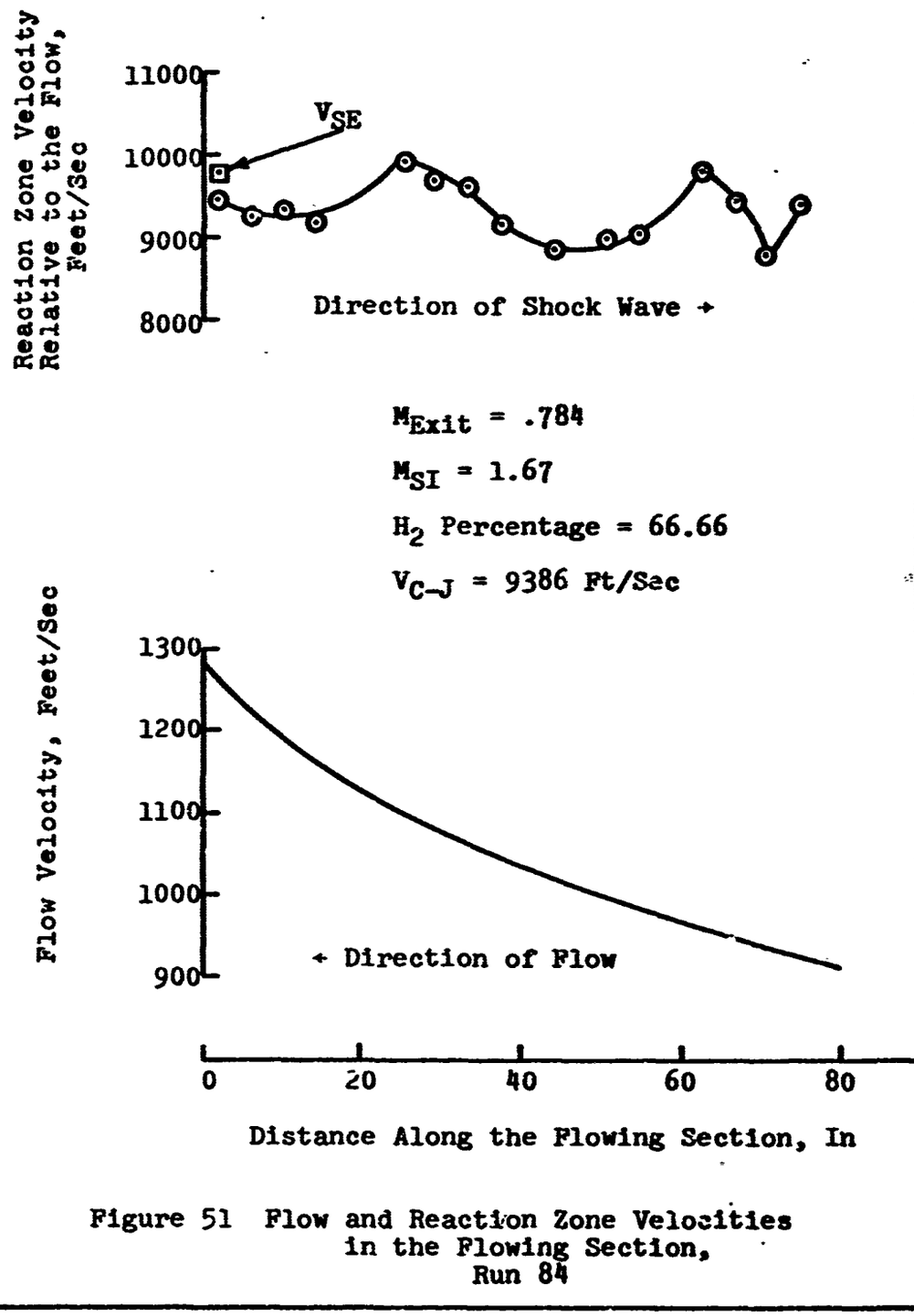

Figure 51 Flow and Reaction Zone Velocities in the Flowing Section, Run 84

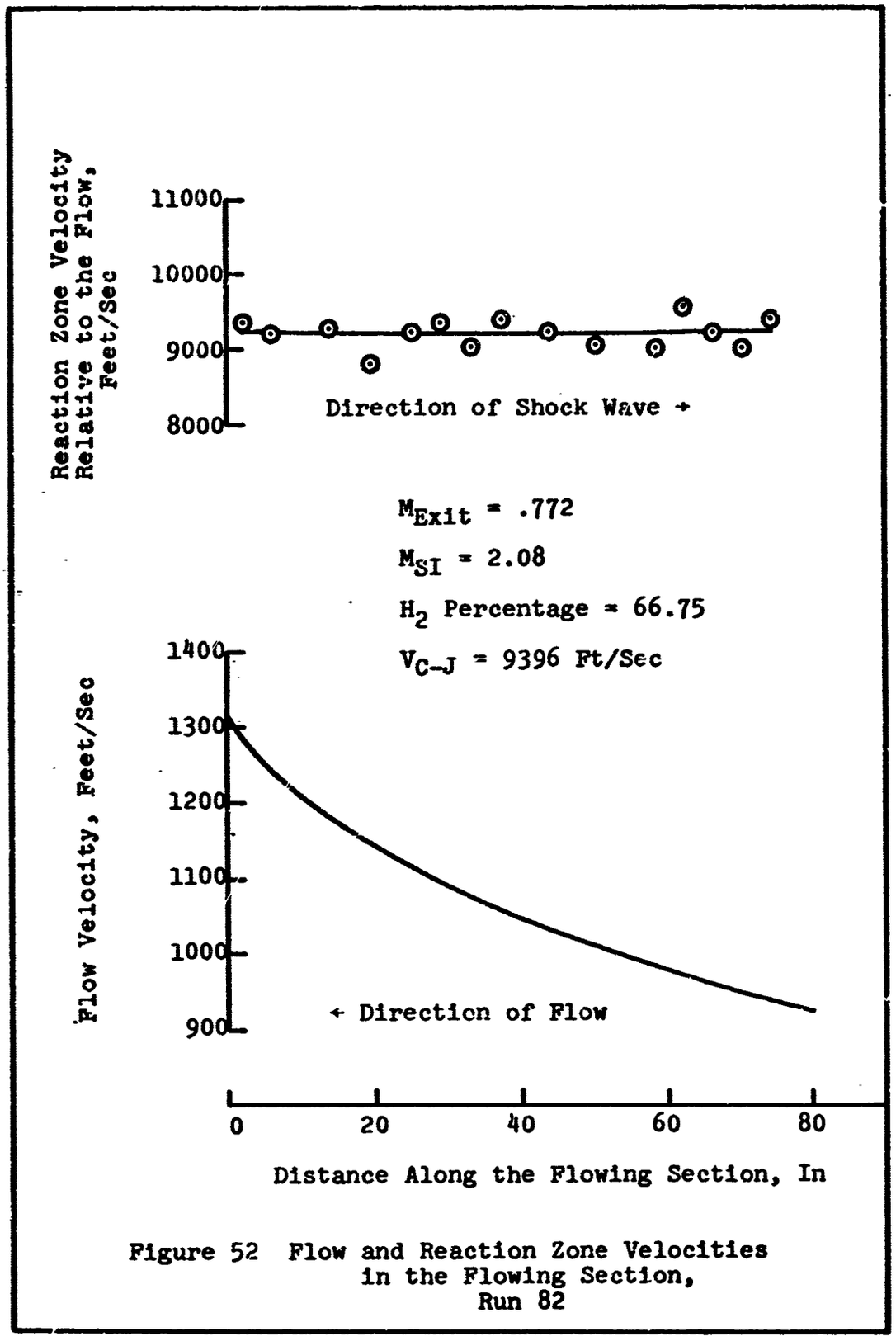

Figure 52 Flow and Reaction Zone Velocities in the Flowing Section, Run 82

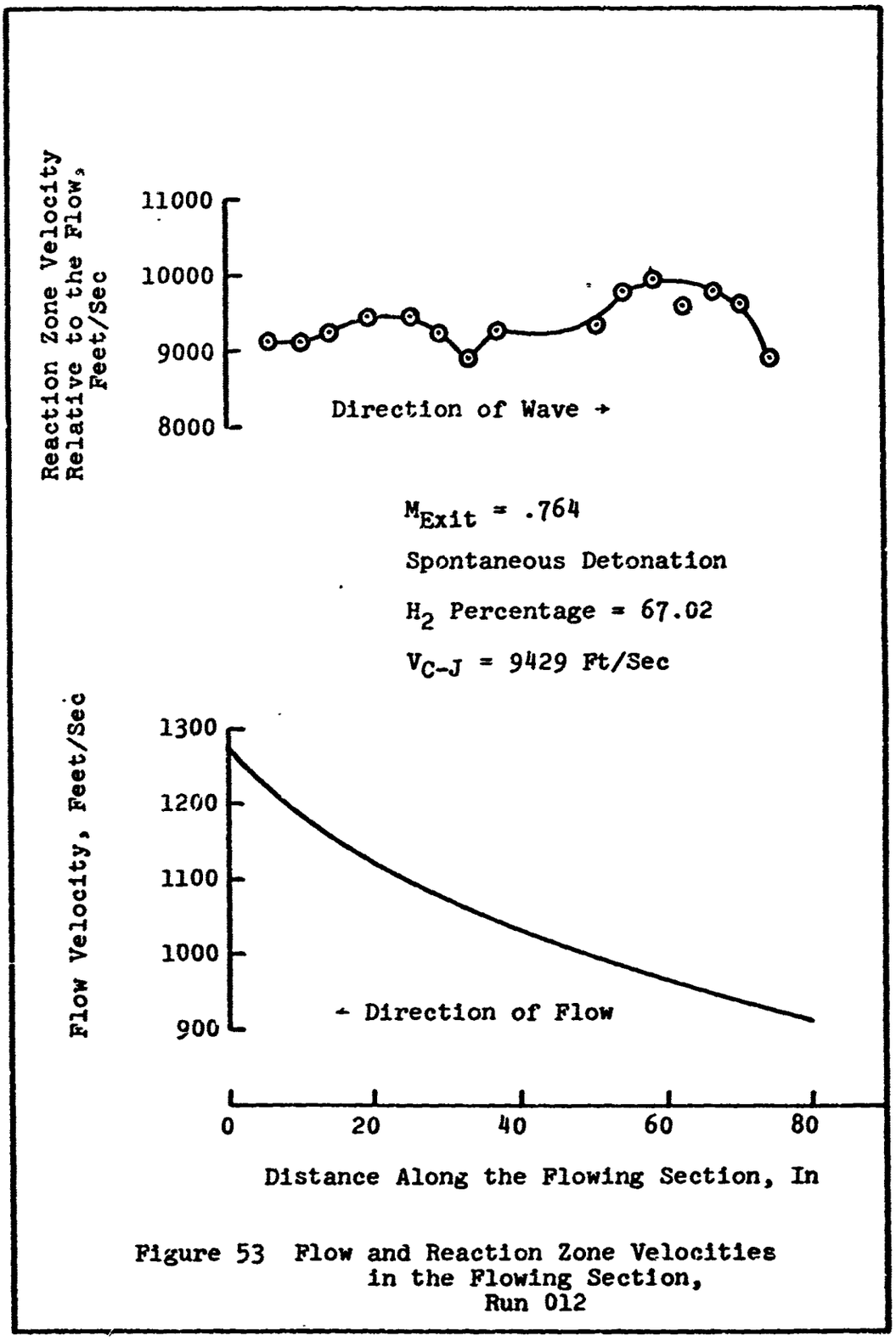

Figure 53 Flow and Reaction Zone Velocities in the Flowing Section, Run 012

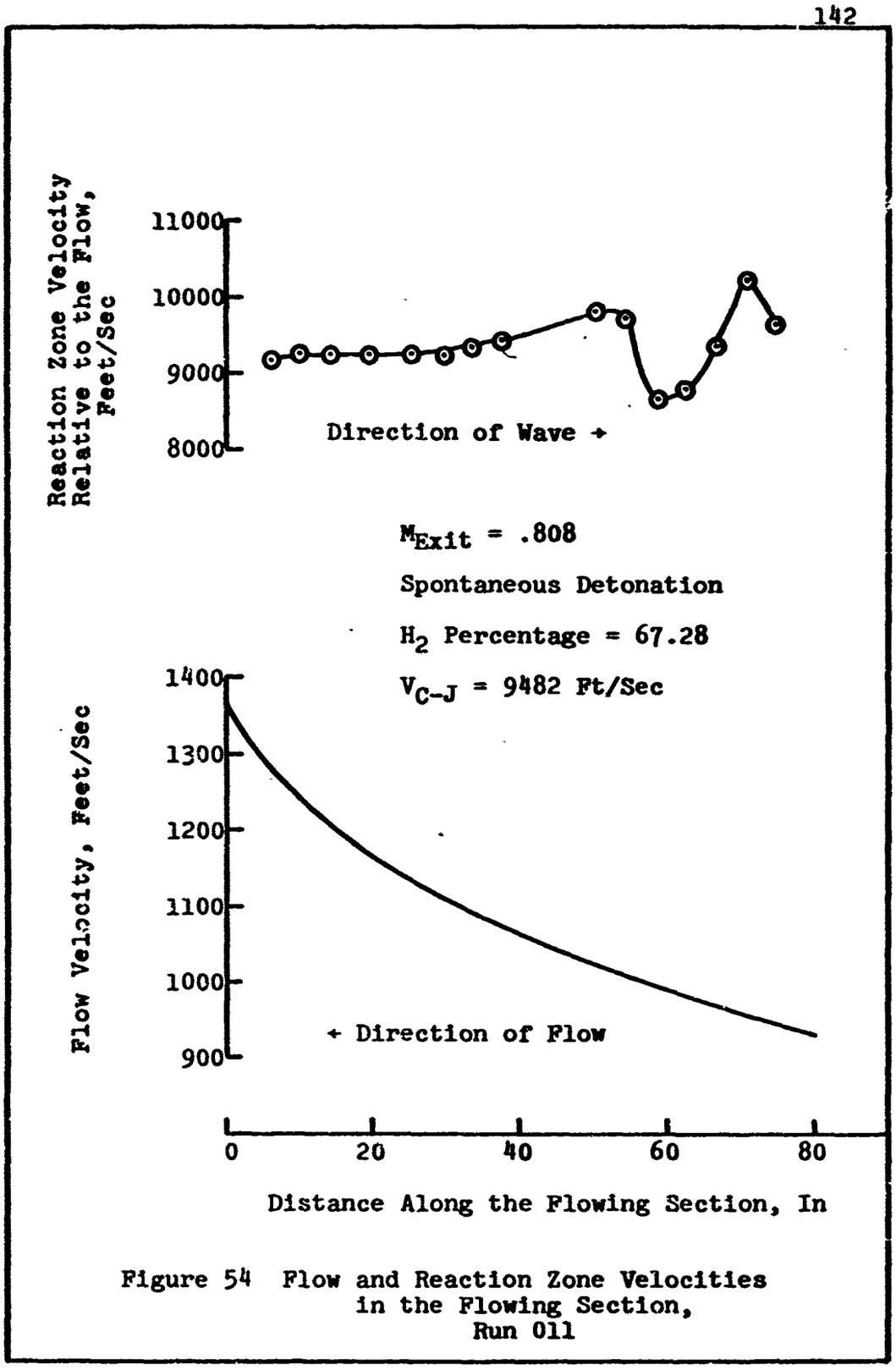

Figure 54 Flow and Reaction Zone Velocities in the Flowing Section, Run 011

Run 011

Run 012

Figure 55 Pictures of Ionization Probe Output for Two Runs in Which Spontaneous Detonation Occurred

Upper Trace - Kistler Transducer Output

Lower Trace - Time Mark Generator Output

Heat Transfer Gage Output

Ionization Probe Output

Figure 56 Wave Speed Data for Run 85

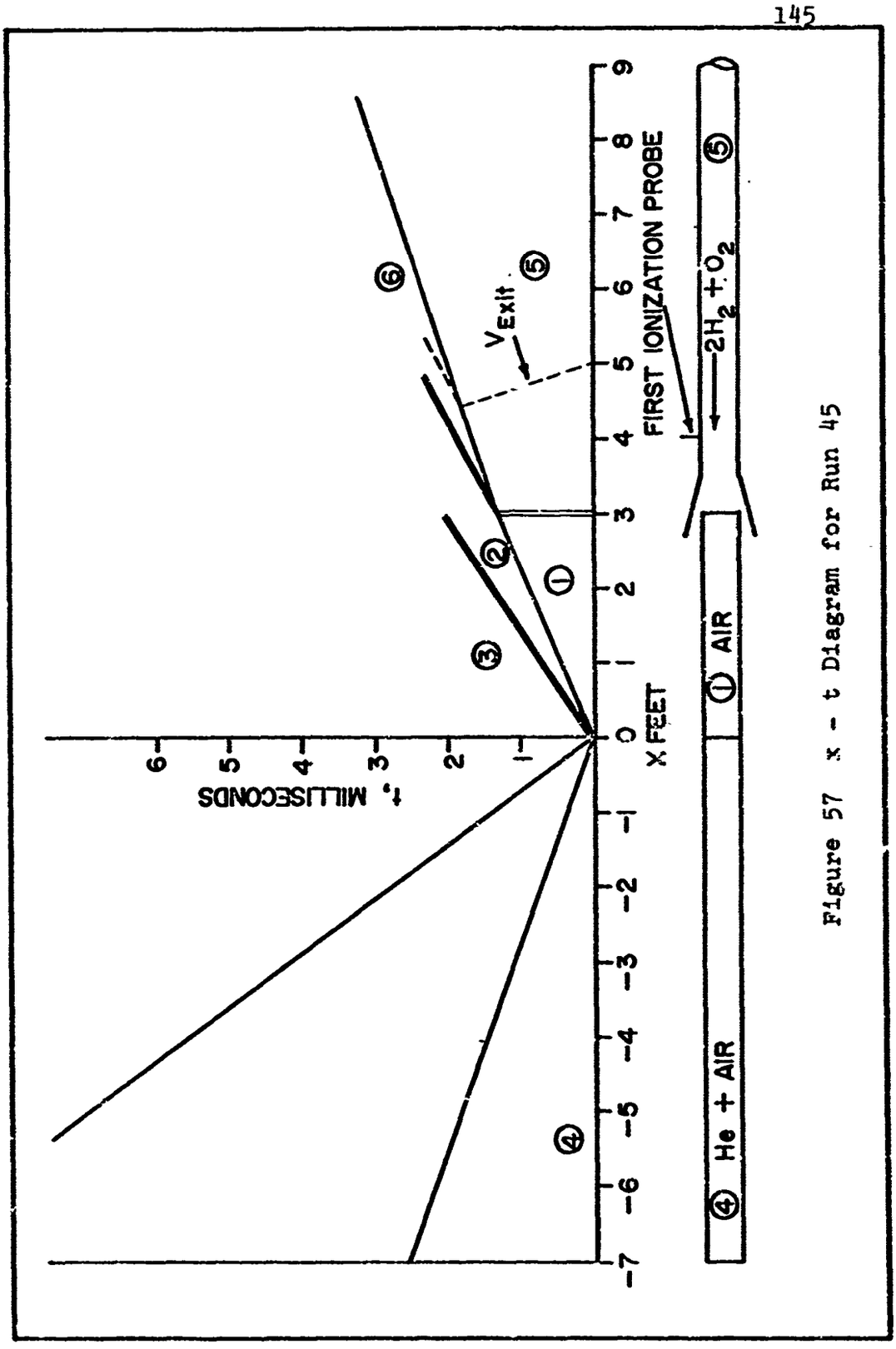

Figure 57 x - t Diagram for Run 45

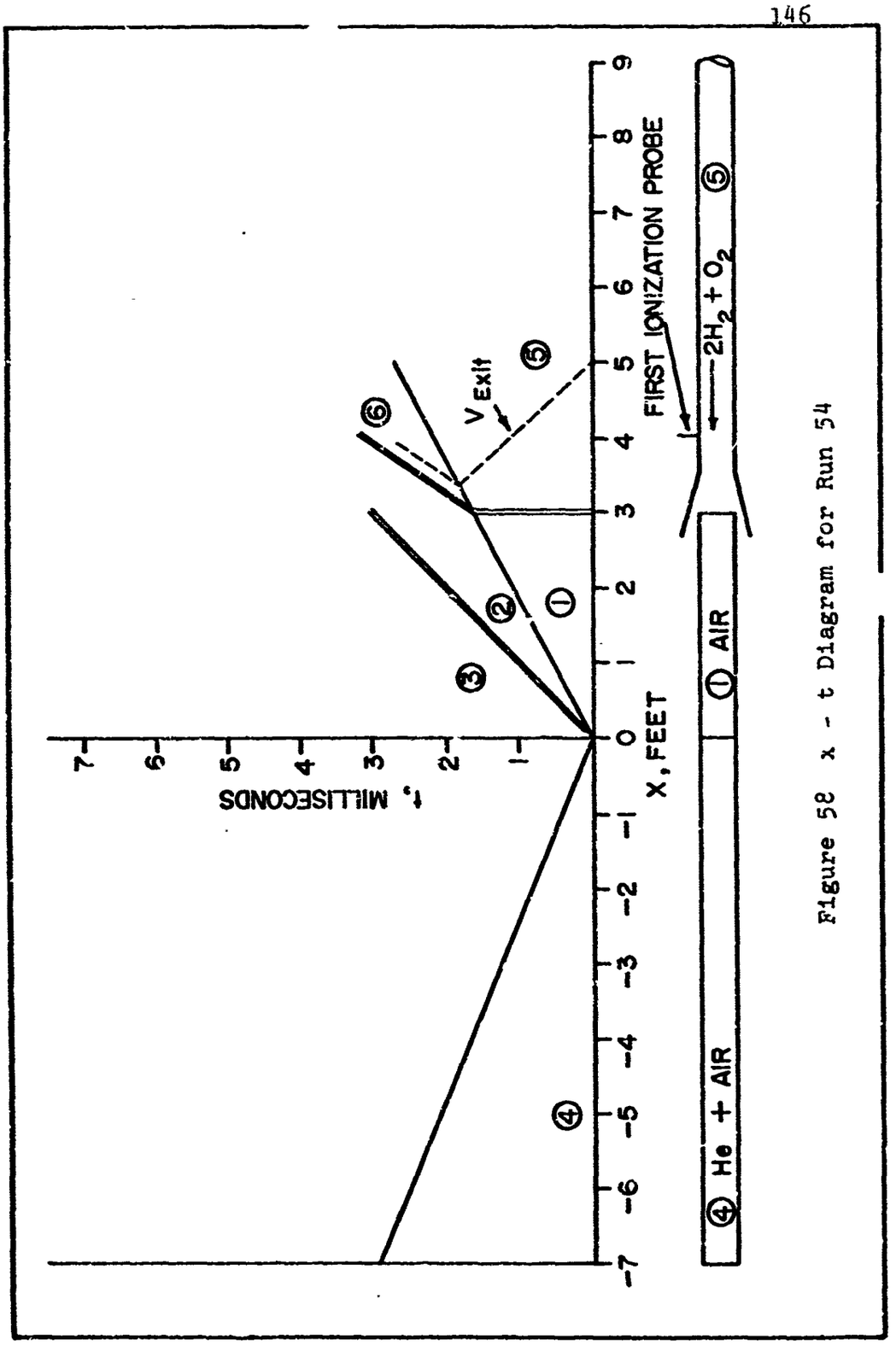

Figure 58 x - t Diagram for Run 54

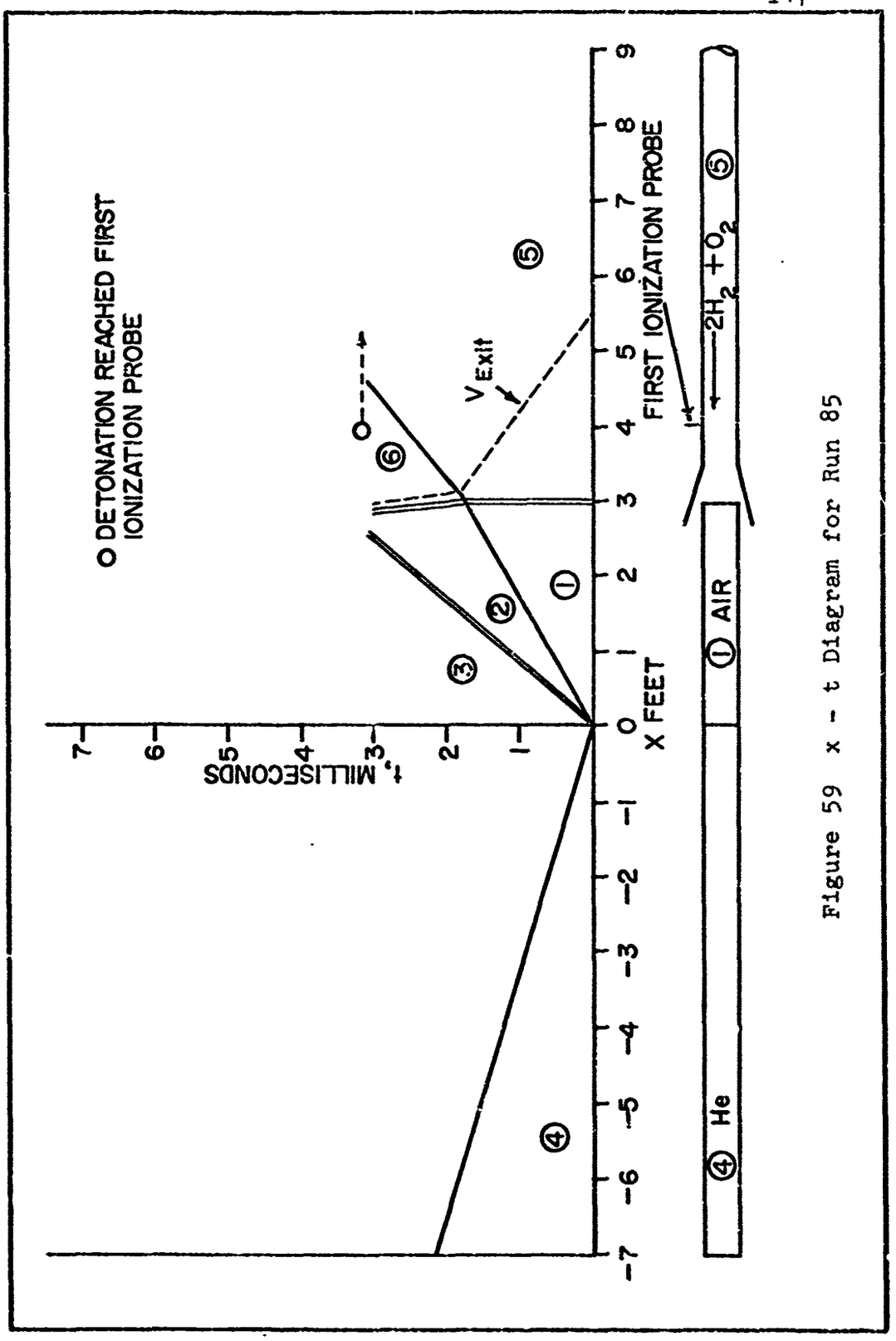

Figure 59 x - t Diagram for Run 85

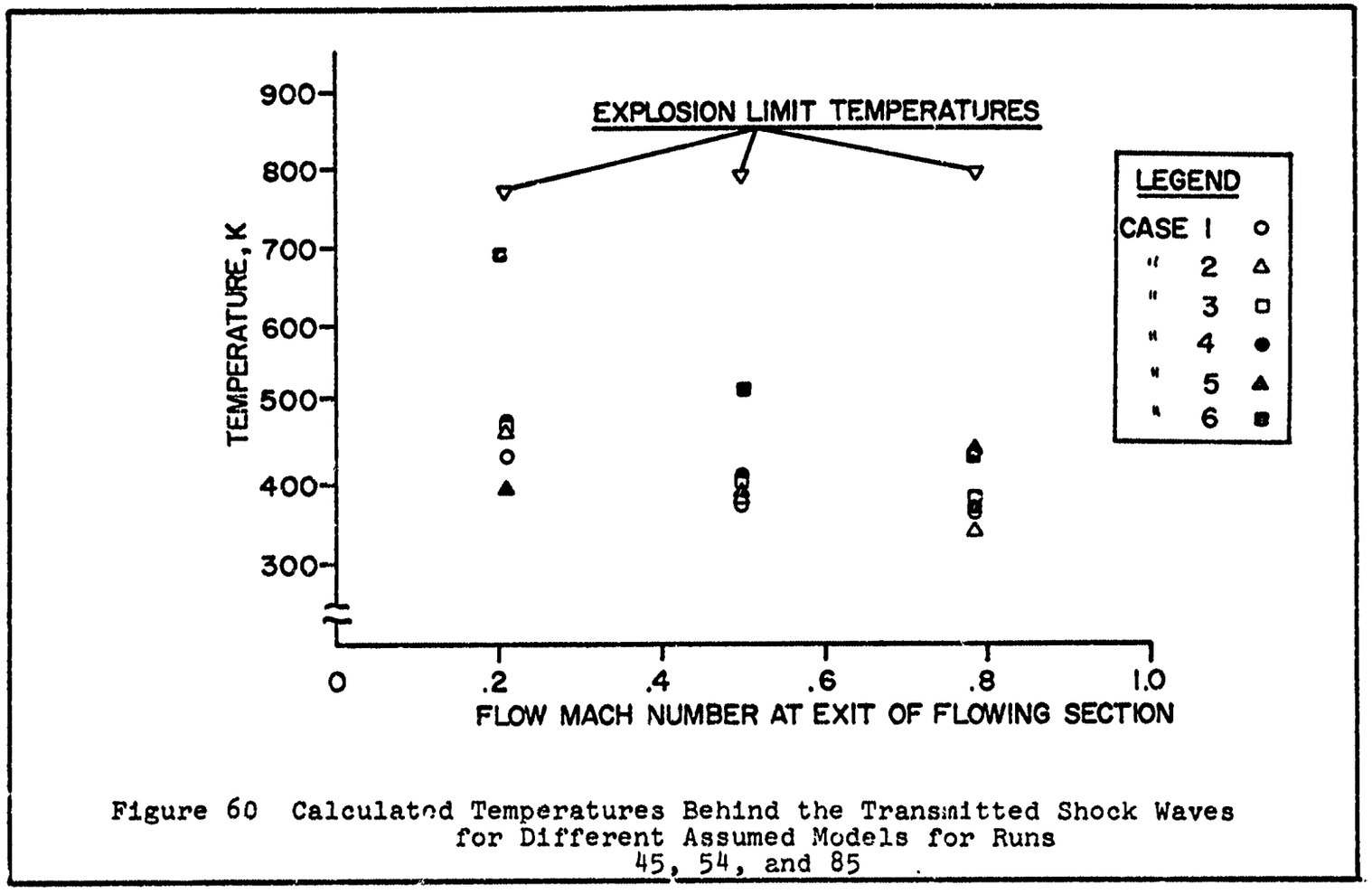

Figure 60 Calculated Temperatures Behind the Transmitted Shock Waves for Different Assumed Models for Runs 45, 54, and 85

APPENDIX
DATA REDUCTION AND CALCULATIONS

APPENDIX

DATA REDUCTION AND CALCULATIONS

The experimental data obtained in this investigation were in two basic forms -- the data associated with the mass flow rates through the system, and the data associated with the speeds of the various waves caused to move into and through the flowing gas. The mass flow rates and other flow parameters were calculated from data recorded by the oscillograph, and the wave speeds were calculated from measurements taken from the oscilloscope pictures.

Mass flow rates

Data required for the calculation of the oxygen and hydrogen mass flow rates were the pressure and temperature upstream of the respective venturi meters, and the pressure drop across the meters. These quantities were obtained from the oscillograph record by measuring the amount of deflection of the appropriate trace from its zero reference position, using a pair of dividers. This distance was transferred to the corresponding calibration curve, where it was converted into a pressure, pressure difference, or temperature, depending on which recorder trace

was being measured. These deflection readings were always taken from the steady values on the records just prior to the occurrence of the pressure rise which signified the arrival of the shock wave at the upstream end of the flowing section. The static pressures measured in this manner were gage pressures, and they were converted to absolute pressures by adding the barometric pressure to them.

The individual mass flow rates were calculated from the following equation, which is applicable to the flow of compressible gases through orifice and venturi meters [34]:

$$\dot{m} = .525 \frac{Y_a C_d d^2}{(1 - B^4)^{1/2}} (\rho \Delta P)^{1/2} \qquad (1)$$

where

$\dot{m}$ = the mass flow rate in lb_m/sec

Y_a = compressibility correction factor

C_d = discharge coefficient = .984

d = venturi throat diameter = .376 inches for both venturis

$P = \frac{\text{venturi throat diameter}}{\text{venturi inlet diameter}} = .575$

ρ = inlet density in lb_m/ft^3

ΔP = pressure difference across the venturi in psi

Introducing a reference temperature of 560 R, the perfect gas equation of state,

$$\rho = \frac{P \mathfrak{M}}{R_o T} ,$$

and a linear approximation for Y_a for $k = 1.4$ [19],

$$Y_a = \left(1 - .644 \frac{\Delta P}{P}\right) ,$$

the mass flow rate equations become

$$\dot{m}_H = .001419 \left(1 - .644 \frac{\Delta P_H}{P_H}\right) \left(P_H \Delta P_H \frac{560}{T_H}\right)^{1/2} \ldots \quad (2)$$

and $$\dot{m}_O = .00565 \left(1 - .644 \frac{\Delta P_O}{P_O}\right) \left(P_O \Delta P_O \frac{560}{T_O}\right)^{1/2} \ldots \quad (3)$$

These equations were solved by the AFIT IBM Model 1620 digital computer using the program shown in Figure 61. This program must be run with the FOR-TO-GO processor because of the length of the format statements. Statement 1 specifies the input data requirement for the program which is: Run number, P_H in psia, ΔP_H in psi, T_H in degrees Rankine, and P_O, ΔP_O, T_O in the same units, respectively. This program also calculates the total mass flow rate, the mixture ratio ($\dot{m}_O/\dot{m}_H$), the molar percentages of oxygen and hydrogen in the mixture, and the average molecular weight of the mixture. A

sample of the input data for Run Number 36, is included in Figure 61, and the output data for this same run is included in Figure 62. The other runs denoted 360 through 365 will be discussed in a later paragraph.

Flow Mach Number at the exit of the mixing section

In order to find the flow Mach Number at the exit of the mixing section it was assumed that the flow was one dimensional, adiabatic, steady flow of a perfect gas with constant specific heats in a constant area duct. Under these assumptions the continuity equation, energy equation, perfect gas equation of state, Mach Number definition, and the equation for the speed of sound in a gas can be combined to give the relation:

$$\frac{\dot{m}}{AP}\sqrt{\frac{T_o}{\mathfrak{M}}} = M\sqrt{\frac{kg_c}{R_o}\left(1 + \frac{k-1}{2}M^2\right)} \quad . \quad . \quad . \tag{4}$$

The quantities $\dot{m}$, $\mathfrak{M}$, A, k, and T_o are constant for all axial stations in the flow; $\dot{m}$ and $\mathfrak{M}$ are calculated as discussed above, A is calculated from the diameter of the tube, T_o is measured as the gases enter the mixing section, and k is assigned the value of 1.4, or 1.41, depending on whether the temperature of the mixture is greater than 490 R, or not. Thus, if P is measured at any axial station in the flow, the left side of

Equation (4) is known, and the equation can be solved for M at the point where P was measured, by trial and error. The static pressure at the exit of the mixing section was measured on all runs, and Equation (4) was used to calculate the flow Mach Number at that station. This calculation is included in the computer program presented in Figure 63. A trial and error solution was necessary, and iteration was continued until the difference between successive values of the Mach Number was less than .0005.

Friction factor

The friction factors of the flowing gas section for nominal flow Mach Numbers of .2, .5, and .8 were determined early in the experimental program. These factors were then used in the calculation of mixture velocities and exit conditions in all later tests. The procedure employed to find the friction factors was to determine the flow Mach Number at two stations in the flow which were a known distance apart, and then apply the well known Fanno Line Theory. The two stations chosen were the exit of the mixing section, and the plane of the ionization probe nearest the exit of the flowing gas section. The distance between those points was determined to be 78.07 inches for the particular arrangement of the three tube sections used in these tests. The static pressure at the downstream end was determined

by subtracting the pressure difference, measured by a differential pressure transducer connected between the two points, from the pressure measured at the upstream station. Equation (4) was used to calculate the Mach Numbers at both stations. The particular equation from the Fanno Line Theory which was applied in the determination of the friction factors was obtained from Keenan and Kaye [23, p. 211], and is

$$\frac{4fL_{max}}{D} = \frac{1 - M^2}{k\,M^2} + \left(\frac{k+1}{2k}\right)\log_e \left[\frac{(k+1)\,M^2}{2\left(1 + \frac{k-1}{2}M^2\right)}\right] \quad . \quad . \quad . \tag{5}$$

In this equation f is the friction factor, and L_{max} is the distance required for the Mach Number to change from M to 1. In all tests conducted in this experimental program, the flow was subsonic, and thus the Mach Number of the flow increased as it progressed down the flowing section. The assumptions used in deriving this equation are the same as those listed above for the determination of the Mach Number. Inspection of Equation (5) shows that if M is known at a point, then a value can be calculated for the parameter on the left (called the friction parameter). If an average friction factor is effective between two points in a fixed diameter tube, the difference between the friction parameters at the

two points is due to the difference in L_{max} at the two points. This difference in L_{max} is simply the distance between the two points, as expressed by the equation:

$$\left(\frac{4fL_{max}}{D}\right)_1 = \left(\frac{4fL_{max}}{D}\right)_2 - \frac{4f\Delta L_{1-2}}{D} \quad . \quad . \quad . \qquad (6)$$

where 1 denotes an upstream station, 2 denotes a downstream station, and ΔL_{1-2} is the distance between them. Rearranging Equation (6) leads to

$$f = \frac{D}{4\Delta L_{1-2}}\left[\left(\frac{4fL_{max}}{D}\right)_1 - \left(\frac{4fL_{max}}{D}\right)_2\right] \quad . \quad . \quad . \qquad (7)$$

In summary, knowing the Mach Number at stations 1 and 2, the respective friction parameters were calculated from Equation (5). Then, knowing the distance between the points, and the diameter of the tube, Equation (7) was used to calculate the friction factor. These calculations were facilitated by making use of tables of solutions of Equations (4) and (5) which were prepared for a Mach Number increment of .01. Linear interpolation was employed for values between the tabulated values.

Flow parameters and exit conditions

The flow velocity as a function of position in the flowing gas section was desired in order to be able to determine the relative velocity between the flow and

the shock and detonation waves, the speed of which were determined with respect to the tube. In addition, the exit pressure and temperature of the gas were desired as input data for the calculation of the Chapman-Jouget detonation velocity in the mixture. For the purpose of these calculations, also, the exit of the flowing section was taken as the plane of the ionization probe near the downstream end. A second computer program (Figure 63) was prepared to perform these tedious calculations. This program, like the previously described one, was run on the IBM Model 1620 computer, using the FOR-TO-GO processor. A brief description of this program, with emphasis on the gas dynamics, rather than on the numerical analysis and programming techniques, will now be presented. In statement 1 an estimated value of the Mach Number at the exit of the mixing section was entered. The computer started with this value and then iterated until an accurate value was determined. The next four entries are values of the parameter $\frac{4f\Delta L_{1-2}}{D}$ calculated for distances of 20, 40, 60, and 80.01 inches, respectively, from the exit of the mixing section (80.01 inches was the length of the instrumented portion of the flowing gas section when it was put in the final configuration used for all runs reported herein). An appropriate value of f was used, depending on the expected exit Mach Number. Some iteration was accomplished for

the runs in which the exit Mach Number was near .8, since the calculated Mach Number in this range was fairly sensitive to the value of f used. In statement 2 the run number, the total mass flow rate in lb_m/sec, the total temperature in degrees R, the static pressure at the exit of the mixing section in psia, the molecular weight, and two values of the specific heat ratio were entered. The capability of using two values of the specific heat ratio was included in the program so that a large temperature drop in the tube could be accounted for, if necessary. With this input data, the computer solved Equation (4), for the Mach Number at the exit of the mixing section, and using this value of M, it solved Equation (5) for $\frac{4fL_{max}}{D}$ at this point (called 1). The temperature at station 1 was then calculated from the equation

$$T = T_o \left(1 + \frac{k-1}{2} M^2\right)^{-1} \quad . \quad . \quad . \qquad (8)$$

Then, knowing P_1, the value of P* was calculated from the equation [23, p. 211]:

$$\frac{P}{P^*} = \frac{1}{M} \sqrt{\frac{k+1}{2\left(1 + \frac{k-1}{2} M^2\right)}} \quad . \quad . \quad . \qquad (9)$$

Next, the velocity at station 1 was calculated from

$$V = Ma = M \sqrt{\frac{kg_c R_o T}{m}} \quad . \quad . \quad . \qquad (10)$$

The computer then solved Equation (5) for the friction parameter at station 1, and following this, the values of the friction parameter at stations 2, 3, 4, and 5 were calculated using the relationship expressed in Equation (6). Then, having the values of the friction parameter at each of the above stations, Equation (5) was solved for the Mach Numbers, from which the temperatures, and then the velocities were determined. Then, at the exit (Station 5) Equation (9) was solved for P, P* having been calculated previously. The final calculation was for the speed of sound at the exit station. A sample calculation using the data from Run Number 36 has been included in Figures 63 and 64.

The flow exit temperature and pressure along with its molar composition were used as input parameters for a third computer program which calculated the detonation parameters, such as the theoretical speed of the Chapman-Jouget detonation wave. This computer program was developed for use on the IBM Model 7094 computer by Bowman [35], and was used also by McKenna [13]. The theoretical detonation velocity was calculated for each of the experimental runs in which a detonation occurred, and has been included in the data presented herein for comparative purposes.

Wave speeds and Mach Numbers

The waves for which the speed was determined in this investigation were the incident shock wave, the transmitted shock wave, and the detonation wave, when one was produced. The raw data from which the wave speeds were determined was in the form of a photograph of an oscilloscope trace.

The same basic technique was employed in reducing the data for each wave. The first step in each case was to determine the scale factor for the picture in microseconds per inch. The scale factor was determined from measurements taken from a calibration photograph which was obtained for each oscilloscope each day on which experiments were conducted. The photographs showed vertical deflections of the electron beam corresponding to the output pulses from the time mark generator, which was always adjusted to give an output pulse every 50 microseconds. The distance between the oscilloscope trace deflections was accurately measured, using a photographic comparator which could be read to 4 decimal places. The time increment selected (in microseconds) was divided by the distance between deflections (in inches) to yield the scale factor. This calculation was performed with a desk calculator, and the answer was rounded off to the nearest one hundredth of a microsecond. It was found that the sweep rate of the Model 551 oscilloscope (used

for the incident shock wave speed) was not linear; therefore, a calibration curve of average scale factor vs total distance from the beginning of the sweep was prepared for this oscilloscope daily. The two Model 545B oscilloscopes with the raster modification operated with an essentially constant sweep rate, although its value depended to a small degree on whether the beam was moving to the right or to the left. For these reasons, a scale factor based on a time increment of 300 microseconds was determined for each of these oscilloscopes for each direction of the sweep motion. The scale factors were approximately 140 microseconds per inch, and the differences between them were of the order of 1 microsecond per inch.

With the scale factors known, distances measured on the photographs taken during an experimental run could be converted into time increments, i.e., the time required for the particular wave to travel the known distance between the respective wave detectors. For the incident shock wave, the beginning of the horizontal trace in the photograph marked the time at which the shock wave passed the first Kistler pressure transducer. The time of arrival of the shock wave at the second Kistler pressure transducer, which was located 5.012 ± .001 inches from the first one, was marked by the almost vertical rise of the trace, due to the pressure

rise associated with the wave passage. The distance between the beginning of the trace and the point on the sharply rising portion corresponding to a deflection of .2 volts was measured. (The end point of the distance measurement was selected as noted above because the oscilloscope sweep triggering level was set at .2 volts. It was desired to determine the time increment required for corresponding points of the shock wave pressure profile to travel between the transducers.) With this distance from the photograph the calibration curve was used to obtain the scale factor for the sweep rate. The distance was then multiplied by the scale factor to give the time increment required for the wave to traverse the distance between the transducers. The time increment was then divided by the distance between the transducers (converted to feet) to give the wave velocity in feet per second. This shock wave was travelling through stationary air in the inert section. The speed of sound in the air was calculated using the ambient temperature measured in the test cell at the same vertical level as the inert section. The incident shock wave Mach Number was then determined by dividing the wave speed by the speed of sound.

The transmitted shock wave was defined to be the shock wave which moved upstream into the flowing mixture of hydrogen and oxygen as a result of the appearance of the

incident shock wave in the transition section. The speed of the transmitted shock wave was determined from signals generated by two heat transfer gages which were 4.005 ± .001 inches apart. (The midpoint between these gages was defined to be the exit station of the flowing mixture when referring to the speed of the transmitted shock wave. This point was approximately 5.44 inches upstream from the end of the constant area flowing gas section of the tube.) The distance between the two vertical trace deflections produced by the heat transfer gages was measured, the proper scale factor was applied, and the same calculations described above were performed to yield the speed of the transmitted shock wave with respect to the tube. Since this shock wave was progressing into a gas which was moving in the opposite direction, its speed relative to the gas was the sum of its speed with respect to the tube and the speed of the flowing gas. The speed of the flowing gas at the point midway between the heat transfer gages was determined from a curve of the calculated flow velocity vs position in the flowing gas section. The Mach Number of the transmitted shock wave was calculated by dividing the speed of the wave relative to the flowing gas by the speed of sound in the flowing gas, which was calculated as indicated previously.

The same procedures, as outlined above, were used to determine the speed of the detonation wave, except the oscilloscope trace picture showing the output of the ionization probes was used. The detonation wave velocity was determined at 17 points along the flowing gas section, corresponding to the midpoints between the 18 ionization probes used. The velocity was measured with respect to the tube, and it was converted to velocity with respect to the gas in which the wave was moving, as indicated above for the transmitted shock wave. The Mach Number of the detonation wave was not needed, and, therefore, was not calculated.

Error analysis

The numerical results of this investigation were calculated from the experimentally determined values of several quantities. Since all experimental measurements are subject to a certain amount of error, it was necessary to consider the effect of possible adverse combinations of these errors on the accuracy of the results calculated from them. Considering the care which was exercised in the calibration of the instrumentation, and in transforming the oscillograph deflections into numerical data, it is felt that the accuracy of the pressure data was well within ± 2% and that the temperatures were certainly accurate to within ± 5 degrees Rankine. These values were chosen as the possible errors for each of the

measured pressures and temperatures, respectively, and the data from Run 36 was analyzed to determine the effect of various combinations of these errors on the values of the calculated parameters. The mass flow rate and mixture composition calculations were considered first. The error combinations considered are shown in the computer input data included in Figure 61 for the runs designated numbers 360-365. For Runs 360-363 the same error combinations were applied to both gases. In Runs 364 and 365 the error combination which led to the maximum mass flow rate was applied to one gas, while the combination which led to the minimum mass flow rate was applied to the other one. The results of these calculations are shown in Figure 62. These calculations show that the maximum error in the calculated mass flow rates occurs when the pressure and pressure drop errors are of one sign and the temperature error is of the opposite sign (Runs 362 and 363). By comparing the values of the mass flow rates for Runs 362 and 363 with the values for Run 36, it is seen that the maximum possible errors in the hydrogen mass flow rate were + 2.52% and -2.47%; the maximum possible errors in the oxygen mass flow rate were + 2.55% and -2.53%. When the errors were assumed to be in the same direction for both gases, there was a negligible change in the mixture composition and, therefore, the average molecular weight

of the mixture. When the errors were combined so as to give the maximum mass flow rate of the hydrogen and the minimum mass flow rate of oxygen (Run 364), the hydrogen molar percentage increased by 1.10%, and the molecular weight decreased by 2.76%. When the conditions were reversed (Run 365), the hydrogen molar percentage decreased by 1.13%, and the molecular weight increased by 2.84%. For the last two cases the total mass flow rate changed by $\pm$ 1.98%, respectively.

The parameters mentioned above were used in the second computer program for the calculation of mixture velocities and exit conditions for the flowing gas mixture. The only way they affected these calculations was in the determination of the Mach Number at the exit of the mixing section, which required the solution of Equation (4). Considering this equation, it is seen that the combination of errors which results in the maximum Mach Number is a high value of $\dot{m}$ and T_o, and a low value of $\mathfrak{M}$ and P. This combination is represented by the values of $\dot{m}$ and $\mathfrak{M}$ obtained in Run 362, which were combined with values of P and T_o having maximum errors in the proper directions to form the input data for a run designated number 3621 in Figure 63. The minimum Mach Number results from errors in the opposite directions, which are represented by the values of $\dot{m}$ and $\mathfrak{M}$ from Run 363, combined with a high value of P and a low value

of T_o. These conditions were incorporated into the run designated number 3631. The results of these calculations, along with the values calculated for Run 36, are included in Figure 64. When the results of Runs 3621 and 3631 were compared with the values obtained for Run 36, the values listed in Table 5 were obtained. It is emphasized that the errors indicated in Table 5 are the results of the maximum possible experimental errors being combined in the most adverse way. The probability of such a combination is quite low.

TABLE 5

MAXIMUM POSSIBLE ERRORS IN MIXTURE VELOCITIES AND EXIT CONDITIONS

Parameter	Maximum Positive Error	Maximum Negative Error
M(1)	4.85%	5.34%
M(5)	5.66%	5.19%
V(5)	5.82%	5.82%
P(5)	2.28%	2.28%
A(5)	.40%	.47%
T(5)	4 R	5 R

Considering the fact that the time bases of the oscilloscopes were calibrated daily, and that all distances involved were measured to within ± .001 inches, the maximum possible error in the calculated values of the various wave speeds was 1%. This statement ignores any erratic behavior of the individual sensing elements due to possible improper installation, deterioriation, or other causes, which were not amenable to analysis. The consistency of the results obtained seems to rule out this possibility except for one of the ionization probes which consistently gave low values of detonation wave velocity on several of the runs, but gave results comparable to adjacent probes after being cleaned and adjusted.

```
C  C  HAMILTON      MASS  FLOW  RATES  AND  COMPOSITION
 2     PUNCH 3
       DUN  . 4
 4     READ,I,PH,DPH,TH,PO,DPO,TO
       DOTMH=.001419*(1.-(.644*(DPH/PH)))*(SQRTF(PH*DPH*560./TH))
 5     DOTMO=.00565*(1.-(.644*(DPO/PO)))*SQRTF(PO*DPO*560./TO)
 6     TOTM=DOTMH+DOTMO
 7     RATM=DOTMO/DOTMH
 8     XNO=2.016*RATM/32.
 9     XPCTO=100.*XNO/(1.+XNO)
10     XPCTH=100.-XPCTO
11     XMW=XPCTO*.32+XPCTH*.02016
12     PUNCH 13,I,DOTMH,DOTMO,TOTM,RATM,XPCTO,XPCTH,XMW
13     FORMAT(/I3,F10.5,F9.5,F8.4,F8.2,F10.2,2F8.2)
14     GO TO 1
 3     FORMAT(7X29HMDOT      MDOT     TOTAL   MDOT,7X3HPCT,5X3HPCT,5X3HMOL)
 4     FORMAT(3HRUN,5X2HH2,7X2HO2,5X4HMDOT,4X5HRATIO,6X2HO2,6X2HH2,6X2HWT
      1.///)
       END
36,54.95,2.5,503.,.76.45,7.3,486.
340,53.85,2.55,498.,.74.92,7.45,481.                                    LHL
341,56.05,2.45,508.,.77.98,7.15,491.                                    HLH
342,56.05,2.55,498.,.77.98,7.45,481.                                    HHL
343,53.85,2.45,508  74.72,7.15,491.                                     LLH
344,56.05,2.55,49   .4.92,7.15,491.                                    HHL*LLH
345,53.85,2.45,508.,.77.98,7.45,481.                                    LLH*HHL
```

Figure 61 IBM 1620 Computer Program for Calculating Mass Flow Rates and Mixture Composition with Sample Input Data

C C HAMILTON MASS FLOW RATES AND COMPOSITION

RUN	MDOT H2	MDOT O2	TOTAL MDOT	MDOT RATIO	PCT O2	PCT H2	MOL WT
36	.01703	.13447	.1515	7.89	33.21	66.79	11.97
360	.01710	.13480	.1519	7.89	33.19	66.81	11.97
361	.01697	.13406	.1510	7.90	33.23	66.77	11.98
362	.01746	.13790	.1554	7.90	33.22	66.78	11.98
363	.01661	.13107	.1477	7.89	33.20	66.80	11.97
364	.01746	.13107	.1485	7.51	32.11	67.89	11.64
365	.01661	.13790	.1545	8.30	34.34	65.66	12.31

Figure 62 Parameters Calculated by the Mass Flow Rate and Mixture Composition Program

```
C  C   AMILTON      MIXTURE VELOCITIES AND EXIT CONDITIONS
      DIMENSION FRIC(5),T(5),V(5),XM(5),CM(5),D(5),SM(5),FNM(5),FPRIM(5)
 1    READ,XM(1),ST2,ST3,ST4,ST5
 2    READ,J,XMT,TO,P1,XMBAR,GAM1,GAM2
10    CALCX=(XMT/P1)*SQRTF(TO/XMBAR)
11    SQMX=(GAM1-1.)*XM(1)*XM(1)*.5
12    CALCM=CALCX/(.2771*SQRTF(GAM1*(1.+SQMX)))
13    IF(ABSF(CALCM-XM(1))-.0005)16,16,14
14    XM(1)=CALCM
15    GO TO 11
16    T(1)=TO/(1.+SQMX)
      SQM=XM(1)*XM(1)
      X=(GAM2+1.)/(2.*(1.+(GAM2-1.)*SQM*.5))
      PST=P1*XM(1)/SQRTF(X)
      V(1)=222.95*XM(1)*SQRTF(GAM1*T(1)/XMBAR)
20    FRIC(1)=(1.-SQM)/(GAM2*SQM)+(GAM2+1.)/(2.*GAM2)*LOGF(X*SQM)
      FRIC(2)=FRIC(1)-ST2
      FRIC(3)=FRIC(1)-ST3
      FRIC(4)=FRIC(1)-ST4
      FRIC(5)=FRIC(1)-ST5
      DO 42 I=2,5
      XM(I)=XM(I-1)
36    D(I)=1.+(GAM2-1.)*XM(I)*XM(I)*.5
37    SM(I)=XM(I)*XM(I)
38    FNM(I)=((1.-SM(I))/(GAM2*SM(I)))+(((GAM2+1.)/(2.*GAM2))*LOGF(((GAM
     12+1.)*SM(I)*.5)/D(I)))-FRIC(I)
381   FPRIM(I)=(-2./(GAM2*XM(I)*SM(I)))+(GAM2+1.)/(GAM2*XM(I)*D(I))
382   CM(I)=XM(I)-FNM(I)/FPRIM(I)
39    IF(ABSF(CM(I)-XM(I))-.0005)41,41,40
40    XM(I)=CM(I)
      GO TO 36
```

Figure 63 IBM 1620 Computer Program for Calculating Mixture Velocities and Exit Conditions with Sample Input Data

```
 41    T(I)=TO/(1.+(GAM2-1.)*.5*SM(I))
 42    V(I)=222.95*SQRTF(SM(I)*GAM2*T(I)/XMBAR)
 43    P5=(PST/(14.696*XM**5)))*SQRTF((GAM2+1.)*.5*D(5))
       A5=222.95*SQRTF(GAM2*T(5)/XMBAR)
       PUNCH 50,J,XM(1),T(1),FRIC(1)
       PUNCH 51,(V(I),I=1,5)
       PUNCH 52,XM(5),T(5),P5,A5
       GO TO 2
 50    FORMAT(7HRUN NR.,I4,4X,6HM(1) =,F7.3,2X,6HT(1) =,F6.0,2X,15HFRICTI
      1ON FCT. =,F12.5)
 51    FORMAT(6HV(1) =,F6.0,3X,6HV(2) =,F6.0,3X,6HV(3) =,F6.0,3X,6HV(4) =
      1,F6.0,3X,6HV(5) =,F6.0)
 52    FORMAT(6HM(5) =,F6.3,3X,6HT(5) =,F5.0,3X,6HP(5) =,F7.3,3X,6HA(5) =
      1,F6.0,///)
       END
.2,.2455,.491,.7365,.9822                                                    CBA
36,.1515,501.,14.48,11.97,1.4,1.4
3621,.1554,506.,14.19,11.98,1.4,1.4
3631,.1477,496.,14.77,11.97,1.4,1.4
```

Figure 63 (Continued) IBM 1620 Computer Program for Calculating Mixture Velocities and Exit Conditions with Sample Input Data

```
C  C  HAMILTON        MIXTURE VELOCITIES AND EXIT CONDITIONS

RUN NR.  36     M(1) =   .206  T(1) =  497.  FRICTION FCT. = 0.13616E+02
V(1) =  349.    V(2) =  352.   V(3) =  355.   V(4) =  358.   V(5) =  361.
M(5) =  .212    T(5) = 497.    P(5) =  .963   A(5) = 1699.

RUN NR.3621     M(1) =   .216  T(1) =  501.  FRICTION FCT. = 0.12094E+02
V(1) =  369.    V(2) =  372.   V(3) =  375.   V(4) =  378.   V(5) =  382.
M(5) =  .224    T(5) = 501.    P(5) =  .941   A(5) = 1706.

RUN NR.3631     M(1) =   .195  T(1) =  492.  FRICTION FCT. = 0.15340E+02
V(1) =  331.    V(2) =  333.   V(3) =  335.   V(4) =  338.   V(5) =  340.
M(5) =  .201    T(5) = 492.    P(5) =  .985   A(5) = 1691.
```

Figure 64 Parameters Calculated by the Mixture Velocities and Exit Conditions Program

REFERENCES

1. Lewis, B. and von Elbe G. Combustion, Flames and Explosions of Gases. 2d ed. New York: Academic Press, Inc., 1961.

2. Jost, W. Explosion and Combustion Processes in Gases. 1st ed. New York and London: McGraw-Hill, 1946.

3. Wolfson, B. T. The Effect of Additives on the Mechanism of Detonation in Gaseous Systems. Ph.D. Dissertation, The Ohio State University, Columbus, Ohio, 1963.

4. Oppenheim, A. K., Manson, N., and Wagner, H. Gg. "Recent Progress in Detonation Research", AIAA Journal, V.1 (October 1963), 2243-2252.

5. Bollinger, L. E. "Formation of Detonation Waves in Combustible Gaseous Mixtures," (Paper presented at the Western States Section Meeting of the Combustion Institute), Paper No. WSS/CI 64-15, AD 625489, Stanford University (April 1964).

6. Berets, D. J., Greene, E. F., and Kistiakowski, G. B. "Gaseous Detonations. II. Initiation by Shock Waves", Journal of Chemical Physics, V. 72 (March 1950), 1086-1091.

7. Shepherd, W. C. F. "The Ignition of Gas Mixtures by Impulsive Pressures", Third Symposium on Combustion Flame and Explosion Phenomena. Baltimore: The Williams and Wilkins Company, 1949, 301-316.

8. Fay, J. A. "Some Experiments on the Initiation of Detonation in $2H_2$-O_2 Mixtures by Uniform Shock Waves", Fourth Symposium (International) on Combustion. Baltimore: The Williams and Wilkins Company, 1953, 501-507.

9. Steinberg, M. and Kaskan, W. E. "The Ignition of Combustible Mixtures by Shock Waves", Fifth Symposium (International) on Combustion. New York: Reinhold Publishing Corp., 1955, 664-671.

10. Belles, F. E. and Ehlers, J. "Shock Wave Ignition of H_2-O_2-Diluent Mixtures Near Detonation Limits", ARS Journal, V. 32, No. 2 (February 1962), 215-220.

11. Jost, W. Investigation of Gaseous Detonations and Shock Wave Experiments with Hydrazine. ARL 62-330, Wright-Patterson AFB, Ohio, April 1962.

12. Bollinger, L. E., et al. "Formation of Detonation Waves in Flowing Hydrogen-Oxygen and Methane-Oxygen Mixtures", AIAA Journal, V. 4, No. 10 (October 1966) 1773-1776.

13. McKenna, W. W. An Investigation of the Behavior of a Detonation Wave in a Flowing Combustible Mixture. Ph.D. Dissertation, The Ohio State University, Columbus, Ohio, 1966. (Also ARL 66-0112, Wright-Patterson AFB, Ohio, June 1966.)

14. Nichols, J. A. "Stabilized Gaseous Detonation Waves", ARS Journal, V. 29, No. 8 (August 1959), 607-608.

15. Nichols, J. A. "Standing Detonation Waves", Ninth Symposium (International) on Combustion. New York and London: Academic Press, 1963.

16. Hall, J. G. Shock Tubes - Part II; Production of Strong Shock Waves; Shock Tube Applications, Design, and Instrumentation. Institute of Aerophysics, University of Toronto, UTIA Review No. 12, Part II, May 1958.

17. Nagamatsu, H. T. and Martin, F. D. "Combustion Investigation in the Hypersonic Shock Tunnel Driver Section", Journal of Applied Physics, V. 30, No. 7 (July 1959), 1018-1021.

18. Keller, R. G., et al. Operations Manual for the Rocket Engine Test Facility of the Department of Mechanical Engineering. Air Force Institute of Technology (AU), Wright-Patterson AFB, Ohio, August 1961.

19. Frye, J. W., Jr. Thin Film Heat Transfer Gages. Thesis, GAM/ME/66A-4, Air Force Institute of Technology, Wright-Patterson AFB, Ohio, March 1966.

20. Gaydon, A. G. and Hurle, I. R. The Shock Tube in High Temperature Chemical Physics. New York: Reinhold Publishing Corp., 1963.

21. Berets, D. J., Greene, E. F., and Kistiakowski, G. B. "Gaseous Detonations. I. Stationary Waves in Hydrogen-Oxygen Mixtures", Journal of Chemical Physics, V. 72 (March 1950), 1080-1086.

22. Bollinger, L. E., Fong, M. C., and Edse, R. "Experimental Measurements and Theoretical Analysis of Detonation Induction Distances", ARS Journal, V. 31, No. 5 (May 1961), 588-595.

23. Keenan, J. H. and Kaye, J. Gas Tables. New York: John Wiley and Sons, Inc., 1948.

24. Glass, I. I. Shock Tubes - Part I: Theory and Performance of Simple Shock Tubes. Institute of Aerophysics, University of Toronto, UTIA Review No. 12, Part I, May 1958.

25. Obert, E. F. Thermodynamics. 1st Ed. New York: McGraw-Hill Book Co., Inc., 1948.

26. Perrot, G. St. J. and Gawthrop, D. B. "Apparatus for Studying the Ignition Process of Inflammable Gas-Air Mixtures by Explosives", Journal of Industrial and Engineering Chemistry, V. 19 (1927), 1293-1295.

27. Shepherd, W. C. F. Ignition of Fire Damp by Explosives - A Study of the Process of Ignition by the Schlieren Method. U. S. Department of Commerce, Bureau of Mines Bulletin 354, U. S. Government Printing Office, Washington, D. C., 1932.

28. Shine, A. J. Unpublished results of research conducted at the Air Force Institute of Technology, Wright-Patterson AFB, Ohio, June 1967.

29. Mawbey, M. W. S. A Scale Model Investigation of the Flow from the Open End of a Shock Tube of Rectangular Cross Section. Atomic Weapons Research Establishment, AWRE Report No. O-61/65, United Kingdom Atomic Energy Authority, August 1965. AD 472055.

30. Edse, R. Unpublished results of research conducted at The Ohio State University, Columbus, Ohio, June 1967.

31. Lewis, B. "Kinetics of Gas Explosions. IV. Ozone Explosions Induced by Hydrogen", Journal of the American Chemical Society, V. 55 (October 1933), 4001-4006.

32. Finch, G. I. and Cowen, L. G. "Gaseous Combustion in Electric Discharges", Proceedings of the Royal Society of London, V. 116, Series A (1927), 529-539.

33. Guest, P. G. Static Electricity in Nature and Industry. U. S. Department of Commerce, U. S. Bureau of Mines Bulletin 368, U. S. Government Printing Office, Washington, D. C., 1933.

34. ASME Special Research Committee on Fluid Meters. Fluid Meters: Their Theory and Application. 5th ed. New York: American Society of Mechanical Engineers, 1959.

35. Bowman, G. P. Computer Program for Calculating Detonation Wave Parameters for Hydrogen-Oxygen-Nitrogen Mixtures. Unpublished Notes. Air Force Institute of Technology (AU), Wright-Patterson AFB, Ohio, 1965.

UNCLASSIFIED

Security Classification

DOCUMENT CONTROL DATA - R & D

(Security classification of title, body of abstract and indexing annotation must be entered when the overall report is classified)

1. ORIGINATING ACTIVITY (Corporate author) Aerospace Research Laboratories Fluid Dynamics Facilities Research Laboratory Wright-Patterson AFB, Ohio 45433	2a. REPORT SECURITY CLASSIFICATION UNCLASSIFIED 2b. GROUP

3. REPORT TITLE

"AN EXPERIMENTAL INVESTIGATION OF SHOCK INITIATED DETONATION WAVES IN A FLOWING COMBUSTIBLE MIXTURE"

4. DESCRIPTIVE NOTES (Type of report and inclusive dates)

Scientific Final June 1966 to June 1967

5. AUTHOR(S) (First name, middle initial, last name)

Leonard Anthony Hamilton, Lt Col, USAF

6. REPORT DATE October 1967	7a. TOTAL NO. OF PAGES 194	7b. NO. OF REFS 35
8a. In-House Research b. PROJECT NO. 7065-00-16 c. DoD/Element 61445014 d. DoD/SubElement 681307	9a. ORIGINATOR'S REPORT NUMBER(S) 9b. OTHER REPORT NO(S) (Any other numbers that may be assigned this report) ARL 67-0202	

10. DISTRIBUTION STATEMENT

1. This document has been approved for public release and sale; its distribution is unlimited.

11. SUPPLEMENTARY NOTES TECH OTHER	12. SPONSORING MILITARY ACTIVITY Aerospace Research Laboratories(ARL) Wright-Patterson AFB Ohio 45433

13. ABSTRACT

This investigation was concerned with the initiation of detonation waves in a subsonically flowing mixture of gaseous hydrogen and oxygen by means of shock waves injected opposite to the direction of the flow. Nominally stoichiometric mixtures at near ambient pressure and stagnation temperature were flowed through a constant area tube at Mach Numbers of approximately .2, .5, and .8. The shock waves were produced by a simple shock tube driver employing helium and mylar diaphragms. Piezoelectric pressure transducers, thin film heat transfer gages, and ionization probes were used to measure the various wave velocities. Results showed that detonation waves can easily be produced in such a flowing mixture. The minimum incident shock wave Mach Number above which detonation always occurred was 2.12 for $M_{Exit} = .2$; 1.75 for $M_{Exit} = .5$; and 1.56 for $M_{Exit} = .8$. The temperatures behind these shock waves were far below the ignition temperature predicted by the thermal explosion limit theory. It was suggested that the low temperature ignition phenomena could be accounted for by an increase in the degree of ionization of the flowing mixture with flow velocity, due to frictional effects and possible impurities normally present in the gases. Additional experimental work is required in order to establish conclusively the explanation of the observed phenomena.

DD FORM 1 NOV 65 1473

UNCLASSIFIED

Security Classification

UNCLASSIFIED
Security Classification

14 KEY WORDS	LINK A		LINK B		LINK C	
	ROLE	WT	ROLE	WT	ROLE	WT
detonation waves						
shock waves						
shock tube						
ignition phenomena						
flowing-gas detonation tube						

UNCLASSIFIED
Security Classification

END